

Thermoplastic Polyurethane-Modified Laponite Clay Nanocomposites

*Thesis submitted to the
Indian Institute of Technology, Kharagpur
For award of the degree*

of

Doctor of Philosophy

by

Ananta Kumar Mishra

Under the guidance of

Professor Golok B Nando & Dr. Santanu Chattopadhyay



**RUBBER TECHNOLOGY CENTRE
INDIAN INSTITUTE OF TECHNOLOGY, KHARAGPUR**

JULY 2010

© 2010 Ananta Kumar Mishra. All rights reserved.

Dedicated to.....

My loving Parents

APPROVAL OF THE VIVA-VOCE BOARD

Date

Certified that the thesis entitled “THERMOPLASTIC POLYURETHANE-MODIFIED LAPONITE CLAY NANOCOMPOSITES” submitted by ANANTA KUMAR MISHRA to Indian Institute of Technology, Kharagpur, for the award of the degree of Doctor of Philosophy has been accepted by the external examiners and that the student has successfully defended the thesis in the viva-voce examination held today.

Prof. D. R. Mal
(Member of the DSC)

Prof. N. K. Singha
(Member of the DSC)

Prof. S. Banerjee
(Member of the DSC)

Prof. G. B. Nando
(Supervisor)

Dr. S. Chattopadhyay
(Supervisor)

(External Examiner)

(Chairman)

CERTIFICATE

This is to certify that the thesis entitled “**Thermoplastic Polyurethane-Modified Laponite Clay Nanocomposites**” submitted by **Mr Ananta Kumar Mishra**, to Indian Institute of Technology, Kharagpur, is a record of bonafide research work under our supervision and we consider it worthy of consideration for the award of the degree of Doctor of Philosophy of the Institute. Six research papers from the thesis have been published /communicated for publication in the reputed international journals.

Prof. Golok B. Nando
Supervisor

Dr. Santanu Chattopadhyay
Supervisor

Date:

ACKNOWLEDGEMENTS

I express my deep sense of gratitude to **Prof. Golok B. Nando** and **Dr. Santanu Chattopadhyay** of Rubber Technology Centre, Indian Institute of Technology, Kharagpur, for suggesting this research problem and their keen interest, unfailing encouragement, constructive suggestions and esteemed guidance throughout the course of the investigation.

I am grateful to **Dr. A. Phadke, Dr. N. K. Singha, Mr. S. Praveen and Dr. P. R. Rajamohanam** for their help during different stage of the present work.

I express my sincere gratitude to the Head of the Centre for extending all facilities of the Rubber Technology Centre during my research work and to the Indian Space Research Organization, Bangalore & IIT Kharagpur, for the financial support.

Despite the impossibility of giving credit to everyone who has been of help, I should like to single out certain people who have been especially instrumental, directly or indirectly, in completing this piece of work. **Kavitha, Thrirumal, Dhruba, Suman, Pijus, Basuli, Radhasyam, Saroj** and **Nabin** deserve special mention as they have helped when I needed their unique help most.

I appreciate the company and help of other faculty members, staffs and scholar friends/brothers for a cordial atmosphere they maintained through out my research work.

Finally, I deeply acknowledge my indebtedness to **my Parents, my sisters 'Namita' & 'Anita' and my brother 'Jayanta'** and all other family members for their good wishes and continuous encouragement which have enabled me to complete the work.

Dated: July 2010.

(Ananta Kumar Mishra)

DECLARATION

I certify that

- a. The work contained in the thesis is original and has been done by myself under the general supervision of my supervisor(s).
- b. The work has not been submitted to any other Institute for any degree or diploma.
- c. I have followed the guidelines provided by the Institute in writing the thesis.
- d. I have conformed to the norms and guidelines given in the Ethical Code of Conduct of the Institute.
- e. Whenever I have used materials (data, theoretical analysis, and text) from other sources, I have given due credit to them by citing them in the text of the thesis and giving their details in the references.
- f. Whenever I have quoted written materials from other sources, I have put them under quotation marks and given due credit to the sources by citing them and giving required details in the references.

Ananta Kumar Mishra

List of Symbols

Symbol	Description	Unit
d	Spacing between two nearby clay platelets	nm
E	Activation energy	J/mole
E'	Storage modulus	Pa
E''	Loss modulus	Pa
G'	Shear storage modulus	Pa
G''	Shear loss modulus	Pa
k	Rate constant	s ⁻¹
k ₃₀₀	Rate constant at 300 °C	s ⁻¹
k ₃₂₅	Rate constant at 325 °C	s ⁻¹
k ₃₅₀	Rate constant at 350 °C	s ⁻¹
k'	Consistency index	Pa.s ⁿ
\overline{Mn}	Number average molecular weight	gms per gm mole
n	Flow behavior index	--
T _g	Glass transition temperature	°C
T _m	Melting temperature	°C
T _i	Onset degradation temperature	°C
T _{1max}	Temperature corresponding to 1 st maximum degradation	°C
T _{2max}	Temperature corresponding to 2 nd maximum degradation	°C
T ₅	Temperature corresponding to 5% degradation	°C
T ₁₀	Temperature corresponding to 10% degradation	°C
T ₅₀	Temperature corresponding to 50% degradation	°C
T ₈₀	Temperature corresponding to 80% degradation	°C
$\dot{\gamma}$	Shear rate	s ⁻¹
δ	Loss angle	° (degree)
tan δ	Loss tangent (E''/ E')	--
tan δ _{max}	Maximum height of loss tangent peak	--
δ ppm	Chemical shift	ppm
ΔC _p	Heat capacity	kJ/kg °C
ε	Strain	%
η*	Complex viscosity	Pa.s
θ	Angle of X-ray diffraction	° (degree)
τ	Characteristic relaxation time	s
χ _c	Percentage of crystallinity	%

List of Abbreviations

Abbreviation	Description
AFM	Atomic force microscopy
ASTM	American society for testing and materials
1,4-BD	1,4-butanediol
DBTDL	Dibutyltin dilaurate
CEC	Cation exchange capacity
DMA	Dynamic mechanical analysis
DSC	Differential scanning calorimetry
EB	Elongation at break
FESEM	Field emission scanning electron microscopy
FTIR	Fourier transformed infrared
HRTEM	High resolution transmission electron microscopy
HTPB	Hydroxy terminated polybutadiene
MDI	4,4'-Methylenebis (phenyl isocyanate)
MMT	Montmorillonite
NMR	Nuclear Magnetic Resonance
-OEt	Ethoxy
-OMe	Methoxy
-OH	Hydroxy
PDI	Polydispersity index
PTMEG	Polytetramethylene glycol
RPA	Rubber process analyzer
rpm	revolution per minute
TGA	Thermogravimetric Analysis
TPU	Thermoplastic polyurethane
TPUCN	Thermoplastic polyurethane clay nanocomposite
TS	Tensile strength

ABSTRACT

The thesis aims to explore the structure-property relationship between the TPU and the TPU-modified Laponite clay nanocomposites prepared following solution mixing, *ex-situ* and *in-situ* techniques by using various modified clays. Laponite clay has been modified by ionic, covalent and dual modification techniques. Initially, modified clays were dispersed in the commercial TPU by using simple solution mixing technique. Finally, the most suitable grade of the modified Laponite clay was used for the preparation of TPU-clay nanocomposite by using *ex-situ* and *in-situ* techniques using the in-house synthesized TPU as a matrix. Effect of tethering with functional modifiers has also been compared by using another grade of modified Laponite prepared in a similar technique. The modified Laponite clays have been found to act as hard domain markers. Improvements in technical properties including the thermal stability have been observed to be a strong function of the degree of dispersion of the modified nanoclays in the TPU matrix. Novel tubular and elliptical morphologies have been evolved by using dual modified Laponite clays in combination with the hard domains of the TPU. The thermal stability of the nanocomposite has been found to increase by 35 °C, as compared to the neat TPU. The tensile strength has been observed to increase by 67% as compared to the neat TPU with merely 3% clay content. Increased numbers of tethering in the modified clays have been observed to be detrimental to the improvements in technical properties of the TPU-clay nanocomposite systems. In the system studied *ex-situ* prepared nanocomposites have been found to offer better improvements in technical properties as compared to the *in-situ* prepared nanocomposites.

Key Words: Thermoplastic polyurethane, Laponite clay, Dual modification, Nanocomposite, Morphology, Thermal stability

Contents

	<u>Page No.</u>
Title Page	i
Dedication	ii
Approval of the viva-voce board	iii
Certificate	iv
Acknowledgements	v
Declaration	vi
List of Symbols	vii
List of Abbreviations	viii
Abstract	ix
Contents	x
CHAPTER 1	1–34
Introduction	
1.1 Polymer-clay nanocomposite	5
1.2 Polyurethanes	5
1.3 Thermoplastic Polyurethane (TPU)	9
1.4 TPU-clay Nanocomposites	10
1.5 Literature Review on TPU-clay Nanocomposites	12
1.5.1 Structure and Morphology	12
1.5.2 Mechanical Properties	15
1.5.3 Thermal Properties	18
1.5.4 Rheological Characteristics	20
1.6 TPU-Laponite clay Nanocomposites	22
1.7 Summary of the Literature Review	24
1.8 Scope and Objectives	25
1.9 References	27

CHAPTER 2 Experimental 35–48

2.1	Materials Used	35
2.1.1	Thermoplastic Polyurethane (TPU)	35
2.1.2	Nanoclays	35
2.1.3	Other Chemicals	36
2.2	Modification of Nanoclays	38
2.2.1	Ionic Modification of Laponite	38
2.2.2	Covalent Modification of Laponite	39
2.2.3	Dual Modification of Laponite	40
2.3	Preparation of Nanocomposites	41
2.3.1	Solution Mixing Technique	41
2.3.2	Synthesis of TPU	41
2.3.3	Preparation of TPUCN by <i>Ex-situ</i> Technique	42
2.3.4	Preparation of TPUCN by <i>In-situ</i> Technique	42
2.4	Characterization Techniques Adopted	44
2.4.1	Fourier Transform Infrared Spectroscopy (FTIR)	44
2.4.2	Solid State NMR Spectroscopy	44
2.4.3	X-Ray Diffraction (XRD) Studies	44
2.4.4	Transmission Electron Microscopy (TEM)	45
2.4.5	Field Emission Scanning Electron Microscopy (FESEM)	45
2.4.6	Atomic Force Microscopy (AFM)	45
2.4.7	Differential Scanning Calorimetry (DSC)	45
2.4.8	Thermogravimetric Analysis (TGA)	46
2.4.9	Dynamic Mechanical Analysis (DMA)	46
2.4.10	Rubber Process Analyzer (RPA)	46
2.4.11	Tensile Property Studies	47

CHAPTER 3 Characterization of Modified Nanoclays 49–65

3.1	Introduction	49
3.2	FTIR Studies of Clay with and without Modification	49
3.2.1	Ionic Modification	49
3.2.2	Covalent Modification	51
3.2.3	Dual Modification	51
3.3	Solid State NMR Spectroscopy of the Modified Clays	53
3.3.1	Ionic Modification	53
3.3.2	Covalent Modification	54
3.3.3	Dual Modification	54
3.4	Wide Angle X-ray Diffraction (WAXRD) Studies	58
3.4.1	Ionic Modification	58
3.4.2	Covalent Modification	59
3.4.3	Dual Modification	59
3.5	Thermogravimetric Analysis of Nanoclays	60
3.5.1	Ionic Modification	60
3.5.2	Covalent Modification	62
3.5.3	Dual Modification	62
3.6	Conclusions	63
3.7	References	63

CHAPTER 4A TPU-clay Nanocomposite based on Modified Laponite and Cloisite® 67–89

4A.1	Introduction	67
4A.2	Wide Angle X-Ray Diffraction	67
4A.3	Transmission Electron Microscopy	70
4.3.1	Morphology of Solution Cast Nanocomposites	70
4.3.2	Morphology of Annealed Nanocomposites	70

4A.4	Field Emission Scanning Electron Microscopy	73
4A.5	Atomic Force Microscopy	74
4A.6	Differential Scanning Calorimetry	75
4A.7	Dynamic Mechanical Analysis	76
4A.8	Thermogravimetric Analysis	81
4A.9	Isothermal TGA	84
4A.10	Conclusions	88
4A.11	References	88

CHAPTER 4B Rheological Characteristics of TPUCN Based on Modified Laponite and Cloisite® 91–112

4B.1	Introduction	91
4B.2	Strain Sweep	92
4B.3	Temperature Sweep	96
4B.4	Frequency Sweep	98
	4B.4.1 Effect on Complex Viscosity at 140 °C	99
	4B.4.2 Effect on Complex Viscosity at 170 °C	103
	4B.4.3 Effect on Modulus at 140 and 170 °C	106
4B.5	Stress Relaxation	108
	4B.5.1 A Brief Theoretical Background on Stress Relaxation	108
	4B.5.2 Instantaneous (0.1 s) and 30 s Stress Relaxation time at 120 °C	109
4B.6	Conclusions	111
4B.7	References	111

CHAPTER 5 TPUCN based on Modified Laponite RDS 113–134

5.1	Introduction	113
-----	--------------	-----

5.2	Wide Angle X-Ray Diffraction (WAXRD)	113
5.3	Transmission Electron Microscopy	115
5.4	Field Emission Scanning Electron Microscopy	118
5.5	Differential Scanning Calorimetry	119
5.6	Dynamic Mechanical Analysis	120
5.7	Dynamic Rheological Analysis	123
	5.7.1 Strain Sweep	123
	5.7.2 Temperature Sweep	125
	5.7.3 Frequency Sweep	127
	5.7.3.1 Effect on Complex Viscosity at 140 °C	127
	5.7.3.2 Effect on Complex Viscosity at 170 °C	127
5.7	Thermogravimetric Analysis	128
5.8	Isothermal TGA	131
5.9	Conclusions	133
5.10	References	134

CHAPTER 6 TPUCN based on Covalent and Dual Modified Laponite RD 135–149

6.1	Introduction	135
6.2	Wide Angle X-Ray Diffraction (WAXRD)	135
6.3	Transmission Electron Microscopy	137
6.4	Differential Scanning Calorimetry	139
6.5	Dynamic Mechanical Analysis	140
6.6	Dynamic Rheological Analysis	144
	6.6.1 Strain Sweep	144
	6.6.2 Temperature Sweep	145
	6.6.3 Frequency Sweep	145
	6.6.3.1 Effect on Complex Viscosity at 140 °C	145
	6.6.3.2 Effect on Complex Viscosity at 170 °C	146
6.7	Thermogravimetric Analysis	147
6.8	Isothermal TGA	147

6.9	Conclusions	149
6.10	References	149
CHAPTER 7	<i>Ex-situ</i> and <i>In-situ</i> Prepared TPUCN based on Dual Modified Laponite RD	151–174
7.1	Introduction	151
7.2	Wide Angle X-Ray Diffraction (WAXRD)	151
	7.2.1 WAXRD at Lower Angular Range	151
	7.2.2 WAXRD at Higher Angular Range	154
7.3	Transmission Electron Microscopy	158
7.4	Differential Scanning Calorimetry	161
7.5	Dynamic Mechanical Analysis	163
7.6	Dynamic Rheological Analysis	165
	6.6.1 Strain Sweep	165
	6.6.2 Temperature Sweep	167
	6.6.3 Effect on Complex Viscosity at 140 °C	168
7.7	Tensile Properties	170
7.8	Thermogravimetric Analysis	172
7.9	Conclusions	174
7.10	References	174
CHAPTER 8	Summary and Conclusions	175–180
8.1	Summary and Conclusions	175
8.2	Contribution of the Present Work	179
8.3	Limitations and Scope for Future Work	180

CHAPTER 1

INTRODUCTION AND LITERATURE SURVEY

1. Introduction

A composite may be defined as a material made up of multiple phases within a single matrix differing in their physical and chemical properties leading to a material with properties different from those of the individual constituents. In a composite, one of the phases is usually continuous and is called the matrix phase, while the other phase (or phases) is usually a reinforcing material and is called the dispersed phase. The materials embedded inside the matrix in a composite normally overcome the deficiencies of the matrix material. The term composite was coined in the year 1937 when salesmen from the Owens Corning Fiberglass Company began to sell fiberglass. In a broader sense, composites may be divided into three classes depending upon their matrix material composition, such as; polymeric, metallic or ceramic matrices. Polymers are the most abundantly used matrix material in preparing the composites, because of their excellent processibility, lower cost, low specific gravity and easy formability. However, the stiffness and strength of the polymers are quite low as compared to those of the metals and ceramics. Thus, reinforcement achieved by preparing polymer composites is highly beneficial for ultimate product performance as compared to other matrix composites. Moreover, polymer composites can be processed at lower temperatures as compared to metallic and ceramic counterparts. Thus, the problems associated with the processing as well as degradation in reinforcement during preparation are the least in polymer matrices as compared to other matrices.

In most of the conventional composite materials, the structural units (dispersed phases) are either in the macro or in the micrometer length scale. However, the first discovery of polymer clay nanocomposite by Toyota research group [Kojima et al. (1993); Usuki et al. (1993)] has brought a significant change in the research on

polymer composites. It has been observed that about 87 °C improvement in heat distortion temperature (HDT) of the Nylon-6 montmorillonite clay nanocomposite can be achieved, as compared to the neat Nylon-6 along with significant improvement in mechanical properties. It has been assumed that the improvement in the physicochemical properties of the nanocomposites may be due to the large interfacial area per unit volume of interaction which is far less in case of conventional composites.

Layered silicates, metal oxides, layered titanate, inorganic nanotubes and polymeric nanomaterials like expandable graphite, cellulose nano-whiskers, polyhedral oligomeric silsesquioxanes (POSS), carbon nanotubes, and many others are among the popular choice of nanofillers used today. Nanoclay is still the most preferred and popularly used nanomaterial to prepare the nanocomposites because of its easy availability, unique layered structure (absent in other nanomaterials) and lower cost as compared to other nanomaterials [Alexandre and Dubois (2000)].

Some of the technologically important classes of clay minerals used in making polymer-clay nanocomposites are listed in Table 1.1. Layered silicates are divided into three main types based on the relative ratio of two unit crystal sheets, like:

- 1:1 type: one silica tetrahedron following one alumina octahedron present in unit lamellar crystal
- 2:1 type: two silica tetrahedron with one alumina octahedron sandwiched in unit lamellar crystal
- 2:2 type: four crystal sheets in which silica tetrahedron and alumina or magnesium octahedron are alternately arranged.

Table 1.1: Important clay minerals used to prepare polymer clay nanocomposites

Type	Name of Clay*	General Formula
1:1	Kaolinite ^{b,N}	$Al_2Si_2F_5(OH)_4$
	Halloysite ^{b,N}	$Al_2Si_2F_5(OH)_4 \cdot n H_2O$
2:1	Montmorillonite ^{a,N}	$M_x(Al_{2-x}Mg_x)Si_4O_{10}(OH)_2 \cdot n(H_2O)$
	Hectorite ^{a,N}	$M_x(Mg_{3-x}Li_x)Si_4O_{10}(OH)_2 \cdot n(H_2O)$
	Saponite ^{a,N}	$M_xMg_3(Si_{4-x}Al_x)O_{10}(OH)_2 \cdot n(H_2O)$
	Laponite ^{a,S}	$M_x(Mg_{3-x}Li_x)Si_4O_{10}(OH)_2 \cdot n(H_2O)$
	Fluorohectorite ^{a,S}	$M_x(Mg_{3-x}Li_x)Si_4O_{10}F_2 \cdot n(H_2O)$
	Fluoromica ^{a,S}	$Na Mg_{2.5}Si_4O_{10}F_2$
	2:2	Sapiolite ^S
Attapulgite ^S		$Mg_5Si_8O_{20}(HO)_2(OH_2)_4 \cdot 4H_2O$

*“a” represents clays with negative surface charges; “b” represents clays with positive charge; N-Natural; S-synthetic

Amongst these nanoclays, the most abundantly explored and used variety of nanoclay is Montmorillonite (MMT), popularly known as ‘Cloisite[®]’ and is available commercially in various grades depending on the types of modifiers used (almost exclusively marketed by Southern Clay Limited, USA). However, other varieties of nanoclays lag behind in bulk production and application as compared to the Cloisite[®]. MMT is a natural hectorite clay whereas, Laponite is a synthetic variety of hectorite clay. The diameters of individual diskettes (or platelets) of MMT vary from 150 to 250 nm whereas, diameter of the platelets of Laponite vary from 25 to 30 nm. Laponite platelets possess well controlled dimension, smaller in size and is chemically pure as compared to MMT. In case of MMT interstitial charge deficiency is created by the replacement of Al^{3+} with Mg^{2+} or Fe^{2+} but in case of Laponite the same is possible by the replacement of Mg^{2+} with Li^{1+} .

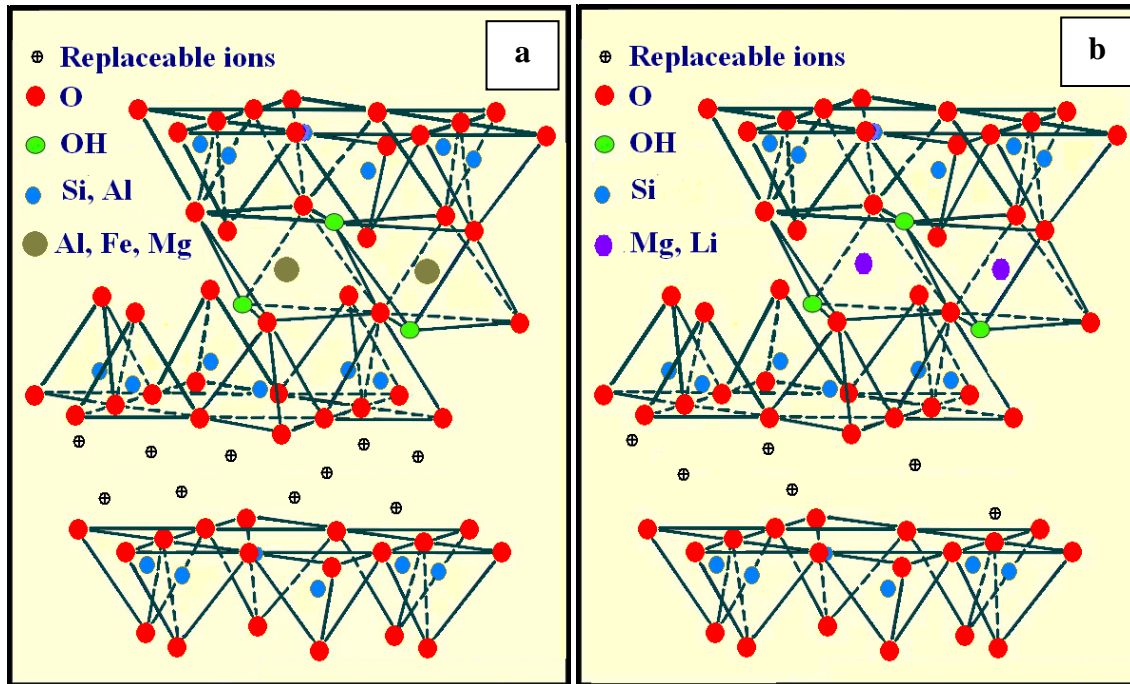


Figure 1.1: Structure of platelets of (a) Montmorillonite and (b) Laponite

These negative charge deficiencies are counterbalanced by the alkali or alkaline earth metal cations. These alkali or alkaline earth metal cations generally present in between the lamellar spacing of the clay galleries (since clay possesses layered structure, Fig. 1.1a and b). These alkali or alkaline earth metal cations can be ion exchanged with alkyl ammonium halides (known as modifier or surfactant in the literature) [Herrera et al. (2006); Ni et al. (2004, 2006); Tien and Wei (2001a, 2002)]. The $-OH$ groups present at the edge of lamellae, provides site for covalent modification of the nanoclay by using alkoxy silanes [Herrera et al. (2004, 2005); Park et al. (2004); Wheeler et al. (2005, 2006)]. Modification of the interlayer space and/or surface of the platelets renders the clay surface hydrophobic. The modification also increases the gallery spacing of the clay. The clay becomes more compatible with the polymer as a whole, due to such modifications.

1.1 Polymer-clay Nanocomposite

In the last few decades polymer clay nanocomposite has come to the forefront and has been recognized as one of the frontier areas of research in the field of polymer science and technology. This is possible only because of the many fold increase in property spectrum of the nanocomposite as compared to those of the neat polymers and conventional macro- and micro- composites. Nanoclay is the most popular nanomaterial because of its unique layered structure. The state of dispersion of the nanoclay in the polymer matrix is classified into three categories, e.g., intercalated, exfoliated and aggregated/agglomerated. Successful thermal and mechanical property enhancement of polymer matrices through nanoclay reinforcement is expected because of complete exfoliation of the clay platelets [William et al. (2005)]. Complete exfoliation is often very difficult because of the hydrophilic-hydrophobic repulsion between clay and polymer matrices. Large viscosity barrier for both polymer melts and solutions makes the situation even more unfavorable. Generally, the unmodified clay surface is hydrophilic, but most of the polymers are hydrophobic in nature. Several attempts have been made to render the clay surface organophilic [Blumstein et al. (1974); Solomon (1968); Theng (1974, 1979)] for achieving better dispersion of clays into the polymer matrices.

1.2 Polyurethanes

Polyurethanes find plenty of applications in a wide range of engineering works including in the biomedical field. Polyurethane is a class of polymer containing organic segments joined to each other by urethane linkages. Otto Bayer and co-workers have invented this polymer at the I.G. Farbenindustrie, Germany in 1937, but production in the industrial scale started only in 1940 when DuPont and ICI recognized its extraordinary elastic properties.

The key components required for the synthesis of polyurethanes are:

- a. Diisocyanate (aliphatic or aromatic)
- b. Polyol (polyester or polyether)
- c. Chain extender (low molecular weight diol or diamine).

The most commonly used diisocyanates are 4,4'-methylene bis(phenyl isocyanate) (MDI), 2,4-toluene diisocyanate (TDI), 1,6-hexamethylene diisocyanate (HDI), isophoron diisocyanate (IPDI), etc.

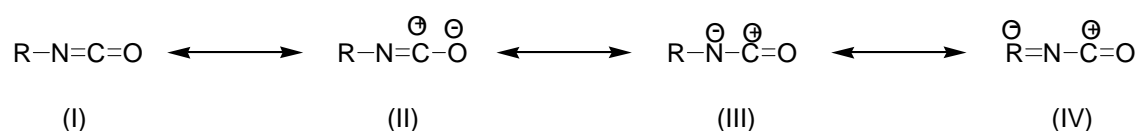
Although isocyanates play a vital role in the polyurethane synthesis (due to the differences in their reactivity depending on the presence of aromatic and aliphatic moieties) but the final property of the polyurethane is mostly determined by the type of polyol used. Functionality of the polyols may vary from 2 to 8 with an average molecular weight of 400 to 6000 gms per gm mole (\bar{M}_n). In practice, polyol with molecular weight 1000 and 2000 gms per gm mole are most widely used [Petrovic and Ferguson (1991)]. Polyether polyol based polyurethanes are more resistant to hydrolysis, whereas, the polyester polyol based counterparts are thermally more stable. Polytetramethylene glycol (PTMEG) based polyurethane possess excellent hydrolytic stability and microbial resistance, outstanding dynamic properties including resilience and low temperature flexibility.

The third most important component is the chain extender. The most widely used chain extender in preparing polyurethanes is 1,4-butane diol but methylene bis (o-chloro aniline) is normally used for the preparation of polyurethane urea [Hepburn (1982)].

Catalysts play an important role in the synthesis of polyurethanes. Tertiary amines are mostly used in the synthesis of polyurethane foams (as it also promotes the reaction of the isocyanate with water). However, organometallic compounds

especially dibutyl tin dilaurate is most widely used catalyst for the synthesis of thermoplastic polyurethanes (TPUs) [Hepburn (1982)].

In the synthesis of polyurethanes, chemistry of diisocyanate plays a vital role. The isocyanate group contains a highly electrophilic carbon atom, which possess the resonating structures as shown in Scheme 1.1.



If R= Aromatic

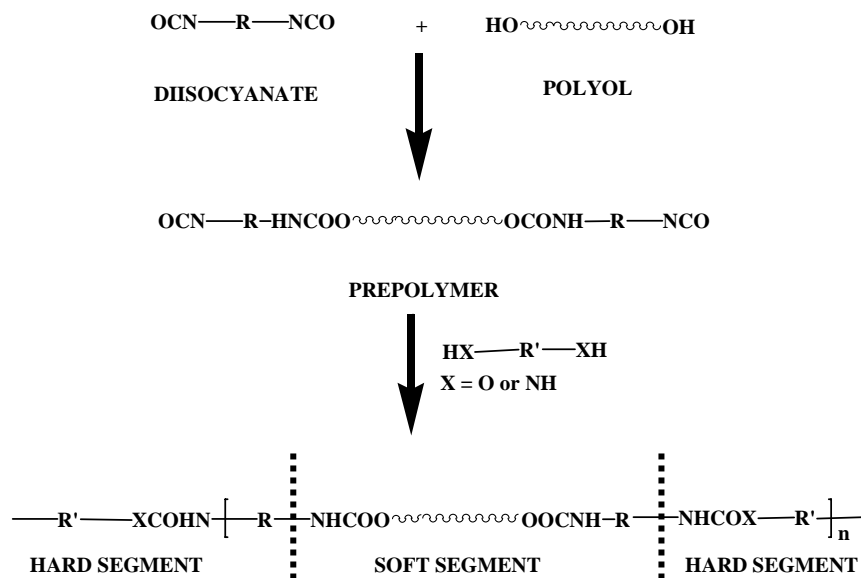
Scheme 1.1: Resonating structures of isocyanate

This electrophilic carbon present in the –NCO group plays a pivotal role in polyurethane chemistry. Three resonating structures (II, III and IV), out of the four, contain carbon atom having positive charge on it with the delocalization of negative charge on oxygen, nitrogen and R group (provided ‘R’ is aromatic). This is the only reason for the high reactivity of isocyanates towards nucleophiles and higher reactivity of aromatic isocyanates over aliphatic isocyanates. It is also found that the reactivity of aromatic isocyanate containing electron withdrawing group on the aromatic ring increases when present in ortho- and para- positions. Similarly, the reactivity diminishes significantly when the aromatic ring(s) contains electron donating substituents.

The methods of synthesis of polyurethanes can be differentiated according to the medium of preparation (bulk, solution, aqueous) and the addition sequence of the reactants (one shot process, two step prepolymer process). Bulk polymerization (either one shot or two step prepolymer process) is generally preferred in industries as the process is cost effective and environment friendly because of solvent-free

synthesis, whereas, solution polymerization is being used for laboratory synthesis [Hepburn (1982); Woods (1990)]. However, reaction in aqueous media via miniemulsion polymerization technique is mostly limited to the preparation of certain coatings and adhesives [Dieterich (1994)].

In one shot process, all the ingredients (polyol, diisocyanate, chain extender and catalyst) are mixed together. However, in the prepolymer process, polyol is first reacted with the diisocyanate to prepare the prepolymer, followed by chain extension reaction. In case of one shot process, high degree of shear is required to render homogeneous mixing. Prepolymer process is most widely used method as one can precisely control the morphology of the final product by this method. Scheme 1.2 depicts the schematic representation of synthesis of polyurethanes by the prepolymer route.



Scheme 1.2: Preparation of polyurethane by prepolymer method

Polyurethanes can be classified into various categories depending on their properties and applications, e.g.,

- a. Thermoplastic Polyurethane (Segmented polyurethane) – ranging from thermoplastic to thermoplastic elastomer
- b. Castable Polyurethane
- c. Millable Polyurethane
- d. Polyurethane foams (Rigid and Soft)
- e. Coatings
- f. Adhesives.

1.3 Thermoplastic Polyurethane (TPU)

Amongst all the grades of polyurethanes, TPU is the most widely used material. This is because of its higher mechanical strength, excellent abrasion resistance, ease in processing and bio-compatibility. TPU is a block copolymer composed of hard segments and soft segments arranged in a (A-B-A)_n fashion. The soft segment is prepared by the reaction between the polyol and the diisocyanate, but hard segment is formed by the reaction between the diisocyanate and the chain extender. Phase separation (segregation) between the hard and soft segments occurs due to the difference in secondary forces (van der Waals, dipole-dipole, H-bonding interactions, etc. [Hepburn (1982)]). Thus, the degree of segregation between the hard and soft segments depend on the extent of interaction of the hard segments with each other and also with the soft segments [Senich and Macknight (1980); Seymour et al. (1970); Sheneider and Paiksung (1977); Srichatrapimuk and Cooper (1978)]. The phase segregation is less pronounced in polyester polyurethane than in polyether polyurethane and is most pronounced in polybutadiene based (e.g., HTPB) polyurethane. Also a drastic development in phase segregation and domain organization can be encountered due to the incorporation of urea moiety in the hard segment [Bonart et al. (1974); Sung et al. (1980a)], which causes improved

mechanical strength such as higher mechanical properties, lower hysteresis, greater toughness and slower rate of stress relaxation [Sung et al. (1980b)]. Phase separation increases with increasing chain length of soft segment or with the increasing polarity leading to lesser hard-soft segment interactions. Bonart (1968) and Clough et al. (1968) reported the first direct evidence of the occurrence of two-phase morphology from small angle X-ray scattering (SAXS) study.

Despite several advantages, TPU suffers from lower thermal stability and flame retardancy as compared to other engineering thermoplastics (polyether imides, polyether esters etc.) for similar applications [Holden et al. (2004); Troughton (2008)].

1.4 TPU-clay Nanocomposites

The aforesaid limitations of TPU may be overcome by three different ways:

- a. Changing the three basic building blocks i.e. polyester/polyether polyol, diisocyanates and chain extender
- b. Blending with a suitable polymer
- c. Incorporation of inorganic fillers especially the nanofillers into the polyurethane matrix.

Amongst these three techniques, incorporation of inorganic nanofillers is found to be most effective commercially and technically viable process. This is because, nanofillers have the advantage of improving barrier property along with improvement in mechanical properties and thermal stability (which is difficult to achieve in other cases) and cost effectiveness. Segmented polyurethane (TPU)-clay nanocomposite was first introduced by Wang and Pinnavaia (1998). It has been observed that montmorillonite clay modified with long chain onium ions (carbon number ≥ 12) exhibited very good compatibility with several polyols commonly used

for polyurethane synthesis. Also an increase in the chain length of alkyl groups in the long chain onium ions results in the increased interlayer distance between the clay platelets in the nanocomposites.

TPU- clay nanocomposites (TPUCNs) may be prepared by three distinct methods, e.g.,

- a. Melt blending
- b. Solution mixing and
- c. *In-situ* synthesis.

In case of melt blending technique, nanoclay is mixed with the molten TPU in an internal mixer or extruder. Solution mixing involves the intermixing of solution of TPU and the solvated nanoclay utilizing mechanical stirring and/or ultrasonic vibration, followed by the evaporation of solvent. Whereas, in case of *in-situ* synthesis technique, clay is dispersed either with the polyol or with the prepolymer followed by further course of polymerization.

Several factors responsible for the dispersion of nanoclays [Takeichi et al. (2002)] in the polymer matrix which can be listed below, as:

- a. method of preparation
- b. mixing temperature and thermal history
- c. mixing time
- d. shear rate and extent of deformation
- e. solvent used (especially in solution mixing and *in-situ* preparation method)
- f. concentration of polymer solution (for solution mixing and *in-situ* preparation)
- g. Molecular weight of the monomer (for *in-situ* preparation method) or polymer
- h. Types of modifier used for modification of nanoclay
- i. Extent of modification of the nanoclay.

1.5 Literature Review on TPU-clay Nanocomposites

1.5.1 Structure and Morphology

First successful dispersion of nanoclays in polyurethane matrix by Wang and Pinnavaia (1998), have attracted tremendous interest among the scientific community. It has been observed that morphology of clay platelets play a vital role in improving the properties of the TPU-clay nanocomposites (as discussed earlier). Several techniques have been utilized to visualize the surface and bulk morphology of the nanocomposites like SEM, FESEM, AFM, XRD and TEM.

The effect of hard segment content and the amount of clay on the morphology has been reported by Hu et al. (2001). Increased hard segment content has been observed to increase the basal spacing of the clay platelets at lower clay content but reverse phenomenon has been observed at higher clay contents.

Two varieties of modified MMT have been dispersed in TPU matrix by Chen et al. (2000) (clay modified with 12 aminolauric acid and benzidine) to study the effect of modifier on the morphology and property of the resulting nanocomposites. Complete exfoliation has been observed upto 5% and 3% of clay modified with 12 aminolauric acid and benzidine, respectively.

An intercalated to exfoliated morphology has been observed with the incorporation of clay modified with dilauryldimethyl ammonium bromide and 4,4'-diaminodiphenylmethane, respectively [Chen-Yang et al. (2004)].

Intercalated structures have been predominantly observed when the clay was used as a pseudo chain extender [Rehab and Salahuddin (2005)]. However, Xia and Song (2006) have observed preponderance of intercalated morphology with nontethered clay (physically mixed clay), and exfoliated morphology with the tethered clay (clay having active functional group) for the nanocomposite prepared by

in-situ synthesis technique. It has been observed that nanoclay possessing active functional groups can form H-bonding if physically mixed and if it can act as a pseudo chain extender by *in-situ* method.

The surface –OH group of the nanoclays has been reacted with the isocyanate and dispersed in polyurethane matrix. Highly exfoliated morphology has been observed by *in-situ* synthesis technique [Seo et al. (2006)] while intercalated morphology has been pronounced by solution mixing technique [Cheng et al. (2006)]. Both solution mixing and twin screw extrusion have been observed to give higher degree of delamination and slight intercalation of Cloisite[®] 30B with two varieties of polyurethanes differing from each other by the content of hard segment [Finnigan et al. (2004)]. These have been explained on the basis of the formation of H-bonding (acting as a driving force) for the intercalation of the modified clay in the TPU matrix. A comparative study between four varieties of clay (unmodified MMT, Cloisite[®] 15A, Cloisite[®] 25A and Cloisite[®] 30B) in two types of TPU (polyether and polyester based TPU) has been reported by Dan et al. (2006). A very poor dispersion has been observed with natural clay (unmodified clay) in both types of TPU. Partially intercalated morphology has been obtained with both Cloisite[®] 15A and Cloisite[®] 25A. Cloisite[®] 25A has been found to give better dispersion as compared to Cloisite[®] 15A. However, presence of –OH groups (tethered) on the modifier has been observed to render mostly exfoliated morphology in case of Cloisite[®] 30B. Similarly, dominant intercalated and exfoliated morphology has been obtained by *in-situ* polymerization of Cloisite[®] 20A (non-tethered) and Cloisite[®] 30B (tethered), respectively [Xia et al. (2005)]. It has been reported by several other researchers also that tethering of the clay leads to exfoliation of the clay platelets [Gorrasi et al. (2005); Kuan et al. (2005b); Pattanayak and Jana (2005a); Ni et al. (2004)]. Interestingly, occurrence of

highly exfoliated morphology upto 40 wt% of nanoclay has been reported by Ni et al. (2004, 2006) by using clay as a pseudo chain extender.

Intercalated morphology has been predominantly obtained by using Cloisite[®] 30B as pseudo chain extender by bulk polymerization method due to high viscosity barrier for exfoliation of clay [Pattanayak and Jana (2005c)].

The effect of changing the number of end tethered –OH functional groups on the tail of the modifier (for the modification of Montmorillonite) have been studied (from 1 to 3) by Tien and Wei (2001b). The morphology of clay has changed from intercalated to exfoliated, with the increase in number of –OH groups in the modifier. Moon et al. (2004) have modified Montmorillonite with tris(hydroxymethyl) aminomethane to prepare a tethered clay having three –OH groups and it has been used as a pseudo chain extender. Intercalated to exfoliated morphology has been observed for all the nanocomposites but increased aggregation tendency has also been reported at higher clay contents.

Interestingly, a contrasting result has been reported by Pattanayak and Jana (2005b). High mechanical shearing (not the tethering of the clay) has been found to be the main reason for the complete exfoliation of the nanoclay. Similar observations have also been reported by Meng et al. (2008). The degree of exfoliation has been found to increase with increase in time of mixing.

Choi et al. (2005) modified the clay with in-house synthesized organifier (modifier) and subsequently dispersed such modified clays into the TPU matrix. It has been observed that 60 minutes of sonication provided better dispersion of modified nanoclays as compared to the nanocomposite prepared without sonication.

Song et al. (2005) have found that hard domain of TPU can self organize to form spherical aggregates. Size of these aggregates has been found to decrease from 800 nm to 500 nm with the incorporation of Cloisite[®] 20A.

1.5.2 Mechanical Properties:

Mechanical properties of TPU are of great importance due to their usefulness in many engineering applications, where strength properties play a vital role. It is observed that addition of nanoclay into the polyurethane matrix improves the tensile properties significantly. Addition of conventional fillers into the polyurethane matrix has been reported to improve the modulus by sacrificing the long range elastic properties [Torro-palau et al. (1997)]. However, addition of 10% of modified clay has been reported to increase the tensile strength, modulus and strain at break by more than 100% [Wang and Pinnavaia (1998)]. More than 100% increase in tensile strength and elongation at break have also been reported by several other researchers [Ni et al. (2004); Pattanayak and Jana (2005a,b,d)]. Xiong et al. (2004) have used Cetyl trimethyl ammonium bromide (CTAB) and methylene bisortho-chloro aniline to prepare C16-MMT and MOMMT, respectively (modified MMT). Addition of 5% of modified clay has been found to increase the mechanical properties by 600% and 450% for MOMMT and C16-MMT, respectively. Dia et al. (2004) have prepared TPU clay nanocomposites by *in-situ* polymerization technique from MDI, PTMEG and 1,3-propylenediamine in DMF solvent. It has been observed that 1700% increase in elongation at break along with the increase in tensile strength and Young's modulus occur with only 2% CTAB modified montmorillinite.

Addition of modified clays has been found to increase the tensile strength by 2 fold as compared to the neat TPU [Chen et al. (2000); Ni et al. (2004, 2006); Song et al. (2003a)]. Young's modulus of the TPUCN has been found to increase with the

addition of modified nanoclays [Choi et al.(2005); Finnigan et al. (2004); Tien et al. (2001); Zheng et al. (2006)]. However, improved Young's modulus with reduced tensile strength and elongation at break upon the addition of clay has also been reported in the literature [Choi et al. (2006)].

Chen et al. (1999) have prepared polycaprolactam based TPU modified clay nanocomposite by *in-situ* preparation technique. An increase in elongation at break at lower clay content following a reverse effect at higher clay content has been observed. Decrease in H-bonding in the hard segment of TPU with the incorporation of modified nanoclays (nontethered) has been reported by Tien and Wei (2001a). However, it has been found to enhance the strength and modulus values compared to the neat TPU. Destruction of H-bonding in the hard segment of TPU due to the incorporation of tethered nanoclays has also been reported by Pattanayak and Jana (2005b). The destruction in H-bonding stems from the H-bond formation between the carbonyl group of the TPU and the –OH group present on the tail of the modifier to the clay. However, modulus and tensile strength has been found to be increased by 110 and 160%, respectively for the nanocomposite containing 5 wt% of Cloisite[®] 30B.

Reaction of the surface –OH group of the MMT with the isocyanate during *in-situ* synthesis, leading to an improvement in tensile strength and elongation at break has been reported by Zhang et al. (2003).

A comparison between the Cloisite[®] 30B, 25A, 15A and Na⁺MMT has been reported by Dan et al. (2006) with both ether and ester type of TPU. It has been observed that nanocomposites with Cloisite[®] 30B provided greater tensile properties as compared to those of the other types of clay. Higher degree of increase in tensile properties has been reported to be with ester type TPU as compared to the ether type

of TPUCN due to the higher degree of compatibility between the polymer and the modified nanoclay.

Tensile strength and elongation at break of the TPU remaining constant, an increase in the Young's modulus of TPUCN by 3.2 fold by the addition of 7% clay has been reported by Finnigan et al. (2004).

Effect of the modifier on the improvement in property of the TPU has been studied by Tien and Wei (2001b) by using three types of modifiers. Greater extent of improvement in tensile properties has been reported with the clay modified by trihydroxy ammonium ions as compared to those of clay modified with dihydroxy and monohydroxy ammonium ions.

The effect of modifier on the property of TPUCNs has also been studied by Cheng et al. (2006). Montmorillonite has been modified with CTAB to prepare OMMT. This OMMT has been further modified with MDI to prepare MOMMT. Improvement in tensile strength and tear strength has been reported in case of MOMMT as compared to OMMT with the addition of same amount of clay. However, elongation at break has been found to be decreased.

Pattnayak and Jana (2005c) have found an increase in tensile strength and elongation at break by 61% and 47%, respectively over the neat TPU by using Cloisite[®] 30B as a pseudo chain extender in the preparation of TPUCN derived from MDI, polypropylene glycol and 1,4-butanediol.

With the increase in the degree of exfoliation, the tensile strength and elongation at break has been found to increase. However, increasing the mixing time (to achieve greater exfoliation) for prolonged time is found to cause the degradation of TPU matrix [Meng et al. (2008)].

From the review of the above literature, it is observed that better properties are obtained when the degree of exfoliation of the clay platelets are higher. This is due to an increase in the mass to volume interaction between the clay and polymer in the exfoliated state of clay in polymer matrix which in turn is highly dependent on the type of modifier used.

1.5.3 Thermal Properties

Thermal stability of TPU is very important as its degradation commences at around 250-300 °C. TPU also possess two Tg's (one for the soft segment and another for the hard segment) due to its two-phase morphology. However, in most of the cases hard segment Tg is not observed due to the dominance of the soft segment and ordered hard domains. Thermal properties generally include the glass transition temperature, melting temperature, dynamic moduli and thermal stability. Overall, composition, molecular weight, hydrogen bonding and thermal history play vital roles towards the thermal properties of the TPUCNs.

Hard segment content remaining same, neat TPU and TPUCN have been found to register nearly similar glass transition temperatures (Tg) [Tien and Wei (2000)]. Tg of the TPU has not been changed with the modified clay acting as a pseudo chain extender [Moon et al. (2004)]. However, addition of small amount of tethered clay has been reported to increase the Tg of the hard segment by 44 °C [Tien and Wei (2002)]. Similarly, a 13 °C rise in Tg value of the soft segment with the addition of Cloisite[®] 20A has been reported by Zheng et al. (2006). Several researchers have reported an increase in Tg of TPUCNs with the increase in the amount of clay [Chen et al. (2000); Choi et al. (2005); Dia et al. (2004); Finnigan et al. (2004); Kim et al. (2005); Ni et al. (2004, 2006)]. Extent of sonication during the preparation of the TPUCN has been found not to have any influence on the Tg of the

nanocomposites [Choi et al. (2005)]. In contrast, a decrease in T_g and the heat capacity at glass transition temperature (ΔC_p) of the nanocomposites with the increase in the clay content has been reported by Seo et al. (2006). It has been reported that this decrease in ΔC_p is due to the increase in steric hindrance by the exfoliated clay layers. Decrease in ΔC_p with the increase in clay content has also been reported by Yao et al. (2000) and Barick and Tripathy (2010b). Lower T_g of the nanocomposite as compared to the neat TPU has been reported by Pattanayak and Jana (2005b) and Xiong et al. (2004).

TPU have been found to exhibit two stages of degradations during decomposition. The 1st stage of degradation corresponds to the degradation of the hard segment and the 2nd stage of degradation corresponds to the degradation of the soft segment [Petrovic et al. (1994); Shieh et al. (1999)].

TPUs generally have been found to commence degradation at a temperature of 250 °C. However, the major weight loss starts around 300 °C. But presence of the modifier in the interlayer gallery spacing has been observed to start degrading from 275 °C upto 325 °C [Chen et al. (1999); Gorrasi et al. (2005); Ma et al. (2001)]. Song et al. (2005a) have reported that hexadecyl trimethyl ammonium starts degrading at 200 °C and proceeds through the Hoffmann degradation mechanism leaving behind an acidic proton on the surface of clay which catalyses the initial degradation of the organic material within the clay. To avoid the confusion between the degradation of TPU and the modifier, generally 5% weight loss is taken into account as the onset of degradation. The same is reflected by an increase in thermal stability of TPUCN after the complete decomposition of the modifier as compared to that of the neat TPU [Chen et al. (1999); Chen-Yang et al. (2004); Gorrasi et al. (2005); Ma et al. (2001)]. Increase in the amount of clay from 1 to 5% has been reported to increase the thermal

stability of TPU by 12 to 34 °C, respectively by Tien and Wei (2000). The increase in thermal stability with an increase in the amount of modified MMT in the TPU matrix has also been reported by several researchers [Barick and Tripathy (2010a, b); Chang and An (2002); Chen et al. (2000); Finnigan et al. (2004); Kim et al. (2005); Ni et al. (2004, 2006)]. The improvement in thermal stability of the TPUCN has been found to be directly related to the degree of dispersion of the nanoclay in the TPU matrix [Choi et al. (2005)]. Enhancement of the thermal stability as well as flame retardant property of the TPUCN has been reported by Chen-Yang et al. (2004) and Song et al. (2003a). The thermal stability has been found to be enhanced by 25 °C with 5% clay content. The heat release rate (HRR) has also been found to decrease by 63% with the addition of 6% clay as compared to that of the neat TPU. However, HRR has been found to be decreased with further increase in the clay content.

1.5.4 Rheological Characteristics

Rheology plays a vital role to monitor the flow behavior under different conditions, e.g., shear rate, temperature, pressure, time etc. The rheological (rheometry - the measuring arm of rheology) and viscoelastic measurements on TPU are important at least for two reasons. Firstly, rheological techniques can be used as a noninvasive experimental tool (though indirect) for the investigation of the rich phase transition/relaxation behavior of this class of nanocomposites. Secondly, rheology could be useful to investigate the effect of phase transitions or relaxations on the processibility of the TPUCNs.

In most of the published work, viscoelastic property measurements of TPUs at higher temperatures have employed temperature-sweep mode in dynamic mechanical analysis (DMA) [Borgart et al. (1983); Kajiyama et al. (1969)]. But the limitation involved in this experiment is that it ends when the sample begins to flow.

Investigations on the rheological properties in the heating and cooling processes is important for polymer processing operations because TPU is mostly processed under high temperature followed by slow cooling to shape the final product. A direct consequence of the incorporation of nanoclay in molten TPUs is the significant change in their viscoelastic properties. Since, the linear dynamic rheological behavior of nanocomposites are sensitive to the structure, particle size, shape and surface characteristics of the silicate phase, the rheological tool is intensively used to assess the state of dispersion of nanoparticles in the molten state.

Addition of Cloisite[®] 30B to the TPU matrix [Meng et al. (2008)] has been found to increase both storage modulus and complex viscosity, especially in the terminal region. Storage modulus has been found to increase as a strong function of the degree of exfoliation of the nanoclays.

Viscosity of the TPUCN has been found to increase with the increase in clay content in the TPU matrix [Rhoney et al. (2004)]. This has been postulated to be due to the increased polymer-clay interaction. At low shear rate region, a yield stress with a shear thinning behavior has been observed. At high shear region, nanocomposites possess a rapid shear thinning behavior as compared to the neat TPU. Shear thinning behavior of the nanocomposites with modified nanoclays (Cloisite[®] 30B, 25A and 15A) have also been reported by Dan et al. (2006). However, Newtonian behavior has been observed with the neat TPU (both ether and ester based) and their nanocomposites with unmodified clay (within a frequency range of 0.1 to 100 rad/s).

The effect of three varieties of clay (unmodified MMT, Cloisite[®] 30B (tethered) and modified MMT (non-tethered)) on the dynamic rheological behavior of TPU matrix have been studied by Pattanayak and Jana (2005a). An increase in the storage modulus values has been observed with the addition of tethered and non-

tethered clays. However, lower storage modulus value with the unmodified clay has been ascribed to the presence of aggregates of clay in micron size scale and owing to poor clay-polymer interaction. The highest value of storage modulus has been found in case of the nanocomposite containing tethered clay. This has also been argued to be due to the greater interaction between the polymer and clay because of tethering.

1.6 TPU-Laponite clay Nanocomposites

Most of the studies on TPUCNs have been focused on MMT based clays whereas, such studies with Laponite based clays have not been frequently encountered in literature. This is because, clays having high aspect ratio (namely MMT and Cloisite[®]) possess the capability in enhancing the stiffness of the matrix even at small mass fractions due to their high surface area to volume ratios. However, owing to higher aspect ratio, probability of the particle to shield the matrix from straining is greater, which negatively influence the load transfer [Sheng et al. (2004)]. Consequently, this is detrimental to the elastic properties. This can be avoided by using clay with smaller aspect ratio. It has also been reported that reinforcement capabilities of the clay depend primarily on the finer dispersion of the clay in the matrix. In this regard, the type of clay used has little significance [Kuan et al. (2005a); Varghese et al. (2004); Zilg et al. (1999)].

The effect of particle size on the mechanical properties of the TPUs has been studied by Finnigan et al. (2005 and 2007). Clay has been found not to possess any observable effect on the microphase separation process of the TPU during both solution casting and annealing. It has also been found not to affect the morphological response of TPU to deformation regardless of the platelet size [Finnigan et al. (2005)]. Clay particles have been observed to increase the stiffness of TPU, especially at low strains, through mechanical restraintment and hydrodynamic effects. These effects

have been found to increase with the increased diameter of the clay particles. At intermediate strains microphase structure dominates and contribution due to clay is minimum at this stage. However, at high strain regions, clay particles can be well aligned to interact with individual segments. Hence, at higher strain clay can significantly influence the tensile properties of the nanocomposites. A lower platelet size has been found to impart better tensile properties as compared to the clay having higher diameter. This has been found to be due to the prominence in void formation with clay having larger diameter during alignment of clay particles [Finnigan et al. (2005)].

It has been observed that the stiffening effect is relatively less with the clay having smallest particle size (30nm) [Finnigan et al. (2007)]. This has been postulated to be due to reduced long range intercalation and molecular confinement along with ineffective stress transfer from matrix to filler. The permanent set and hysteresis value has also been found to be reduced with the clay of particle size ~30nm.

Thus, the aspect ratio of the clay, interaction between the TPU macromolecules and clay particles in combination with the state of dispersion of the clay are some of the important factors those can be ascertained to influence the properties. Based on this approach, TPU-Laponite clay nanocomposites have been prepared by Korley et al. (2006) and Liff et al. (2007) by using their unique solvent exchange approach. Unmodified Laponite RD is very difficult to disperse in common solvents like tetrahydrofuran (THF), dimethylformamide (DMF) and dimethyl acetamide (DMAc), in which, TPU is highly soluble. But Laponite in the unmodified stage can be easily dispersed in water. 1.5% solution has been prepared by mixing unmodified Laponite RD dispersed in water and subsequently the TPU solution in DMAc has also been prepared. Both were mixed together and sonicated for 1 hr,

before solution casting in an oven at 60 °C, with $\sim 0.02 \text{ m}^3\text{hr}^{-1}$ N_2 flow rate. By this process, complete exfoliation of the unmodified Laponite RD has been observed in the TPU matrix. An increase in initial modulus by 23 fold, 1.5 fold increase in ultimate strength (tensile strength) and 4 fold increase in toughness with 20% clay loading have been reported. Consequently, improvement in heat distortion temperature has also been claimed. This process has been found to lead unmodified Laponite RD to get preferentially associated with the more polar hard domains because of the higher surface energy of the unmodified clay.

However, few demerits like, decrease in onset of degradation temperature of the resultant TPUCNs, use of huge quantities of solvents during preparation, etc., limits this process. A very precise and controlled evaporation of solvent for the preparation of the nanocomposites is often difficult to achieve, which ultimately makes the process technically nonviable.

Later on, Polyurethane urea (PUU) clay nanocomposites have been prepared by Sormana et al. (2008) by *in-situ* synthesis technique using Laponite RD modified with monoamine and diamine based modifiers. The modification has been done by following the standard ion exchange process. A 3 fold increase in tensile strength and 1.4 fold improvement in elongation at break of the nanocomposites have been observed as compared to that of the neat PUU. Laponite with reactive functional groups (Laponite modified by diamine) have been found to impart better tensile strength to the PUU matrix as compared to that of the nontethered clay.

1.7 Summary of the Literature Review

Literature survey on TPU-clay nanocomposites reveals that most of the work carried out till date, encompasses the use of Montmorillonite (MMT) clay as the nanofiller (unmodified or modified). The key features for the improvement in

technical properties of the TPU lie on the dispersion of clay into the TPU matrix. In this regard, modifiers to the clay and the method of preparation of the nanocomposites play vital roles. Tethering of the clay and *in-situ* synthesis technique have been found to impart improved technical properties of the TPU. It has been observed that the dispersion of the nanoclay, rather than the size of the nanoclay, matters more for the improvement in technical properties of the TPU. It has also been reported that the matrix stiffening effect due to the use of clay possessing large aspect ratio can be greatly reduced by using clay with lower aspect ratios. This opens up a new area of research on the use of the nanoclay with smaller dimension like Laponite. Laponite has a well controlled dimension of 25-30 nm as against the 150-300 nm in diameter for MMT. Laponite is also chemically pure and free from impurities as compared to its naturally occurring MMT counterpart. The first attempt towards the use of Laponite RD (unmodified and modified) in the TPU and PUU matrix, respectively has paved the path for further exploration in this area.

1.8 Scope and Objectives

The detailed investigation on the structure-property relationship of the TPU-modified Laponite RD has not yet been fully explored till date. Thus, there is a wide scope for detail investigation in this area. Use of Laponite RDS (possessing larger number of sites for ionic modification) in TPU matrix has also remained an unexplored area. Use of dual modified Laponite RD has been established in other polymer matrices, but its consequence in the TPU matrix has remained untouched. Tethering of Laponite RD (with active functional groups) to make it more useful as a nanofiller in the preparation of TPUCNs by *ex-situ* method and to use it as a pseudo chain extender during the synthesis of TPUCNs by *in-situ* technique, have not been fully explored.

The thesis aims to explore the structure-property relationship between the TPU and the TPU-modified Laponite clay nanocomposites prepared following *ex-situ* and *in-situ* techniques by using various modified clays. The objectives of the thesis are manifold and are presented precisely below:

- To compare the effect of particle size, degree of dispersion and modifier type on the structure-property relationship of TPU-clay nanocomposites prepared by solution mixing technique. For this study, Cloisite 20A, Laponite RD modified by standard ion exchange process utilizing dodecylammonium ion (d) and cetyltrimethyl ammonium ion (c) are used.
- To study the effect of increased extent of ionic modification and effect of modifiers on the degree of dispersion and technical properties of the nanocomposites. For this study, Laponite RDS is modified with ‘d’ and ‘c’, respectively and then the modified clays are dispersed in TPU matrix by solution mixing technique.
- To establish the structure-property relationship between the covalently modified and dual modified Laponite RD (modified by ionic and covalent modification technique in two different routes) dispersed in the TPU matrix by solution mixing technique.
- To study the effect of tethering on the morphology and technical properties of the TPU-clay nanocomposites prepared by *ex-situ* and *in-situ* techniques.

1.9 References

- Alexandre M., Dubois P. (2000) Polymer-layered silicate nanocomposites: preparation, properties and uses of a new class of materials, *Material Science and Engineering* 28, 1-63
- Almdal K., Rodale J. H., Bates F. (1990) The order-disorder transition in binary mixtures of nearly symmetric diblock copolymers, *Macromolecules* 23, 4336-4338
- Barick A. K., Tripathy D. K. (2010a) Effect of organoclay on the morphology, mechanical, thermal, and rheological properties of organophilic montmorillonite nanoclay based thermoplastic polyurethane nanocomposites prepared by melt blending, *Polymer Engineering and Science* 50, 484-498
- Barick A. K., Tripathy D. K. (2010b) Thermal and dynamic mechanical characterization of thermoplastic polyurethane/organoclay nanocomposites prepared by melt compounding, *Material Science and Engineering A* 527, 812-823
- Bharadwaj R. K. (2001) Modeling the Barrier Properties of Polymer-Layered Silicate Nanocomposites, *Macromolecules* 34, 9189-9192
- Blumstein R., Blumstein A., Parikh K. K. (1974) Polymerization of monomolecular layers adsorbed on Montmorillonite: Cyclization in polyacrylonitrile and polymethacrylonitrile, *Applied Polymer Symposium* 25, 81-88
- Bonart R. (1968) X-ray investigations concerning the physical structure of cross-linking in segmented urethane elastomers, *Journal of Macromolecular Science Part B Physics* 2, 115-138
- Bonart R., Morbitzer L., Muller E. H. (1974) X-ray investigations concerning the physical structure of crosslinking in urethane elastomers. III. Common structure principles for extensions with aliphatic diamines and diols, *Journal of Macromolecular Science Part B Physics* 9, 447-461
- Bogart J. W. C. V., Gibson P. E., Cooper S. L. (1983) Structure-property relationships in polycaprolactone polyurethanes. *Journal of Polymer Science Part B: Polymer Physics* 21, 65-95
- Chang J. H., An Y. U. (2002) Nanocomposites of polyurethane with various organoclays: Thermomechanical properties, morphology, and gas permeability, *Journal of Polymer Science Part B: Polymer Physics* 40, 670-677
- Chen T. K., Tien Y. I., Wei K. H. (1999) Synthesis and characterization of novel segmented polyurethane/clay nanocomposite via poly(ϵ -caprolactone)/clay, *Journal of Polymer Science Part A Polymer Chemistry* 37, 2225-2233

Chen T. K., Tien Y. I., Wei K. H. (2000) Synthesis and characterization of novel segmented polyurethane/clay nanocomposites, *Polymer* 41, 1345-1353

Chang J. H., An Y. U. (2002) Nanocomposites of polyurethane with various organoclays: Thermomechanical properties, morphology, and gas permeability, *Journal of Polymer Science Part B: Polymer Physics* 40, 670-677

Cheng A., Wu S., Jiang D., Wu F., Shen J. (2006) Study of elastomeric polyurethane nanocomposites prepared from grafted organic-montmorillonite, *Colloid and Polymer Science* 284, 1057-1061

Chen-Yang Y. W., Yang H. C., Li G. J., Li Y. K. (2004) Thermal and anticorrosive properties of Polyurethane/clay nanocomposites, *Journal of Polymer Research* 11, 275-283

Choi M. Y., Anandhan S., Youk J. H., Baik D. H., Seo S.W., Lee H. S. (2006) Synthesis and characterization of in situ polymerized segmented thermoplastic elastomeric polyurethane/layered silicate clay nanocomposites, *Journal of Applied Polymer Science* 102, 3048-3055

Choi W. J., Kim S. H., Kim Y. J., Kim S. C. (2005) Synthesis of chain-extended organifier and properties of polyurethane/clay nanocomposites, *Polymer* 45, 6045-6057

Clough S. B., Schneider N. S., King A. O. (1968) Small-angle X-Ray scattering from polyurethane elastomers, *Journal of Macromolecular Science Part B Physics* 2, 641-648

Dan C. H., Lee M. H., Kim Y. D., Min B. H., Kim J. H. (2006) Effect of clay modifiers on the morphology and physical properties of thermoplastic polyurethane/clay nanocomposites, *Polymer* 47, 6718-6730

Dia X., Xu J., Guo X., Lu Y., Shen D., Zhao N., Luo X., Zhang X. (2004) Study on Structure and Orientation Action of Polyurethane Nanocomposites, *Macromolecules* 37, 5615-5623

Dieterich D., Schmelzer H. G. (1994) *Polyurethane Handbook*; Oertel G., Ed.: Hanser Publishers: Munich, Germany

Finnigan B., Casey P., Cookson D., Halley P., Jack K., Truss R., Martin D. (2007) Impact of controlled particle size nanofillers on the mechanical properties of segmented polyurethane nanocomposites, *International Journal of Nanotechnology* 4, 496-515

Finnigan B., Jack K., Campbell K., Halley P., Truss R., Casey P., Cookson D., King S., Martin D. (2005) Segmented Polyurethane Nanocomposites: Impact of Controlled Particle size Nanofillers on the Morphological Response to Uniaxial Deformation, *Macromolecules* 38, 7386-7396

- Finnigan B., Martin D., Halley P., Truss R., Campbell K. (2004) Morphology and properties of thermoplastic polyurethane nanocomposites incorporating hydrophilic layered silicates, *Polymer* 45, 2249-2260
- Gorrasi G., Tortora M., Vittoria V. (2005) Synthesis and physical properties of layered silicates/polyurethane nanocomposites, *Journal of Polymer Science Part B Polymer Physics* 43, 2454-2467
- Hepburn C. (1982) Polyurethane Elastomers, Applied Science Publisher: London
- Herrera N. N., Letoffe J. -M., Reymond J. -P., Bourgeat-Lami E. (2005) Silylation of laponite clay particles with monofunctional and trifunctional vinyl alkoxysilanes, *Journal of Materials Chemistry* 15, 863-871
- Herrera N. N., Letoffe J. -M., Putaux J. -L., David L., Bourgeat-Lami E. (2004) Aqueous dispersions of silane-functionalized Laponite clay platelets. A first step towards the elaboration of water-based polymer/clay nanocomposites, *Langmuir* 20(5), 1564-1571
- Herrera N. N., Putaux J. -L., Bourgeat-Lami E. (2006) Synthesis of polymer/Laponite nanocomposite latex particles via emulsion polymerization using silylated and cation exchanged Laponite clay platelets, *Progress in Solid State Chemistry* 34, 121-137
- Holden G., Kricheldorf H. R., Quirk R. P. (2004) Thermoplastic Elastomers, 3rd Edtn., Hanser: Munich, Germany
- Hu Y., Song L., Xu J., Yang L., Chen Z., Fan W. (2001) Synthesis of polyurethane/clay intercalated nanocomposites, *Colloid and Polymer Science* 279, 819-822
- Kajiyama T., MacKnight W. J. (1969) Relaxation in Polyurethanes in the glass transition region, *Journal of Rheology* 13, 527-546
- Kim D. S., Kim J. T., Woo W. B. (2005) Reaction kinetics and characteristics of polyurethane/clay nanocomposites, *Journal of Applied Polymer Science* 96, 1641-1647
- Kojima Y., Usuki A., Kawasumi M., Okada A., Fujushima A., Kurauchi T., Kamigaito O. (1993) Mechanical properties of Nylon-6 clay hybrid, *Journal of Material Research* 8, 1185-1189
- Korley L. T. J., Liff S. M., Kumar N., McKinley G.H., Hammond P.T. (2006) Preferential Association of Segment Blocks in Polyurethane Nanocomposites, *Macromolecules* 39, 7030-7036

Kuan H. C., Chuang W. P., Ma C. C. M. (2005a) Synthesis and characterization of a clay/ waterborn Polyurethane nanocomposite, *Journal of Material Science* 40, 179-185

Kuan H. C., Ma C. C. M., Chuang W. P., Su H. Y. (2005b) Hydrogen bonding, mechanical properties, and surface morphology of clay/waterborne polyurethane nanocomposites, *Journal of Polymer Science Part B Polymer Physics* 43, 1-12

Liff S. M., Kumar N., McKinley G. H. (2007) High-Performance elastomeric nanocomposites via solvent exchange processing, *Nature Material* 6, 76-83

Lu G., Kalyon M. (2003) Rheology and extrusion of medical grade thermoplastic polyurethane, *Polymer Engineering and Science* 43, 1863-1877

Ma J., Zhang S., Qi Z. (2001) Synthesis and characterization of elastomeric polyurethane/clay nanocomposites, *Journal of Applied Polymer Science* 82, 1444-1448

Ma J., Zhang S., Qi Z. (2001) Synthesis and characterization of elastomeric polyurethane/clay nanocomposites, *Journal of Applied Polymer Science* 82, 1444-1448

Meng X., Du X., Wang Z., Bi W., Tang T. (2008) The investigation of exfoliation process of organic modified montmorillonite in thermoplastic polyurethane with different molecular weights, *Composite Science and Technology* 68, 1815-1821

Moon S. Y., Kim J. K., Nah C., Lee Y. S. (2004) Polyurethane/montmorillonite nanocomposites prepared from crystalline polyols, using 1,4-butanediol and organoclay hybrid as chain extenders, *European Polymer Journal* 40, 1615-1621

Ni P., Li J., Suo J., Li S. (2004) Novel polyether polyurethane/clay nanocomposites synthesized with organic-modified montmorillonite as chain extenders, *Journal Applied Polymer Science* 94, 534-541

Ni P., Wang Q., Li J., Suo J., Li S. (2006) Novel polyether polyurethane/clay nanocomposites synthesized with organically modified montmorillonite as chain extenders, *Journal Applied Polymer Science* 99, 6-13

Nichetti D., Cossar S. (2005) Effect of molecular weight and chemical structure on phase transition of thermoplastic polyurethanes, *Journal of Rheology* 49, 1361-1376

Park M., Shim I. -K., Jung E. -Y., Choy J. -H. (2004) Modification of external surface of Laponite by silane grafting, *Journal of Physics and Chemistry of Solids* 65, 499-501

- Pattanayak A., Jana S. C. (2005a) Properties of bulk-polymerized thermoplastic polyurethane nanocomposites, *Polymer* 46, 3394-3406
- Pattanayak A., Jana S. C. (2005b) Synthesis of thermoplastic polyurethane nanocomposites of reactive nanoclay by bulk polymerization methods, *Polymer* 46, 3275-3288
- Pattanayak A., Jana S. C. (2005c) High-strength and low-stiffness composites of nanoclay-filled thermoplastic polyurethanes, *Polymer Engineering and Science* 45, 1532-1539
- Pattanayak A., Jana S. C. (2005d) Thermoplastic polyurethane nanocomposites of reactive silicate clays: effects of soft segments on properties, *Polymer* 46, 5183-5193
- Petrovic Z. S., Ferguson P. J. (1991) Polyurethane elastomers, *Progress in Polymer Science* 16, 695-836
- Petrovic Z. S., Zavargo Z., Flynn J. F., Macknight W. J. (1994) Thermal degradation of segmented polyurethanes, *Journal Applied Polymer Science* 51, 1087-1095
- Rehab A., Salahuddin N. (2005) Nanocomposite materials based on polyurethane intercalated into montmorillonite clay, *Material Science and Engineering A* 399, 368-376
- Rhoney I., Brown S., Hudson N. E., Pethrick R. A. (2004) Influence of processing method on the exfoliation process for organically modified clay systems. I. Polyurethanes, *Journal Applied Polymer Science* 91, 1335-1343
- Ryan A. J., Macosko C. W., Bras W. (1992) Order-disorder transition in a block copolyurethane, *Macromolecules* 25, 6277-6283
- Senich G. A., Macknight W. J. (1980) Fourier Transform Infrared Thermal Analysis of a Segmented Polyurethane, *Macromolecules* 13, 106-110
- Seo W. J., Sung Y. T., Han S. J., Kim Y. H., Ryu O. H., Lee H. S., Kim W. N. (2006) Synthesis and properties of polyurethane/clay nanocomposite by clay modified with polymeric methane diisocyanate, *Journal Applied Polymer Science* 101, 2879-2883
- Seymour R. W., Estes G. M., Cooper S. L. (1970) Infrared Studies of Segmented Polyurethane Elastomers. I. Hydrogen Bonding, *Macromolecules* 3, 579-583
- Shneider N. S., Paiksung C. S. (1977) Transition behavior and phase segregation in TDI polyurethanes, *Polymer Engineering and Science* 17, 73-80

Sheng N., Boyce M. C., Parks D. M., Rutledge G. C., Abes J. I., Cohen R. E. (2004) Multiscale micromechanical modeling of polymer/clay nanocomposites and the effective clay particle, *Polymer* 45, 487-506

Shieh Y. T., Chen H. T., Liu K. H., Twu Y. K. (1999) Thermal degradation of MDI-based segmented polyurethanes, *Journal Polymer Science Part A: Polymer Chemistry* 37, 4126-4134

Solomon D. H. (1968) Clay Minerals as Electron Acceptors and/or Electron Donors in Organic Reactions, *Clays and Clay Mineral* 16, 31-39

Song L., Hu Y., Li B. G., Wang S. F., Fan W. C., Chen Z. Y. (2003a) A Study on the Synthesis and Properties of Polyurethane/Clay Nanocomposites, *International Journal of Polymer Analysis and Characterization* 8, 317-326

Song L., Hu Y., Tang Y., Zhang R., Chen Z., Fan W. (2005a) Study on the properties of flame retardant polyurethane/organoclay nanocomposite, *Polymer Degardation and Stability* 87, 111-116

Song M., Hourston D. J., Yao K. J., Tay J. K. H., Ansarifar M. A. (2003b) High performance nanocomposites of polyurethane elastomer and organically modified layered silicate, *Journal Applied Polymer Science* 90, 3239-3243

Song M., Xia H. S., Yao K. J., Hourston D. J. (2005b) A study on phase morphology and surface properties of polyurethane/organoclay nanocomposite, *European polymer Journal* 41, 259-266

Sormana J. L., Chattopadhyay S., Meredith J. C. (2008) Mechanical and thermal properties of Poly(urethaneurea) nanocomposites prepared with diamine-modified Laponite, *Journal of Nanomaterials* 2008, article ID 869354, 9 pages

Srichatrapimuk V. W., Cooper S. L. (1978) Infrared thermal analysis of polyurethane block polymers, *Journal of Macromolecular Science Part B Physics* 15, 267-311

Sung C. S. P., Hu C. B., Wu C. S. (1980a) Properties of Segmented Poly(urethaneureas) Based on 2,4-Toluene Diisocyanate. 1. Thermal Transitions, X-ray Studies, and Comparison with Segmented Poly(urethanes), *Macromolecules* 13, 111-116

Sung C. S. P., Smith T. W., Sung N. H. (1980b) Properties of Segmented Polyether Poly(urethaneureas) Based of 2,4-Toluene Diisocyanate. 2. Infrared and Mechanical Studies, *Macromolecules* 13, 117-121

Takeichi T., Zeidam R., Agag T. (2002) Polybenzoxazine/clay hybrid nanocomposites: influence of preparation method on the curing behavior and properties of polybenzoxazines, *Polymer* 43, 45-53

Theng K. B. G. (1974) *The Chemistry of Clay-Organic Reactions*, Adam Hilger: London

Theng K. B. G. (1979) *Formation and properties of Clay-Polymer Complex*, Elsevier: Amsterdam

Tien Y. I., Wei K. H. (2001a) Hydrogen bonding and mechanical properties in segmented montmorillonite/polyurethane nanocomposites of different hard segment ratios, *Polymer* 42, 3213-3221.

Tien Y. I., Wei K. H. (2002) The effect of nano-sized silicate layers from montmorillonite on glass transition, dynamic mechanical, and thermal degradation properties of segmented polyurethane, *Journal Applied Polymer Science* 86, 1741-1748

Tien Y. I., Wei K. H. (2000) Thermal transition of Montmorillonite/Polyurethane Nanocomposites, *Journal of Polymer Research* 7, 245-250.

Tien Y. I., Wei K. H. (2001b) High-Tensile-Property Layered Silicates/Polyurethane Nanocomposites by Using Reactive Silicates as Pseudo Chain Extenders, *Macromolecules* 34, 9045-9052

Torro-palau A., Fernandez-garcia J. C., Orgiles-barcelo A. C., Pastor-blas M. M., Martin-martinez J. M. (1997) Characterization of solvent-based polyurethane adhesives containing sepiolite as a filler. Rheological, mechanical, surface and adhesion properties, *Journal of Adhesion Science and Technology* 11, 247-262

Troughton M. J. (2008) *Handbook of Plastics Joining: A practical Guide*, 2nd Edition, William Andrew Inc.: NY, USA

Usuki A., Kojima Y., Kawasumi M., Okada A., Fujushima A., Kurauchi T., Kamigaito O. (1993) Synthesis of Nylon-6 clay hybrid, *Journal of Material Research* 8, 1179-1184

Varghese S., Gatos K. G., Apostolov A. A., Karger-Kocsis J. (2004) Morphology and mechanical properties of layered silicate reinforced natural and polyurethane rubber blends produced by latex compounding, *Journal Applied Polymer Science* 92, 543-551

Velankar S., Cooper S. L. (1998) Microphase Separation and Rheological Properties of Polyurethane Melts. 1. Effect of Block Length, *Macromolecules* 31, 9181-9192

Wang Z., Pinnavaia T. J. (1998) Nanolayer Reinforcement of Elastomeric Polyurethane, *Chemistry of Materials* 10, 3769-3771

Wheeler P. A., Wang J., Baker J., Mathias L. J. (2005) Synthesis and Characterization of Covalently Functionalized Laponite Clay, *Chemistry of Materials* 17, 3012-3018

Wheeler P. A., Wang J., Mathias L. J. (2006) Poly(methyl methacrylate)/Laponite Nanocomposites: Exploring Covalent and Ionic Clay Modifications, *Chemistry of Materials* 18, 3937-3945

William G. E., Aldo B. A., Jinwen Z. (2005) Polymer nanocomposites: Synthetic and natural fillers A Review, *Maderas Ciencia y tecnologia* 7, 159-178

Woods G. (1990) the ICI Polyurethanes Book, John Wiley & Sons: New York, USA

Xia H., Shaw S. J., Song M. (2005) Relationship between mechanical properties and exfoliation degree of clay in polyurethane nanocomposites, *Polymer International* 54, 1392-1400

Xia H., Song M. (2006) Intercalation and exfoliation behaviour of clay layers in branched polyol and polyurethane/clay nanocomposites, *Polymer International* 55, 229-235

Xiong J., Liu Y., Yang X., Wang X. (2004) Thermal and mechanical properties of polyurethane/montmorillonite nanocomposites based on a novel reactive modifier, *Polymer Degradation and Stability* 86, 549-555

Xiong J., Zheng Z., Jiang H., Ye S., Wang X. (2007) Reinforcement of polyurethane composites with an organically modified montmorillonite, *Composites Part A* 38, 132-137

Yao K. J., Song M., Hourtson D. J., Luo D. Z. (2000) Polymer/layered clay nanocomposites: 2 polyurethane nanocomposites, *Polymer* 43, 1017-1020

Yoon P. J., Han C. D. (2000) Effect of Thermal History on the Rheological Behavior of Thermoplastic Polyurethanes, *Macromolecules* 33, 2171-2183

Zhang X. M., Xu R. J., Wu Z. G., Zhou C. X. (2003) The synthesis and characterization of polyurethane/clay nanocomposites, *Polymer International* 52, 790-794.

Zheng J., Ozisik R., Siegel R. W. (2006) Phase separation and mechanical responses of polyurethane nanocomposites, *Polymer* 47, 7786-7794

Zilg C., Thomann R., Mulhaupt R., Finter J. (1999) Polyurethane Nanocomposites Containing Laminated Anisotropic Nanoparticles Derived from Organophilic Layered Silicates, *Advanced Materials* 11, 49-52

CHAPTER 2

EXPERIMENTAL

2.1 Materials Used

2.1.1 Thermoplastic Polyurethane (TPU)

Commercially available Thermoplastic Polyether Polyurethane (trade name Desmopan KU2 8600E) was kindly provided by Bayer Materials Science Ltd., Chennai, India. It was prepared from Poly tetramethylene glycol (PTMEG), 4,4'-Methylenebis(phenyl isocyanate) (MDI) and 1,4- butanediol (BD). It has a specific gravity of 1.11 and molecular weight of $\overline{Mn} = 60,000$ gms per gm mole (PDI: 2.2).

2.1.2 Nanoclays

Cloisite[®] 20A, unmodified Laponite RD and Laponite RDS grades of clay were purchased from the Southern Clay Ltd., Mumbai, India. The details about the nanoclays used are mentioned in Table 2.1.

Table 2.1: Details about the nanoclays used in this work

Properties	Cloisite [®] 20A	Laponite RD	Laponite RDS
Physical Appearance	Grey Powder	Free Flowing White Powder	Free Flowing White Powder
Bulk Density	1.8 gm/cm ³	1.0 gm/cm ³	1.0 gm/cm ³
Platelet Size	150-250 nm	25-30 nm	25-30 nm
Chemical Composition	$M_x(Al_{4-x}Mg_x) \cdot Si_8O_{20}(OH)_4$	$M_x(Mg_{6-x}Li_x) \cdot Si_8O_{20}(OH)_4$	$M_x(Mg_{6-x}Li_x) \cdot Si_8O_{20}(OH)_4 \cdot Na_4P_2O_7$
Exchangable Na ⁺ ion	Na ⁺ ion already exchanged with dimethyl dehydrogenated tallow ammonium ion	70 mequ / 100gm	140 mequ / 100gm

2.1.3 Other Chemicals

Other Chemicals used in this work and their properties are presented in Tables

2.2 to 2.5.

Table 2.2: Monomers and catalyst used in the synthesis of TPU

Materials	Typical Data	Unit	Value	Sources
4,4'-Methylenebis (phenyl isocyanate) (MDI)	Molecular Weight	a.m.u.	250.3	Sigma Aldrich, USA
	Melting Point	°C	42.0-45.0	
	Boiling Point	°C	200.0	
	Density	gm/cm ³ at 25 °C	1.180	
Terathane-1000 (PTMEG)	Molecular Weight (\overline{Mn})	gms per gm mole	1000.0	Sigma Aldrich, USA
	Melting Point	°C	25.0-33.0	
	Density	gm/cm ³ at 25 °C	0.974	
1,4-Butanediol (1,4-BD)	Molecular Weight	a.m.u.	90.1	Sigma Aldrich, USA
	Melting Point	°C	16.0	
	Boiling Point	°C	230.0	
	Density	gm/cm ³ at 25 °C	1.017	
Dibutyltin dilaurate (DBTDL)	Molecular Weight	a.m.u.	631.6	Sigma Aldrich, USA
	Density	gm/cm ³ at 25 °C	1.066	

Table 2.3: Modifiers used for the modification of Laponite

Materials	Typical Data	Unit	Value	Sources
Dodecyl amine	Molecular Weight	a.m.u.	185.4	Sigma Aldrich, USA
	Melting Point	°C	27.0-29.0	
	Density	gm/cm ³ at 25 °C	0.806	
Cetyltrimethyl ammonium bromide (CTAB)	Molecular Weight	a.m.u.	364.5	Sigma Aldrich, USA
	Melting Point	°C	250.0	
Octyl trimethoxy silane (OS)	Molecular Weight	a.m.u.	234.4	Sigma Aldrich, USA
	Density	gm/cm ³ at 25 °C	0.907	
3-mino propyl triethoxy silane (AP)	Molecular Weight	a.m.u.	221.4	Sigma Aldrich, USA
	Density	gm/cm ³ at 25 °C	0.946	

Table 2.4: Other chemicals used and their properties

Materials	Typical Data	Unit	Value	Sources
Concentrated hydrochloric acid (HCl) 37% in water	Molecular Weight	a.m.u.	36.5	Sigma Aldrich, USA
	Density	gm/cm ³ at 25 °C	1.200	
	Solution in water	%	37	
Sodium metal	Molecular Weight	a.m.u.	23.0	Merck, Germany
	Melting Point	°C	97.8	
Benzophenone	Molecular Weight	a.m.u.	182.0	Loba Chemie, India
	Melting Point	°C	47.0-51.0	

Table 2.5: Solvents used and their properties

Materials	Typical Data	Unit	Value	Sources
Tetrahydrofuran (THF)	Molecular Weight	a.m.u.	72.1	Merck, Germany
	Melting Point	°C	-108.0	
	Boiling Point	°C	65.0-67.0	
	Density	gm/cm ³ at 25 °C	0.889	
Methanol	Molecular Weight	a.m.u.	32.0	Merck, Germany
	Melting Point	°C	-98.0	
	Boiling Point	°C	64.7	
	Density	gm/cm ³ at 25 °C	0.791	
Toluene	Molecular Weight	a.m.u.	92.1	Merck, Germany
	Melting Point	°C	-93.0	
	Boiling Point	°C	110.0	
	Density	gm/cm ³ at 25 °C	0.865	

* All the solvents used here were of analytical grades

2.2 Modification of Nanoclays

Unmodified clays were dried at 90 °C in a vacuum oven for 12 hrs prior to modification.

2.2.1 Ionic Modification of Laponite

Laponite RD (L) and RDS (LS) were modified with dodecyl ammonium chloride (an adduct prepared from the reaction between dodecyl amine and concentrated HCl) (d) and cetyltrimethyl ammonium bromide (c), by using the standard ion exchange process to increase the interlayer spacing and to enhance organophilic nature of the clay platelets.

Desired amounts of the surfactant (dodecylamine hydrochloride or cetyltrimethyl ammonium bromide) were dissolved in de-ionized (DI) water to

prepare 1% solution. The solution was heated to 60 °C. To this solution 1% dispersion of Laponite RD or RDS (heated to 60 °C) were added slowly for a period of one hour. The mixture was further stirred for 12 hrs at 60 °C. It was then centrifuged at 10,000 rpm followed by repeated washings with DI water till complete removal of the halide ions (monitored by AgNO₃ solution). Then, it was vacuum dried and made into powder in a mortar pastel. It was ultrasonicated for half an hour in THF for further deagglomeration. Then the THF was evaporated and the clay powder was dried. The dried mass was powdered and then sieved (325 mesh size) to get rid of the large agglomerates.

Desired amounts of surfactants for Laponite RD and Laponite RDS for ionic modifications are given in equation 2.1 and equation 2.2, respectively:

$$\text{Amount of surfactant for RD} = \frac{2.8 \times 1.2}{31 \times 100} \times W \times M \quad \dots\dots\dots(2.1)$$

$$\text{Amount of surfactant for RDS} = \frac{5.6 \times 1.2}{31 \times 100} \times W \times M \quad \dots\dots\dots(2.2)$$

where, 2.8 and 5.6 are the percentage equivalent of Na₂O present in Laponite RD and RDS, respectively. 1.2 is the number of equivalents of surfactant taken (with respect to total exchangeable sodium ions in clay), 31 is the equivalent weight of the replaceable sodium ion present, W is the amount of clay in gms to be modified and M is the molecular weight of the surfactant.

2.2.2 Covalent Modification of Laponite

Laponite RD was dispersed in dry toluene (dried over pressed sodium metal) in a two neck round bottomed flask (RB) under nitrogen atmosphere. Calculated amount of silane (octyl trimethoxy silane) was added to it and the mixture was refluxed for 6 hrs. The solvent was dried and then the excess amount of silane along

with the alcohol (methanol/ethanol obtained as byproduct during modification) were extracted by a soxhlet extractor using toluene as solvent for 12 hrs.

2.2.3 Dual Modification of Laponite

a. Covalent Modification followed by Ionic Modification

The covalently modified Laponite RD (as mentioned in section 2.2.2) was further modified by the same procedure as described in section 2.2.1 except the fact that in this case the medium was 1:1 solution of DI water and acetone in place of only DI water.

b. Ionic Modification followed by Covalent Modification

The ionically modified Laponite RD (as mentioned in section 2.2.1) was modified again by using covalent modification technique as described earlier using the same procedure as described in section 2.2.2. Designations of the modified nanoclays are given in Table 2.6.

Table 2.6: Nomenclature of the modified nanoclays

Designation	Details	Designation	Details
dL	Laponite RD modified by dodecyl ammonium chloride	OSL	Laponite RD modified by OS
cL	Laponite RD modified by cetyltrimethyl ammonium bromide	OScL	OSL modified by cetyltrimethyl ammonium bromide
dLS	Laponite RDS modified by dodecyl ammonium chloride	cOSL	cL modified by OS
cLS	Laponite RDS modified by cetyltrimethyl ammonium bromide	cAPL	cL modified by AP
C	Montmorillonite modified by dimethyl dehydrogenated tallow quaternary ammonium chloride (Cloisite [®] 20A)		

2.3 Preparation of nanocomposites

2.3.1 Solution Mixing Technique

A 20% solution of TPU was first prepared in THF solvent. Calculated amount of nanoclay (C, dL, cL, dLS, cLS, OSCL, cOSL or cAPL) was mixed with THF and stirred under ultrasonic vibration for 30 min and then added slowly to the TPU solution, maintaining gentle stirring. Stirring was continued for further 15 min. The mixture was sonicated for 15 min more to obtain a homogeneous dispersion of clay in the polymer solution. It was then cast on a petridis and allowed to dry. The solvent got evaporated slowly at the room temperature. After complete removal of the solvent, the sample was kept in a vacuum oven at 70 °C till constant weight. Control polyurethane sample was also prepared following the same procedure excluding the addition of nanoclay to accomplish a better comparison. The solution cast films (of the neat TPU and nanocomposites containing 1, 3, 5 and 7% clay, respectively) were taken directly for further study.

2.3.2 Synthesis of TPU

PTMEG was dried in a vacuum oven at 70 °C for 12 hrs prior to use. Calculated amount of PTMEG (6-7 gms) were taken in a dry 3 neck RB under dry nitrogen atmosphere. 0.1% DBTDL catalyst (based on the weight of PTMEG taken) was added to it and stirred at 50 °C and at 850 rpm speed by using a SCOTT magnetic stirrer (model SLR, SCHOTT Instruments GmbH, Germany). 3.5 equivalent of MDI (based on the weight of PTMEG taken) mixed with THF was added dropwise for one hour. After complete addition of MDI, the mixture was allowed to stir for additional 2 hrs at 50 °C, to prepare the **prepolymer**.

2.35 equivalent of 1,4-butanediol was added to the prepolymer and further stirred at 50 °C at 1000 rpm speed for a period of 2 hrs to prepare the final TPU. The

mixture was then purified by precipitating in methanol followed by repeated washings. The precipitate was then dried in a vacuum oven at 60 °C.

The TPU so prepared was mixed with THF to prepare a solution of 10% concentration. It was sonicated for about 30 min and then cast on a petridish. THF was evaporated at room temperature followed by vacuum drying at 70 °C and then molded into sheet under pressure (at 170 °C and at 5 MPa pressure followed by slow cooling) before further characterization.

2.3.3 Preparation of TPUCN by *Ex-situ* Technique

Calculated amount of modified nanoclay was sonicated in dry THF for a period of 30 min and then added to the already prepared 10% solution of the TPU prepared following the procedure as described in Section 2.3.2. The mixture was again stirred for another 15 min and then sonicated for 30 min and cast on a petridish. The solvent was initially allowed to evaporate at room temperature and then finally at 70 °C in a vacuum oven till constant weight. The composite was molded into thin sheets at 170 °C under a pressure (of 5 MPa followed by slow cooling) before further characterization.

2.3.4 Preparation of TPUCN by *In-situ* Technique

Calculated amount of modified clay was dispersed in dry THF by sonicating for a period of 30 min in a sealed container under nitrogen atmosphere and then mixed with the prepolymer solution prepared according to the procedure mentioned in section 2.3.2 at 50 °C. The mixture was stirred for another 15 min and sonicated for 30 min for homogeneous dispersion of the nanoclay. Then 2.35 equivalent of 1,4-BD was added to the prepolymer-nanoclay mixture which was further stirred for a period of 2 hrs at 50 °C and at 1000 rpm to prepare the TPUCN. The reaction mixture was poured into methanol to precipitate the nanocomposite which was washed repeatedly

with methanol to obtain the final TPUCNs. The composite was first dried at room temperature followed by final drying in a vacuum oven at 70 °C till constant weight. The composite was molded into thin sheets under pressure (at 170 °C and at 5 MPa pressure followed by slow cooling) before further characterization. The nomenclatures of the various nanocomposites prepared are given in Table 2.7.

Table 2.7: Nomenclature of the nanocomposites

Designation	Details
S0	Neat TPU (commercial) prepared by solution mixing process
PU	In house prepared TPU molded at 170 °C
S	Nanocomposite prepared by Solution mixing technique
E	Nanocomposite prepared by <i>Ex-situ</i> technique
I	Nanocomposite prepared by <i>In-situ</i> technique
TPUCN	Polyurethane clay nanocomposite
weight % of clay (1, 3, 5 etc.)	
<p>Preparation method of the nanocomposite ← Axy → types of clay</p> <p>Example:</p> <p>S5dL = Nanocomposite prepared by solution mixing technique with 5% of dL</p> <p>E3cOSL = Nanocomposite prepared by <i>Ex-situ</i> technique with 3% of cOSL</p> <p>I1cAPL = Nanocomposite prepared by <i>In-situ</i> technique with 1% of cAPL</p>	
<p>General representation of the nanocomposites based on a particular type of clay:</p> <p>Preparation method of the nanocomposite ← Ay → types of clay</p> <p>Example:</p> <p>SC = Polyurethane clay nanocomposite containing Cloisite® 20A prepared by Solution mixing technique</p> <p>EcOSL = Polyurethane clay nanocomposite containing cOSL prepared by <i>Ex-situ</i> technique</p> <p>IcAPL = Polyurethane clay nanocomposite containing cAPL prepared by <i>In-situ</i> technique</p>	

2.4 Characterization Techniques Adopted

2.4.1 Fourier Transform Infrared Spectroscopy (FTIR)

A Perkin Elmer FTIR Spectrophotometer of resolution 4 cm^{-1} , was used to study the modification of nanoclay. The clay samples were ground with KBr salt (FTIR grade) and made into pellets under pressure and used for the analysis. All the measurements were carried out in the wave number range of $4000\text{-}400\text{ cm}^{-1}$.

2.4.2 Solid State NMR Spectroscopy

^{13}C and ^{29}Si solid state Nuclear magnetic resonance spectroscopy was conducted on a Bruker instrument AV 300 spectrophotometer operating at 75.46 and 59.6 MHz, respectively in the magic angle cross polarization mode.

2.4.3 X-Ray Diffraction (XRD) Studies

Wide angle XRD (WAXRD) study in the lower angular range between 2 and 10 degree 2θ was performed to study the modification of clay and dispersion of nanoclay in the TPU matrix. All the samples were dried at $70\text{ }^{\circ}\text{C}$ in a vacuum oven prior to the experiment. The experiment was performed on a Philips Panalytica X-ray diffractometer (model: XPert Pro) using Cu target ($\text{Cu K}\alpha$) and Ni filter at a scanning rate of 0.001 s^{-1} operating at a voltage of 40 kV and 30 mA beam current. The distance from the detector to the sample was 177 mm. The incident slit used was $\frac{1}{4}$ mm and diffracted slit was 1 mm.

WAXRD in the higher angular range was performed with the same instrument using Cu target ($\text{Cu K}\alpha$) and Ni filter at a scanning rate of 0.003 s^{-1} between 10 to 50° 2θ operating at a voltage of 40 kV and with a beam current of 30 mA to study the effect of clay on the semi-crystalline morphology of TPU.

2θ values could be reproduced within $\pm 0.5\%$.

2.4.4 Transmission Electron Microscopy (TEM)

The TPUCN were cut in to 50 nm thick sections by means of a LEICA ULTRACUT UCT (Austria) microtome equipped with a diamond knife. Preparation of the section was conducted at 1 mm/s knife speed at approximately -60 °C. The microtomed samples were placed over 300 mesh size copper grid and scanned under the electron beam accelerated by 200 kV at different magnifications. Bulk morphology of the clay in the TPU matrix was studied by using JEOL JEM 2100 high resolution Transmission Electron Microscope (TEM).

2.4.5 Field Emission Scanning Electron Microscopy (FESEM)

Bulk morphology of the nanocomposites was studied using a FESEM of Carl Zeiss SMT pvt. Ltd., Germany make, having model number Supra 40. The sample was prepared by removing ~30 nm layer from the 1 mm thick sample surface at -60 °C using a LEICA ULTRACUT UCT (Austria) microtome machine equipped with a diamond knife (at a speed of 0.1 mm/s) followed by auto sputter coating with gold.

2.4.6 Atomic Force Microscopy (AFM)

The bulk morphology of the nanocomposites was also studied by AFM using model Multiview 1000TM, of Nanonics Imaging Ltd., Israel. Topographic height and phase images were recorded in the Tapping mode. The samples were microtomed at room temperature so that the more elastic part of the samples will protrude to a higher elevation.

2.4.5 Differential Scanning Calorimetry (DSC)

The change in T_g and crystalline morphology of TPU and TPUCNs were studied by a Differential Scanning calorimeter (DSC) using model DSC Q100 V8.1 of TA instruments, USA make. The samples were sealed inside aluminium pans and

scanned under the N₂ atmosphere at a heating rate of 10 °C/min from -75 to +250 °C. The percent error associated with the measurements of the characteristic temperatures was within ± 1%.

2.4.6 Thermogravimetric Analysis (TGA)

Thermal stability and degradation kinetics of the TPUCN as well as quantification of the alkyl groups incorporated into the modified nanoclays were analyzed by TGA using TGA Q50 V6.1 of TA instruments, USA make, in N₂ environment in the temperature range from ~50-800 °C, at a heating rate 20 °C/min. The percent error associated with the measurements was within ± 2%.

2.4.7 Dynamic Mechanical Analysis (DMA)

Dynamic mechanical properties of the composites were analyzed by DMA using DMA 2980 V1.7B of TA instrument, USA make in the tension mode. The samples were subjected to a sinusoidal displacement with an amplitude of 0.1% strain at a frequency of 1 Hz from -75 to 100 °C. The heating rate of the sample was 5 °C/min. Storage modulus, loss modulus and damping factor ($\tan \delta_{\max}$) were measured for each sample in above mentioned temperature range. The percent error associated with the measurements was within ± 1%.

2.4.8 Rubber Process Analyzer (RPA)

Dynamic rheological behavior of the TPUCN were studied with the help of a rubber process analyzer, model RPA-2000 of Alpha Technologies, USA make. Strain sweep experiments were carried out at 40 °C and 140 °C, respectively at 0.5 Hz frequency. Strain sweep at 40 °C was performed for evaluating the changes in linear viscoelastic properties due to the addition of modified clay particles. Whereas, strain sweep at 140 °C was carried out only to measure the linear viscoelastic region (LVR). The percent error associated with this experiment was within ± 2%. Forward

temperature sweep experiment was carried out within the temperature range from 130 to 220 °C to access the dynamic rheological behavior at a constant frequency of 0.5 Hz and at 1% strain. The average variation in storage modulus and viscosity was within $\pm 2\%$. Reverse temperature sweep was also conducted by cooling the samples from 180 °C to 40 °C at the cooling rate of 3 °C/min at a constant frequency of 0.5 Hz and 1% strain. The average variation in storage modulus and viscosity was within $\pm 3\%$. Frequency sweep (0.033-30 Hz) was carried out at two different temperatures (140 and 170 °C) at 1% strain which was found to be within the linear viscoelastic region (LVR) for the matrix. The two temperatures were selected relying on the DSC thermogram (corresponding to the destruction of the short range and long range ordering; semi-crystalline melting and final hard segment melting, respectively). The percent error associated with the dynamic viscosity and storage modulus measurements were within $\pm 1\%$ and $\pm 2\%$ at 140 and 170 °C, respectively. Stress relaxation experiment was carried out at 120 °C to access the elastic to viscous response of the nanocomposites at a temperature close enough for the destruction of the short range ordering in the hard domains. In stress relaxation, the samples were deformed by 69.75% shear strain and the stress decay was monitored over 120 s (with a preheat time of 60 s). The percentage errors associated with the stress relaxation experiment was within $\pm 2\%$.

In all the cases, the samples were loaded once the required temperature is reached and samples were equilibrated before the specific test.

2.4.9 Tensile Property Studies

Tensile strength, elongation at break and tensile modulus of the neat TPU and TPUCN were determined by using Hounsfield Universal Testing Machine (Model No. H25KS) of Hounsfield, UK, make. The testing was performed at 25 °C as per

ASTM D 638 at a deformation rate of 500 mm/min. The results reported are based on the average values of the results of five samples. The average variations in tensile strength, elongation at break and tensile modulus were within $\pm 2\%$, $\pm 4\%$ and $\pm 0.5\%$, respectively.

CHAPTER 3

CHARACTERIZATION OF MODIFIED NANOCCLAYS

Different parts of this chapter have been published in:

Designed Monomers and Polymers 11 (2008) 395

Journal of Polymer Science Part B: Polymer Physics 46 (2008) 2341

Journal of Applied Polymer Science 115 (2010) 558

Advanced Science Letters (In press) 4 (2011) 1

3.1 Introduction

The unfavourably high surface energy of the unmodified nanoclays makes them incompatible with most of the non-polar polymers. Replaceable Na^+ ions in the interlayer gallery spacing of the clay platelets and the silanol $-\text{OH}$ groups on the edge of the nanoclays provide sites for modification with suitable organic modifiers. Modification of the nanoclays not only renders the clay surface organophilic but also increases the gallery spacing. Either ionic (e.g., by replacing the Na^+ ions with alkyl ammonium or alkyl phosphonium ions) [Herrera et al. (2006); Ni et al. (2004, 2006); Tien and Wei (2001, 2002)] or covalent (e.g., by reacting surface $-\text{OH}$ groups with alkyl silanes) [Herrera et al. (2004, 2005); Park (2004); Wheeler (2005)] modification are found to be of common practice for the reduction in the surface energy. However, use of dual modified (both ionic and covalently modified) nanoclay is rarely practiced [Borsacchi (2007); Wang et al. (2007); Wheeler et al. (2006)]. Modified Montmorillonites (trade name Cloisite[®]) are most frequently being used among the nanoclays. However, Laponite is rarely used in this regard, especially in the TPU matrix. Laponite is commercially available only in the unmodified state. This chapter deals with the characterization of the modified nanoclays (modified Laponite and Cloisite[®] 20A).

3.2 FTIR Studies of Clay with and without Modification

3.2.1 Ionic Modification

A comparison between the FTIR spectra of unmodified Laponite RD and its modified counterparts (modified by dodecylammonium chloride and cetyltrimethyl ammonium bromide) is shown in Fig. 3.1. New peaks in the FTIR spectrum are observed at 2927 cm^{-1} corresponding to asymmetric C-H_{str} , 2855 cm^{-1} corresponding to symmetric C-H_{str} and 1471 cm^{-1} corresponding to C-H_{def} vibration in the modified

clay as compared to the unmodified one. This confirms the presence of alkyl amine group in the clay, after modification. The peak at 3683 cm^{-1} due to N-H_{str} , further confirms the presence of alkyl amine group that is incorporated after modification.

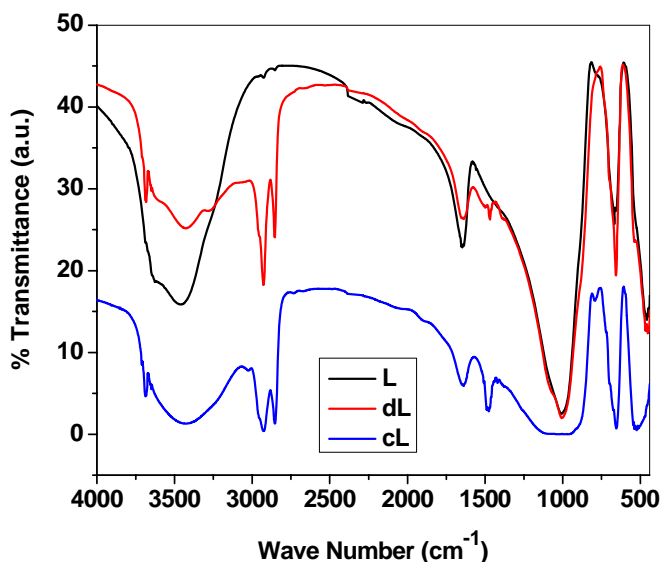


Figure 3.1: FTIR spectra of the unmodified and modified Laponite RD

Unmodified Laponite RDS (LS) does not show any additional peak due to the presence of $\text{Na}_4\text{P}_2\text{O}_7$ in the mid IR region as compared to the unmodified Laponite RD. As observed in earlier case, Laponite RDS when modified with dodecylammonium chloride and cetyltrimethyl ammonium bromide shows new peaks at 2927 cm^{-1} corresponding to asymmetric C-H_{str} , 2855 cm^{-1} corresponding to symmetric C-H_{str} , 1471 cm^{-1} corresponding to C-H_{def} and 3683 cm^{-1} due to N-H_{str} vibrations. This confirms the success of modification of LS.

Similarly, in case of Cloisite[®] 20A (C) new peaks appear at 2886, 2810, 1428 and 3594 cm^{-1} due to asymmetric C-H_{str} , symmetric C-H_{str} , C-H_{def} and N-H_{str} vibrations, respectively as compared to the Cloisite[®] Na (unmodified Cloisite[®] or MMT).

3.2.2 Covalent Modification

An FTIR spectrum of Laponite RD modified by octyl trimethoxy silane (OS) is shown in Figure 3.2. Modification of Laponite RD by OS introduces new peaks at 3429, 2928, 2852, 1469, 796 cm^{-1} due to O-H_{str} , C-H_{str} (asymmetric), C-H_{str} (symmetric), C-H_{def} and Si-C_{str} , respectively. This confirms the covalent modification of Laponite RD.

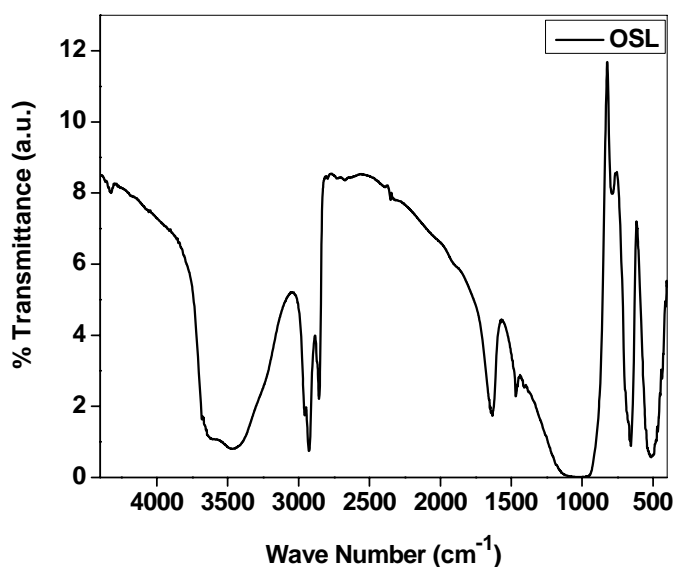


Figure 3.2: FTIR spectrum of the octyl trimethoxy silane modified Laponite RD

3.2.3 Dual Modification

In case of dual modified Laponite RD, ionic modification is carried out by using CTAB. Hence, in addition to other peaks present in cL, new peaks appear corresponding to 796 cm^{-1} due to Si-C_{str} and 3685 and 980 cm^{-1} due to N-H_{str} and C-N_{str} , respectively in addition to other peaks present on OSL (Fig. 3.3). This confirms the successful dual modification of Laponite RD. However, there is no significant change in the position of the FTIR peaks for cOSL and OSCL. In case of cAPL, a new peak at 1568 cm^{-1} due to N-H_{def} is observed in addition to other peaks present in cOSL. Details of FTIR peaks and their corresponding assignments are depicted in Table 3.1.

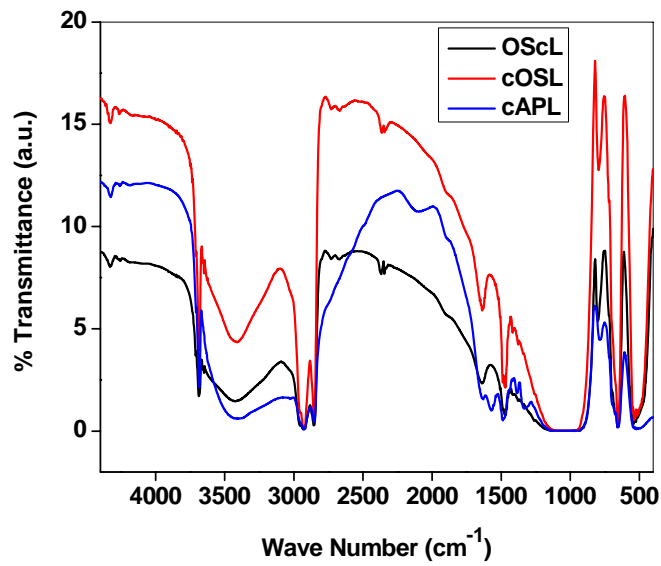


Figure 3.3: FTIR spectra of the dual modified Laponite RD

Table 3.1: FTIR peaks assignment of the nanoclays [Socrates (1980)]

Wave number (cm^{-1})	L	cL	OSL	OScL	cOSL	cAPL	Peak assignment
3685	--	P	--	P	P	P	N-H _{str}
3429	P	P	P	P	P	P	O-H _{str}
2928	--	P	P	P	P	P	C-H _{str} (asymmetric)
2852	--	P	P	P	P	P	C-H _{str} (symmetric)
1636	P	P	P	P	P	P	O-H _{def}
1568	--	--	--	--	--	P	N-H _{def}
1469	--	P	P	P	P	P	C-H _{def}
1042	P	P	P	P	P	P	Si-O-Si _{str}
980	--	P	--	P	P	P	C-N _{str}
796	--	--	P	P	P	P	Si-C _{str}
652	P	P	P	P	P	P	Si-O _{def}
518	P	P	P	P	P	P	Si-O-Si _{def}

*P indicates the presence of the peak

3.3 Solid State NMR Spectroscopy of the Modified Clays

3.3.1 Ionic Modification

Figure 3.4 displays the solid state ^{13}C and ^{29}Si NMR spectra of the unmodified and modified nanoclays.

^{13}C NMR spectrum of unmodified Laponite RD does not register any peak due to the absence of any form of carbon in its structure (not shown). cL shows peaks at 14.6 ppm (due to C_{16}), 23.3 ppm (due to C_3 and C_{15}), 30.7 ppm (due to C_2 and carbons from C_4 to C_{13}), 32.6 ppm (due to C_{14}), 53.8 ppm (due to N-CH_3) and 67.2 ppm (due to N-CH_2 or C_1) [Venkataraman and Vasudevan (2000)] (Fig. 3.4a).

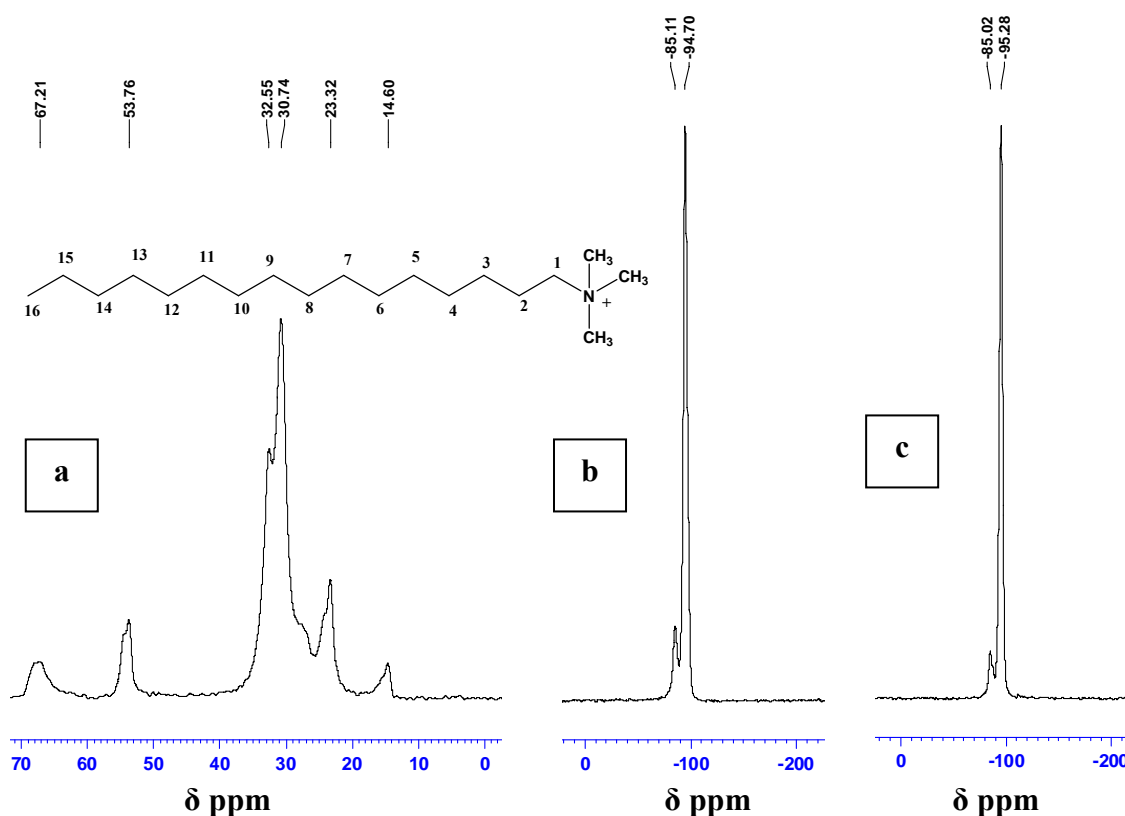


Figure 3.4: Solid state NMR spectra of (a) ^{13}C NMR of cL, (b) ^{29}Si NMR of L and (c) ^{29}Si NMR of cL

^{29}Si NMR spectrum of unmodified Laponite RD registers two peaks at -94.7 and -85.1 ppm due to Q^3 [$\text{Si}^*(\text{OMg})(\text{OSi})_3$] and Q^2 [$\text{Si}^*(\text{OMg})(\text{OSi})_2(\text{OH})$] structures,

respectively [Wang et al. (2007)] (Fig. 3.4b and c). Both the peaks are retained in the similar position with similar intensities in case of 'cL'.

3.3.2 Covalent Modification

Figure 3.5 displays the solid state ^{13}C and ^{29}Si NMR spectra of OSL. ^{13}C NMR spectrum of 'OSL' shows peaks at 14.2 ppm (due to C_8' and C_1'), 23.2 ppm (due to C_2' and C_7'), 29.9 ppm (due to C_4' and C_5') and 32.5 ppm (due to C_3' and C_6') [Gadzała-Kopciuch et al. (2005)] (Fig. 3.5a).

The peak at -94.7 ppm due to $\text{Q}^3 [\text{Si}^*(\text{OMg})(\text{OSi})_3]$ for unmodified Laponite RD remain unchanged in ^{29}Si NMR spectrum. However, a reduction in intensity of the peak at -85.1 ppm due to $\text{Q}^2 [\text{Si}^*(\text{OMg})(\text{OSi})_2(\text{OH})]$ structure is encountered after silane modification along with the development of two new peaks at -65.8 and -55.4 ppm due to $\text{T}^3 [\text{Si}^*(\text{OSi})_3\text{R}]$ and $\text{T}^2 [\text{Si}^*(\text{OSi})_2(\text{OR}')\text{R}]$ structures (Fig. 3.5b). This confirms the reaction of 'OS' with the Si-OH present only on the edge of the clay to produce OSL.

The absence of $\text{T}^0 [\text{Si}^*(\text{OR}')_3\text{R}]$ structure confirms the nonexistence of unreacted silanes. Similarly, absence of $\text{T}^1 [\text{Si}^*(\text{OSi})(\text{OR}')_2\text{R}]$ structure and presence of T^3 and T^2 structures confirms the oligomerization of 'OS' as observed by earlier researchers [Herrera et al. (2005); Park (2004); Wheeler (2005); Wheeler et al. (2006); Wang et al. (2007)].

3.3.3 Dual Modification

Figure 3.6 and 3.7 display the solid state ^{13}C and ^{29}Si NMR spectra of OSCL, cOSL and cAPL, respectively.

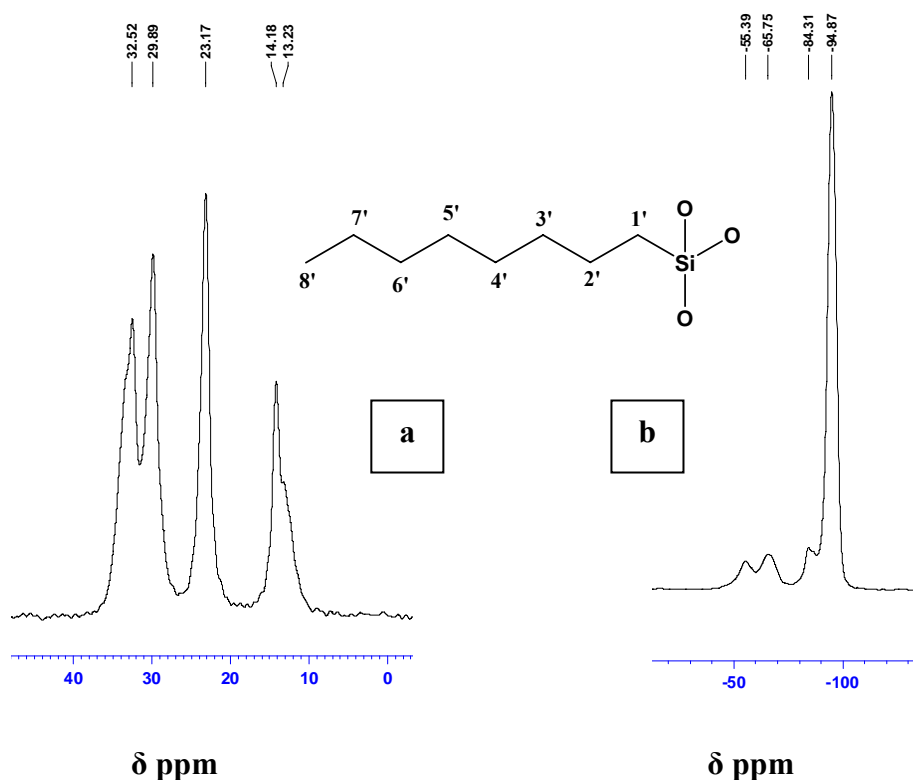


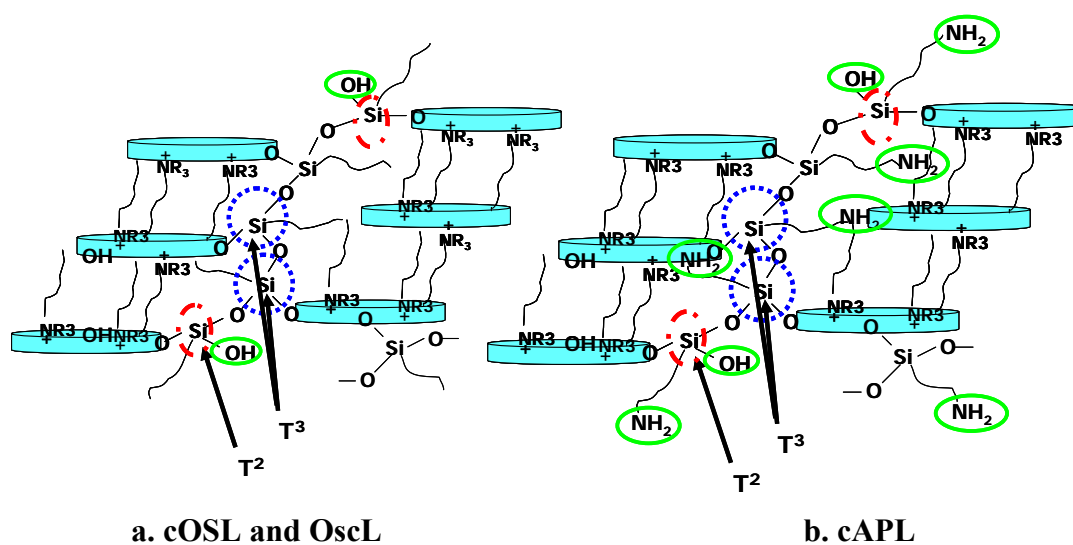
Figure 3.5: Solid state NMR spectra of (a) ^{13}C NMR and (b) ^{29}Si NMR of OSL

^{13}C NMR spectra of both the dual modified clays 'OScL' and 'cOSL' are almost similar with a slight variation in relative peak positions (both contain the combined signature of 'OSL' and 'cL'). In both the cases increase in intensities of all the peaks except the peaks corresponding to 53.8 and 67.2 ppm (characteristic peaks of CTAB) confirms the dual modification. However, a comparison between 'cL' and 'cAPL' shows an increased intensity of the peak at 23.3 ppm. Development of two new peaks corresponding to chemical shift of 10.8 and 43.0 ppm due to Si-CH₂ (C₁"') and N-CH₂ (C₃"') peaks of 3-aminopropyl triethoxy silane confirms the success of the dual modification of cL with 3-aminopropyltriethoxy silane [Ferreira et al. (2008)].

The absence of -OMe (present in OS) peak at 50 ppm and -OEt (present in AP) peaks at 58.4 ppm and 18.4 ppm indicate the complete silylation reaction of the OS and AP during the modification.

^{29}Si NMR spectra of the dual modified Laponites (OScL, cOSL and cAPL) are not different from each other and possess Q^3 , Q^2 , T^3 and T^2 structures with slight difference in their respective chemical shifts. This indicates that structurally there is not much difference between the dual modified clays e.g., OScL, cOSL and cAPL. The absence of T^0 [$\text{Si}^*(\text{OR}')_3\text{R}$] structure confirms the nonexistence of unreacted silanes. Similarly, absence of T^1 [$\text{Si}^*(\text{OSi})(\text{OR}')_2\text{R}$] structure and presence of T^3 and T^2 structures confirm the oligomerization of the respective silanes as observed by several researchers earlier [Herrera et al. (2005); Park et al. (2004); Wang et al. (2007); Wheeler et al. (2005, 2006)].

Appearance of T^2 structure indicates the presence of either $-\text{OMe}$ or $-\text{OH}$ group on the clay after modification. However, absence of any peak corresponding to $-\text{OMe}$ and $-\text{OEt}$ in ^{13}C NMR spectrum of 'OScL', 'cOSL' and 'cAPL', respectively confirms only the presence of $-\text{OH}$ group (as indicated earlier from the FTIR spectrum as well). Based on these observations a scheme has been proposed for structure of the modified clays (Scheme 3.1).



Scheme 3.1: Proposed structure of the dual modified clay platelets

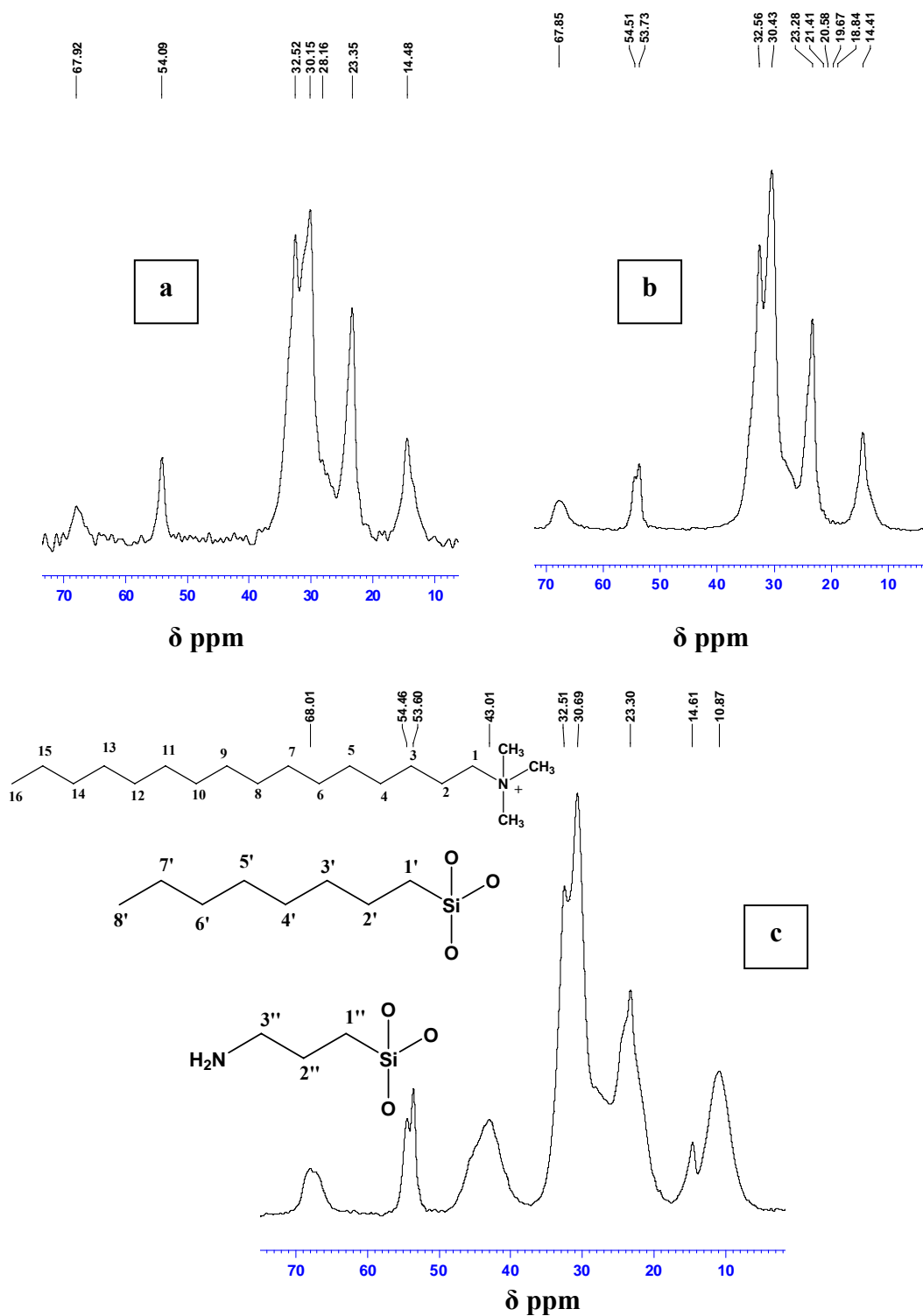


Figure 3.6: Solid state ^{13}C NMR of (a) OSCL, (b) cOSL and (c) cAPL
 (Chemical structures of the modifiers with the assignment of carbon numbers are provided)

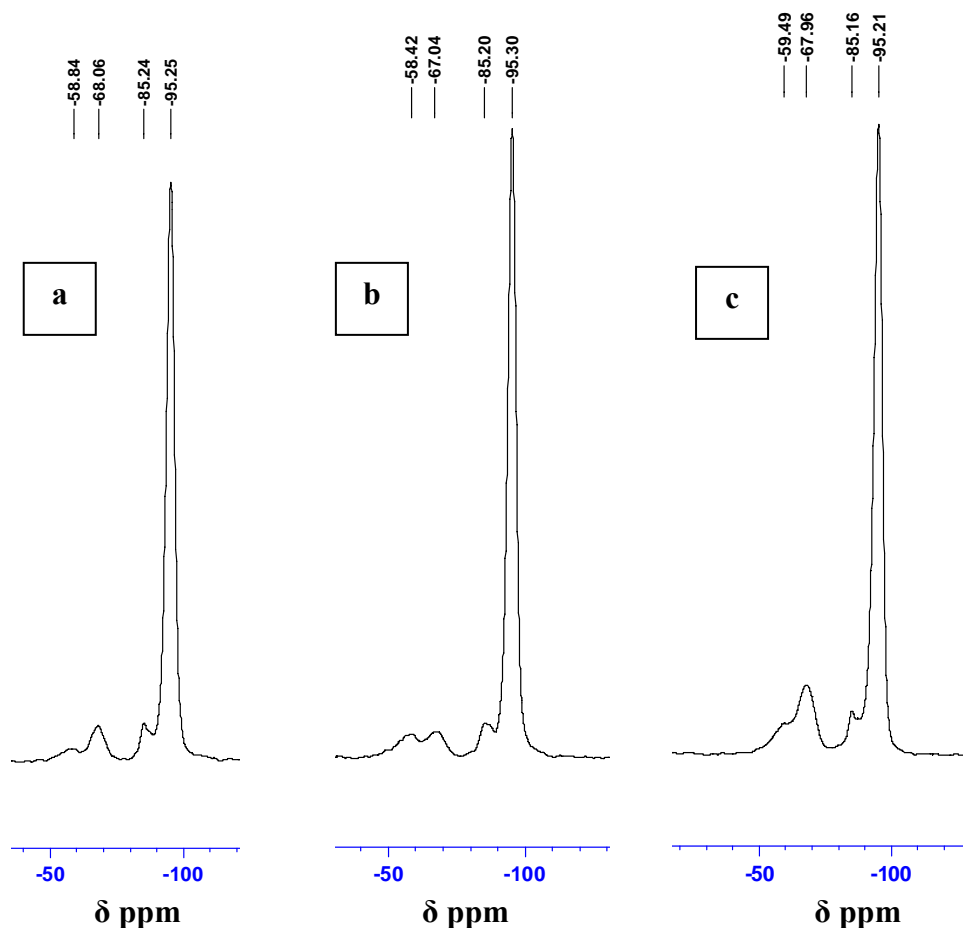


Figure 3.7: Solid state ^{29}Si NMR spectra of (a) OScL, (b) cOSL and (c) cAPL

3.4 Wide Angle X-ray Diffraction (WAXRD) Studies

3.4.1 Ionic Modification

WAXRD diffractograms of the ionically modified nanoclays at lower angular range (2θ value 2 to 10°) are shown in Figure 3.8. It is observed that unmodified Laponite RD and RDS do not show any distinct peak corresponding to the inter layer gallery spacing of the clay platelets. It has been reported recently by Wheeler et al. (2005) that the absence of distinct peak is due to disordered stacking of platelets in pristine Laponite which eventually shows some order upon modification. Modification with dodecyl ammonium hydrochloride (d) or cetyltrimethyl ammonium bromide (c) resulted in a peak nearly at 2θ value 6.0° . The peak is more prominent and distinct in case of cL and cLS as compared to those of dL and dLS, respectively.

This is ascribed to the higher degree of modification in case of 'c' giving rise to greater d-spacing between the clay galleries with cL and cLS (due to longer alkyl chain).

However, in case of Cloisite[®] 20A, two peaks appear corresponding to 2θ values 3.7° and 7.1° . The peak at 2θ value 7.1° corresponds to the presence of small fraction of unmodified clay whereas, the peak at 2θ value of 3.7° corresponds to the modified clay fraction [Song et al. (2003)].

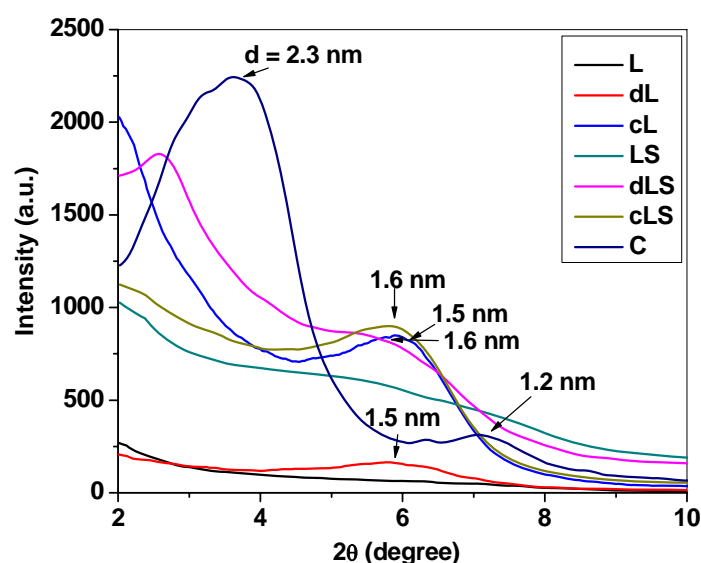


Figure 3.8: WAXRD peaks of unmodified and modified Laponite RD, d-value corresponding to the peaks are calculated and provided in the Figure

3.4.2 Covalent Modification

A broad band in the form of a shoulder (from 2θ value 4.0 - 7.0°) is observed in case of OSL (Fig. 3.9). This is ascribed to the complex structure formation [Sormana et al. (2008)] and oligomerization of the silane.

3.4.3 Dual Modification

WAXRD diffractograms of the dual modified Laponites are shown in Figure 3.9. OScL shows a broad band ranging from 2θ value 4.0 - 7.0° . However, relatively sharp peaks have been observed for cOSL and cAPL centred at 5.8° 2θ .

Hence, in the two varieties of dual modified clays the history of the initial modification persists. The initial covalent modification is expected not to allow the clay platelets to get separated to a greater extent due to the oligomer formation as indicated by solid state NMR studies.

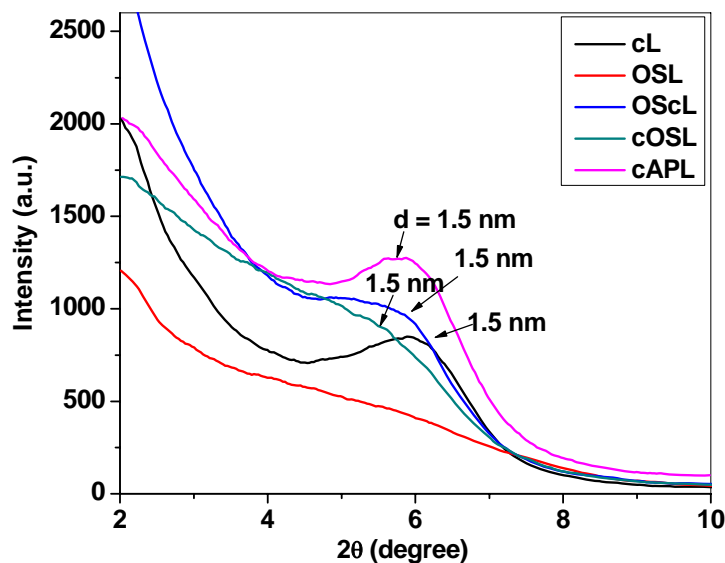


Figure 3.9: WAXRD peaks of covalently modified and dual modified Laponite RD

3.5 Thermogravimetric Analysis (TGA) of Nanoclays

TGA thermograms of unmodified and modified clays are shown in Figures 3.10 and 3.11, respectively. The extent of modification of the clays is calculated by deducting the weight loss of the unmodified clay from the weight loss of the modified clay within the temperature range of 130 to 600 °C. The extents of modification of different varieties of clays are listed in Table 3.2.

3.5.1 Ionic Modification

The higher amount of weight loss of the modified clays as compared to the unmodified Laponites (Fig. 3.10) unveils additional evidence of the modification of the nanoclays. It is observed that the extent of modification is higher in case of cL as compared to dL. This is due to the difference in the molecular weight and alkyl chain

length between ‘c’ and ‘d’. ‘c’ contains alkyl chain with sixteen carbons along with three methyl groups attached to the nitrogen atom, whereas, ‘d’ contains alkyl chain with twelve carbons along with three hydrogens attached to the nitrogen atom. However, by using the same surfactants, modification of Laponite RDS resulted in a reverse trend with greater extent of modification in case of dLS as compared to that of cLS. This may be due to the removal of the surface alkyl ammonium group while washing with water in case of cLS. Laponite RDS registers an additional degree of modification (8 to 10% higher) than that of Laponite RD when modified with the same surfactants (‘d’ or ‘c’). This is due to the involvement of the surface $\text{Na}_4\text{P}_2\text{O}_7$ (adsorbed on the surface of Laponite RDS) during the process of ion exchange with alkyl ammonium ions. *It is worth mentioning here that this is probably the first report on the involvement of the surface $\text{Na}_4\text{P}_2\text{O}_7$ in ion exchange process for Laponite RDS.*

Commercially available modified montmorillonite (C) possess highest extent of modification. This is because of the higher molecular weight of the surfactant and greater cation exchange capacity (CEC) of montmorillonite as compared to the Laponites.

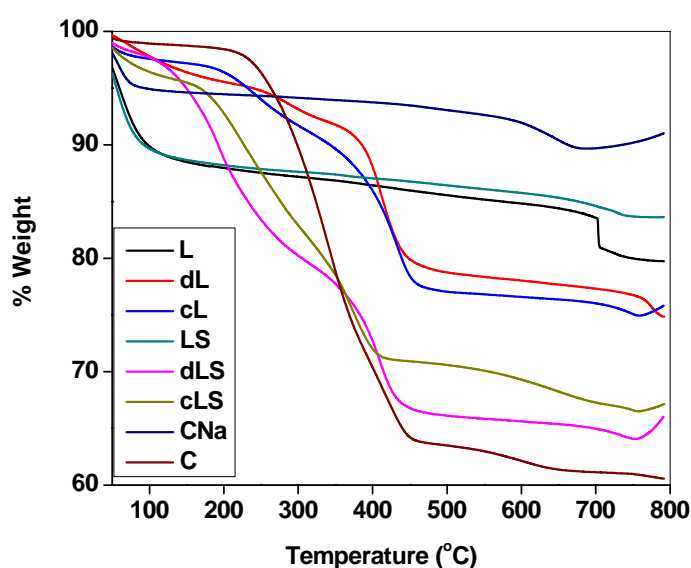


Figure 3.10: TGA thermograms of ionically modified Laponites and Cloisites[®]

3.5.2 Covalent Modification

Presence of lower amount of surface –OH groups and low molecular weight of the silane renders a lower degree of modification in case of OSL. Only 11.2 weight % of alkyl groups have been incorporated by octyl trimethoxy silane modification (Fig. 3.11).

3.5.3 Dual Modification

In case of the dual modified Laponite, the extent of modification of OSCL is less as compared to that of cOSL. This is because of the fact that initial silane modification of Laponite with ‘OS’ leads to the formation of crosslinked structure derived from the oligomeric siloxane chains (Section 3.3). This crosslinked structure partly restricts the entrance of the cetyltrimethyl ammonium group to effectively utilize all the exchangeable Na^+ ions present inside the clay gallery. However, initial ionic exchange by CTAB can effectively utilize the exchangeable Na^+ ions present inside the clay gallery. Hence, extent of modification (Table 3.2) is higher in case of ‘cOSL’ as compared to ‘OSCL’.

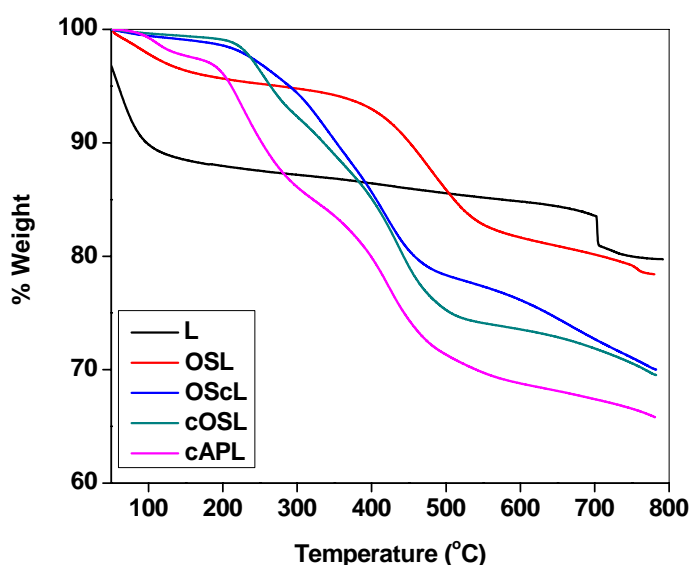


Figure 3.11: TGA thermograms of covalent and dual modified Laponite RD

Table 3.2: Extent of modification of the nanoclays

Designation	Extent of modification (%)	Designation	Extent of modification (%)
dL	14.8	OSL	11.2
cL	15.6	OscL	17.2
dLS	26.4	cOSL	22.0
cLS	22.5	cAPL	25.3
C	32.9	--	--

3.6 Conclusions

Laponite clay is successfully modified by using ionic, covalent and dual modification techniques. Laponite RDS provides additional sites for modification due to the adsorbed $\text{Na}_4\text{P}_2\text{O}_7$. Therefore, it can be modified with larger amount of surfactants by ionic modification technique. Covalent modification of Laponite with trialkoxy silanes leads to oligomerization of the modifiers. Dual modification of Laponite results in maximum extent of modification of Laponite RD. However, the extent of modification depends on the sequence of ionic and covalent modifications.

3.7 References

- Borsacchi S., Geppi M., Ricci L., Ruggeri G., Veracini C. A. (2007) Interactions at the surface of organophilic-modified Laponite: A multinuclear solid state NMR study, *Langmuir* 23, 3953-3960
- Ferreira R. B., da Silva C. R., Pastore H. O. (2008) Aminopropyl-modified magnesium-phyllsilicates: layered solids with tailored interlayer access and reactivity, *Langmuir* 24, 14215-14221
- Socrates G. (1980) Infrared Characteristic group frequencies, John Wiley & Sons, Wiley-Interscience Publication: New York
- Gadzała-Kopciuch R., Kluska M., Wełniak M., Buszewski B (2005) Silicon dioxide surfaces with aryl interaction sites for chromatographic applications, *Materials Chemistry and Physics* 89, 228-237
- Herrera N. N., Letoffe J. -M., Reymond J. -P. and Bourgeat-Lami E. (2005) Silylation of Laponite clay particles with monofunctional and trifunctional vinyl alkoxysilanes, *Journal of Materials Chemistry* 15, 863-871

Herrera N. N., Letoffe J. -M., Putaux J. -L., David L., Bourgeat-Lami E. (2004) Aqueous dispersions of silane-functionalized Laponite clay platelets. A first step towards the elaboration of water-based polymer/clay nanocomposites, *Langmuir* 20 (5) 1564-1571

Herrera N. N., Putaux J. -L., Bourgeat-Lami E. (2006) Synthesis of polymer/Laponite nanocomposite latex particles via emulsion polymerization using silylated and cation exchanged Laponite clay platelets, *Progress in Solid State Chemistry* 34, 121-137

Ni P., Li J., Suo J., Li S. (2004) Novel polyether polyurethane/clay nanocomposites synthesized with organic-modified montmorillonite as chain extenders, *Journal of Applied Polymer Science* 94, 534-541

Ni P., Wang Q., Li J., Suo J., Li S. (2006) Novel polyether polyurethane/clay nanocomposites synthesized with organically modified montmorillonite as chain extenders, *Journal of Applied Polymer Science* 99, 6-13

Park M., Shim I. -K., Jung E. -Y., Choy J. -H. (2004) Modification of external surface of Laponite by silane grafting, *Journal of Physics and Chemistry of Solids* 65, 499-501

Song M., Hourston D. J., Yao K. J., Tay J. K. H., Ansarifard M. A. (2003) High performance nanocomposites of Polyurethane elastomer and organically modified layered silicate, *Journal of Applied Polymer Science* 90, 3239-3243

Sormana J. L., Chattopadhyay S., Meredith J. C. (2008) Mechanical and thermal properties of Poly(urethaneurea) nanocomposites prepared with diamine-modified Laponite, *Journal of Nanomaterials* 2008, article ID 869354, 9 pages

Tien Y. I., Wei K. H. (2001) High-Tensile-Property Layered Silicates/Polyurethane Nanocomposites by Using Reactive Silicates as Pseudo Chain Extenders, *Macromolecules* 34, 9045-9052

Tien Y. I., Wei K. H. (2002) The effect of nano-sized silicate layers from montmorillonite on glass transition, dynamic mechanical, and thermal degradation properties of segmented polyurethane, *Journal of Applied Polymer Science* 86, 1741-1748

Venkataraman N. V., Vasudevan S. (2000) Conformation of an alkane chain in confined geometry: cetyl trimethyl ammonium ion intercalated in layered CdPS₃, *Journal of Physical Chemistry Part B* 104, 11179-11185

Wang J., Wheeler P. A., Jarrett W. L., Mathias L. J. (2007) Synthesis and characterization of dual functionalized Laponite clay for acrylic nanocomposites, *Journal of Applied Polymer Science* 106, 1496-1506

Wheeler P. A., Wang J., Mathias L. J. (2006) Poly(methyl methacrylate)/Laponite Nanocomposites: Exploring Covalent and Ionic Clay Modifications, *Chemistry of Materials* 18, 3937-3945

Wheeler P. A., Wang J., Baker J., Mathias L. J. (2005) Synthesis and characterization of covalently functionalized laponite clay, *Chemistry of Materials* 17, 3012-3018

CHAPTER 4A

TPUCN BASED ON MODIFIED LAPONITE AND CLOISITE®

A part of this chapter has been published in:

Journal of Polymer Science Part B: Polymer Physics 46 (2008) 2341

4A.1 Introduction

Liff et al. (2007) and Korley et al. (2006) have reported that unmodified Laponite RD preferentially associates with the more polar hard segment. Thus in view of these, Laponite RD has been modified by two surfactants to prepare 'cL' and 'dL' (as described in Chapter 2). These modified clays have been dispersed in a commercial TPU matrix (Desmopan 8600E) by using solution mixing technique. To achieve a better comparison a widely used commercially available modified clay Cloisite® 20A has been dispersed in the TPU matrix following the same method. The structure-property correlations of the resulting nanocomposites have been studied in details in this chapter.

4A.2 Wide Angle X-ray Diffraction (WAXRD)

WAXRD diffractograms of the neat TPU and TPUCN at lower angular range are shown in Figure 4A.1. In case of SC, both the parent peaks (at 3.7° and 7.1° 2θ) observed in C, persist with reduced intensity and with a shift towards lower angles. However, the peaks corresponding to dL is not observed at lower clay content in SdL but can be seen at higher clay content with reduced intensity and with a shift towards lower angle as compared to that present in dL. Similarly, in case of ScL, the peaks are visible at all clay contents with reduced intensity and with a shift towards lower angle as compared to cL. In all these cases, an increase in the clay content shifts the peaks towards higher angle. This suggests that increasing clay content increases the aggregation tendency.

WAXRD at higher angular range (from 10 to 50° 2θ value) for C display peaks at 2θ values 19.8° (0.45 nm), 24.1° (0.37 nm) and 35.2° (0.26 nm) corresponding to 110, 101 and 130 planes of reflections respectively (Fig. 4A.2) [Shieh et al. (1999)]. However, the corresponding peaks are observed at 2θ values

19.6° (0.45 nm), 26.3° (0.34 nm) and 35.1° (0.26 nm), respectively for modified Laponites. The peak positions remain indifferent in both dL and cL. The peak corresponding to 2θ value of 27.7° (0.32 nm) in C is due to the (Mg, Fe)SiO₃ and CaCO₃ impurities [Carrado (2000)] which are absent in modified Laponites as it is a synthetic Li-hectorite. However, all these peaks are not observed in TPUCN, either because of lower concentration of clay in the matrix or due to the random dispersion of clay in the matrix breaking the ordered clay tactoids.

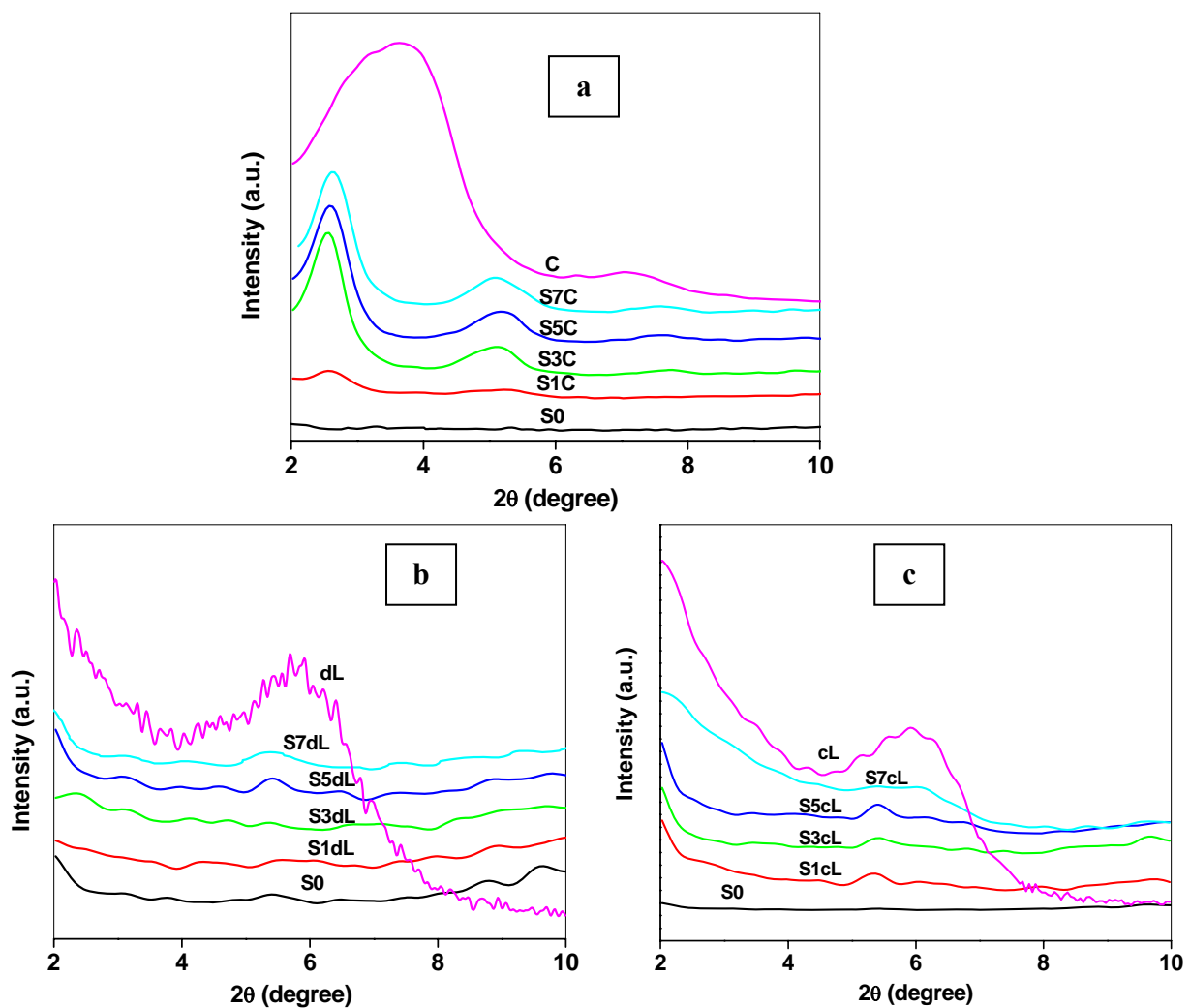


Figure 4A.1: WAXRD at lower angular range of (a) SC, (b) SdL and (c) ScL

A broad band is observed from 2θ value ranging from 10 to 30° along with some sharp peaks, in the neat TPU. The broad band is the indication of the amorphous

or quasi crystalline nature of the TPU. However, sharp peaks correspond to the ordered hard domains of the TPUs resulted during evaporation of the solvent. In case of SC and SdL the broad band is divided into two peaks and a new peak can be seen at $2\theta \sim 13.7^\circ$. The exact reason for this new peak is unknown and further study is required in this regard. However, this behavior is not observed in case of ScL.

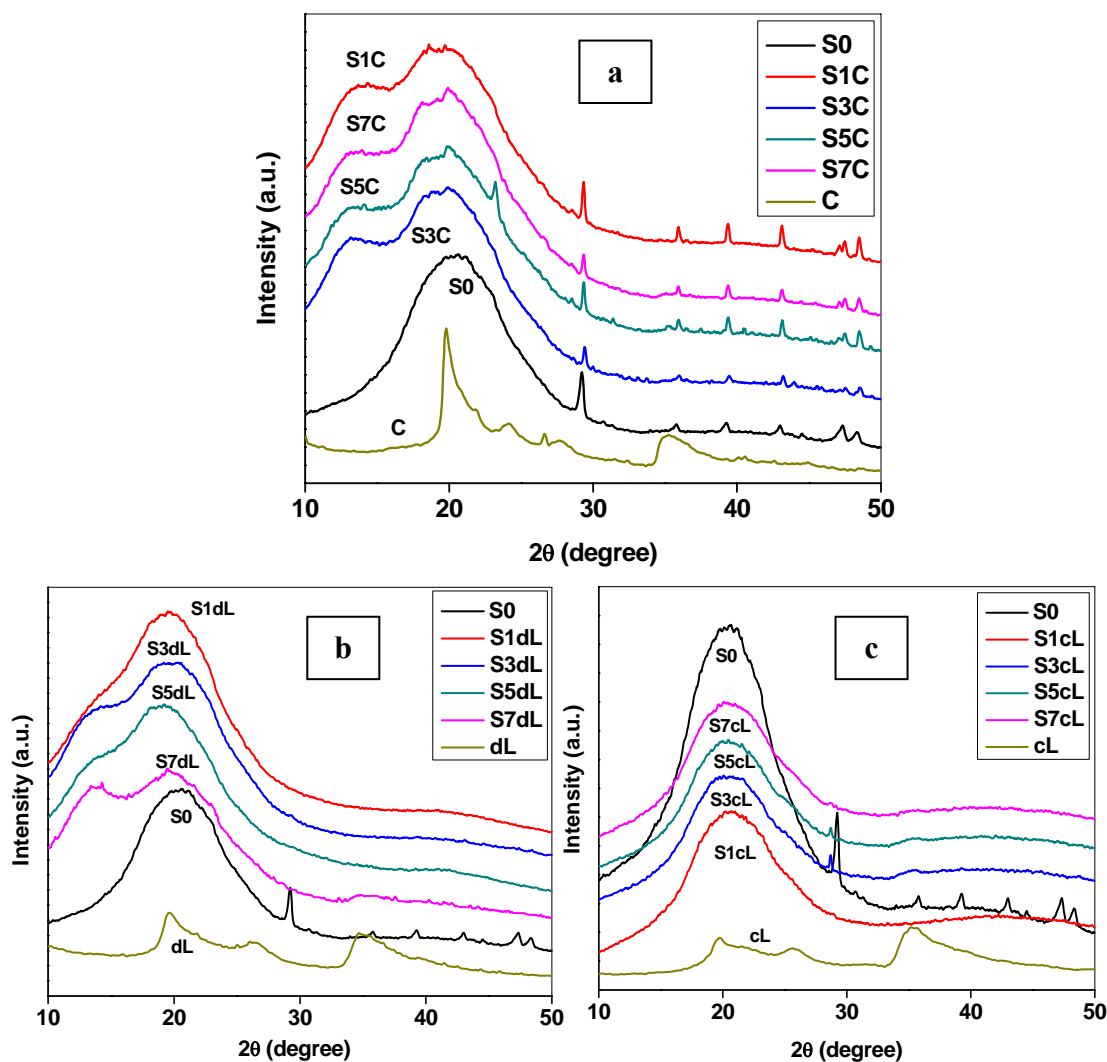


Figure 4A.2: WAXRD of (a) SC, (b) SdL and (c) ScL

Some sharp peaks are seen above 2θ value of 29.3° in the neat TPU. All these peaks remain in the same positions in case of SC, but disappear in case of SdL and partly persist in case of ScL. This is due to the destruction of hard domain ordering in the neat TPU with the addition of dL, which is less effective in case of cL and least

influential in case of C. The affinity of the unmodified Laponite RD to the more polar hard domain is also reported in the literature [Liff et al. (2007) and Korley et al. (2006)]. Hence, it provides an indication that dL preferentially associate with the more polar hard domain, C preferentially associate with the less polar soft segment whereas, cL lacks any preference and gets distributed in both the segments randomly.

4A.3 Transmission Electron Microscopy

4A.3.1 Morphology of Solution Cast Nanocomposites

Figure 4A.3 represents the TEM photomicrographs of the original solution cast samples. Figure 4A.3a shows that C follows a more exfoliated structure compared to the other varieties of clay. However, dL and cL exhibited a combination of loosely aggregated to intercalated structure throughout the matrix (Fig. 4A.3b and 4A.3c). Although TPU exhibits two-phase morphology, SC does not show any phase separation but in case of SdL and ScL, a localized aggregation of clay possibly indicates its association to the hard domain (creating phase separation) is observed. Interestingly, the size scale of such aggregates (25-150 nm) matches well with the approximate size scale of hard domains common with the TPUs [Liff et al. (2007)]. *Thus we can postulate that the modified Laponite particles especially dL, are acting as hard-domain marker.* The TEM observations are inline with our earlier WAXRD results.

4A.3.2 Morphology of Annealed Nanocomposites

Figure 4A.4 represents the annealed morphology of the nanocomposites. The samples were equilibrated at a temperature of 140 °C, (very close to the temperature corresponding to the destruction of the hard domain) and slowly cooled to room temperature to achieve equilibrium morphology due to the self organization of the hard domains. Here the spherical grey colored structures represent the ordered hard

domain, the darker (black) spherical structures represent the hard domain (Fig. 4A.4a) with clay platelets and the linings reveal the distributed clay platelets. It is observed that dL preferentially associate with the hard domain (Fig. 4A.4c), C associates with the soft domain Fig. 4A.4b), whereas, cL gets distributed both in hard and soft domains randomly (Fig. 4A.4d).

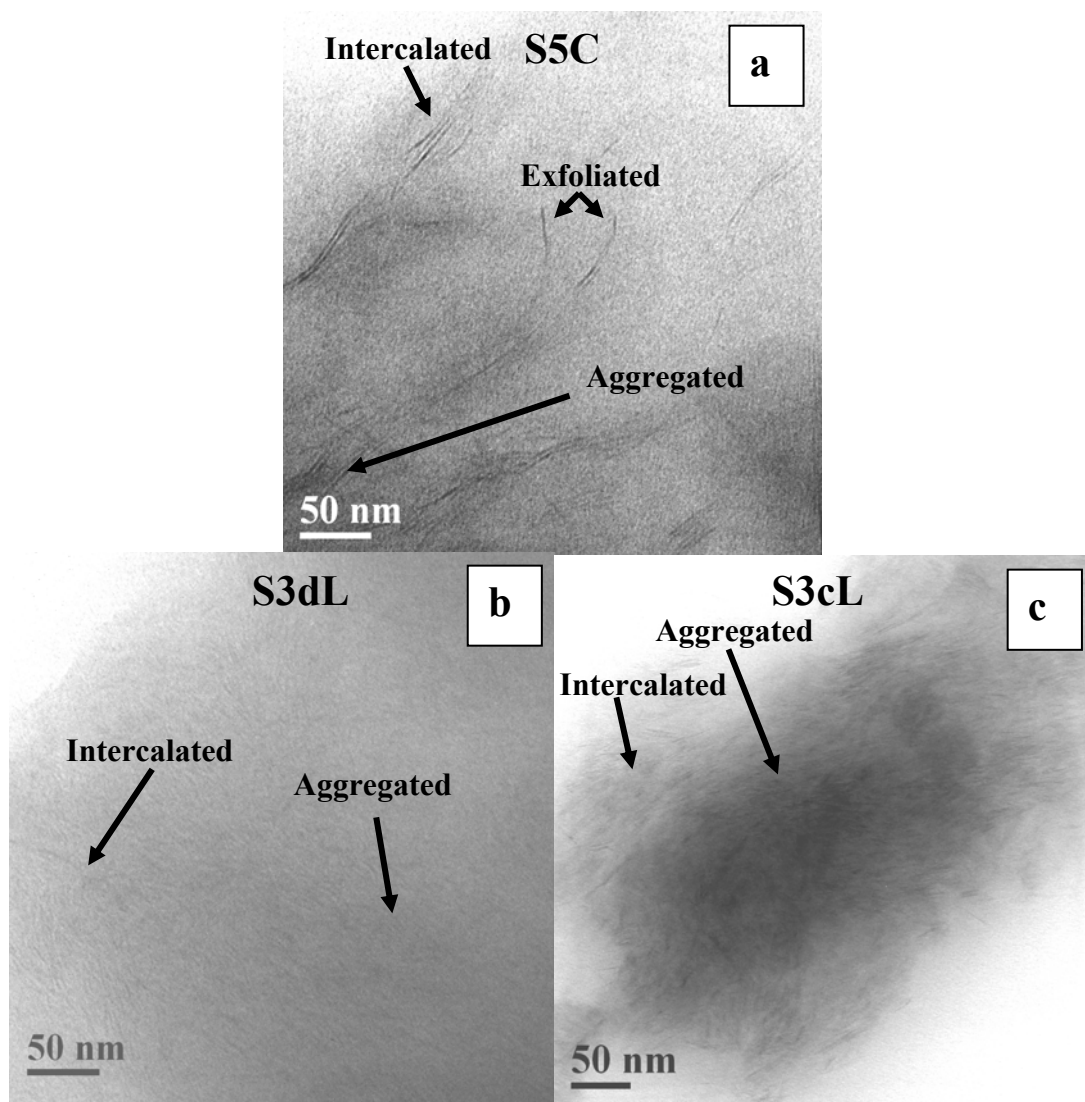


Figure 4A.3: TEM photomicrographs of solution cast nanocomposites (a) S5C (b) S3dL & (c) S3cL

The hard/soft segment preference can be explained based on the hydrophobicity of the clay platelets. Laponite RD is organically modified by two types of surfactants, e.g., dodecylammonium chloride (alkyl group with 12 carbon atoms having primary alkyl ammonium head) and cetyltrimethyl ammonium bromide

(alkyl group with 16 carbon atoms having tertiary alkyl ammonium head). It is expected that due to the primary alkyl ammonium ion, the hydrophilicity still persists with dL. Hence, Laponite modified by dodecylammonium ion preferentially associates with the more polar hard domain. But presence of long alkyl chain and the quaternary alkylammonium ion hinders preferential association of cL with the more polar hard domains. However, C is modified with a greater amount of surfactant containing quaternary ammonium ion. Thus the hydrophobicity of C is greater than both dL and cL (Chapter 3, Table 3.2). Hence, C preferentially associates itself with the soft domains. This further supports the report by Liff et al. (2007) and Korley et al. (2006) that due to more hydrophilic nature of Laponite RD, it showed a preferential association with the more polar hard domains.

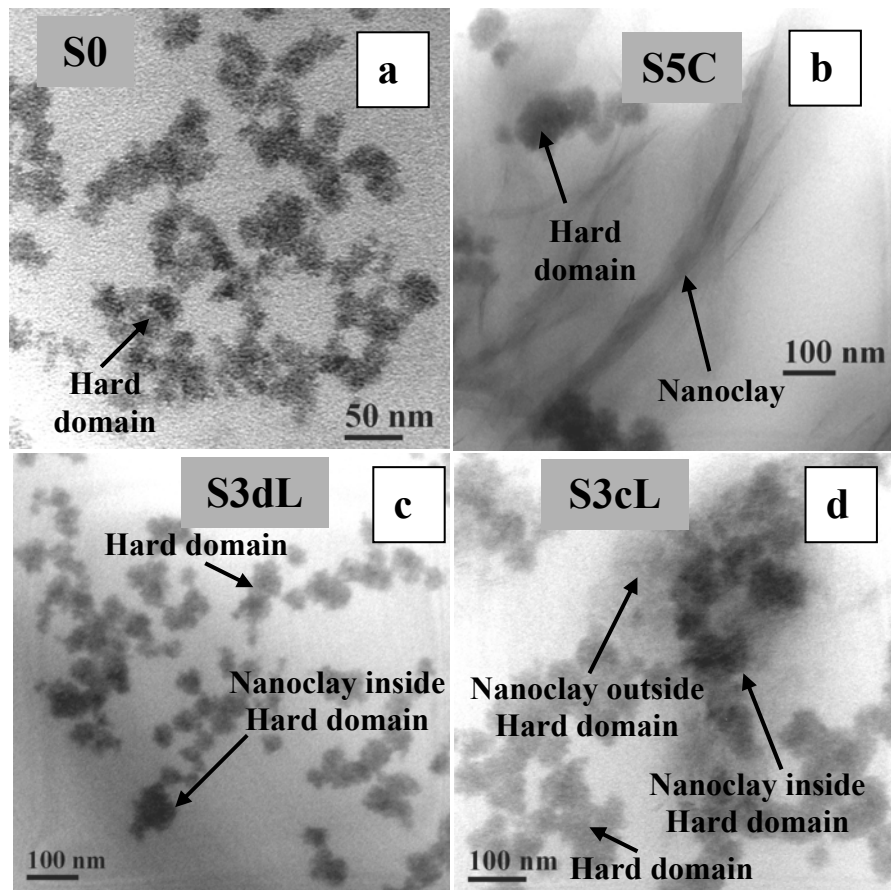


Figure 4A.4: TEM photomicrographs of the annealed TPUCNs

4A.4 Field Emission Scanning Electron Microscopy (FESEM)

Figure 4A.5 displays the FESEM photomicrographs of the nanocomposites with 3 and 5% clay contents. In the photomicrographs the gray coloured regions indicate the bulk of the polymer matrix and the brighter spots indicate the distribution of clay particles. It is observed that the amount of aggregation increases with increased amount of clay. Uniform distribution of clay particles is more clearly visible in case of TC as compared to SdL and ScL. It is observed that Cloisite® based nanocomposites show elliptical type of clay aggregate but Laponite based nanocomposites display spherical type of clay aggregate. This is because of the difference in dimension (diameter to thickness or aspect ratio). However, the phenomenon of exfoliation, intercalation and aggregation is difficult to study from FESEM conclusively, which can be easily reflected from TEM photomicrographs.

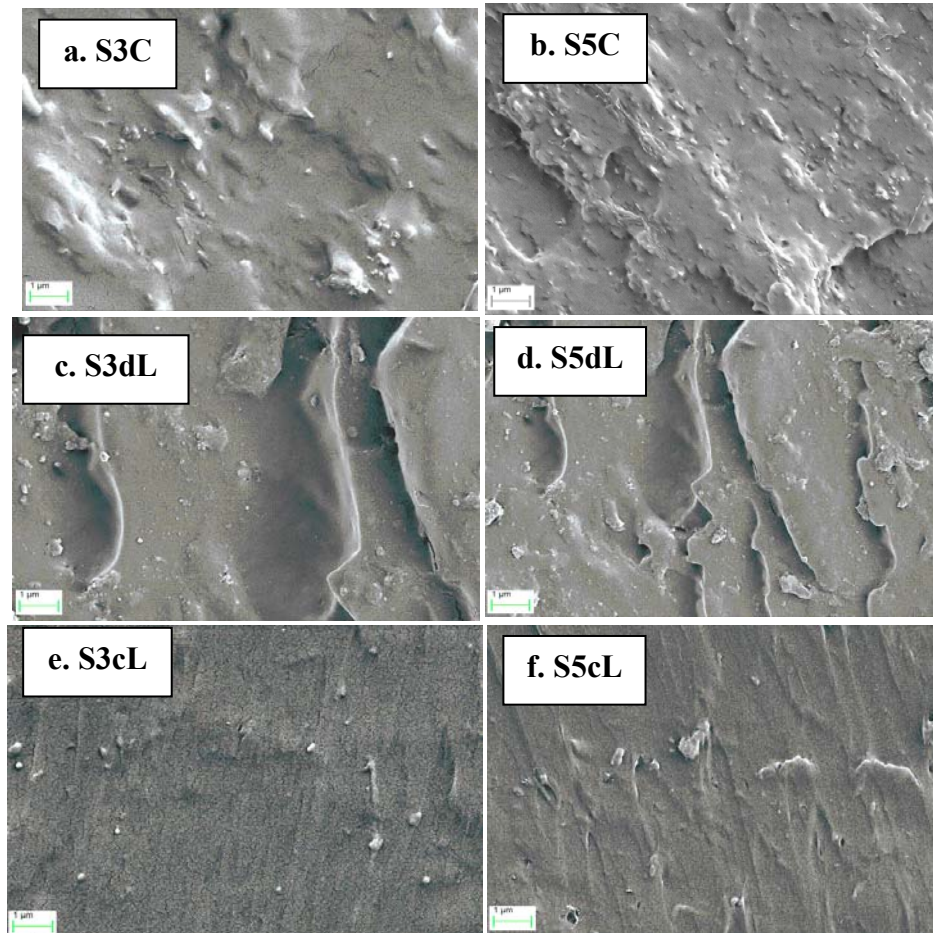


Figure 4A.5: FESEM photomicrographs of TPUCNs

4A.5 Atomic Force Microscopy (AFM) Analysis

Figure 4A.6 (a-d) displays height and phase images of S5C and S3dL. Since, the samples were microtomed at a high knife speed at room temperature, it is most likely that the soft domain which is more elastic as compared to the hard domain would protrude to higher elevation. Based on the comparison of the height and phase images of S5C and S3dL, it is observed that Cloisite® is most preferentially distributed in the higher elevated region, whereas dL is distributed in a reverse way around. This is again in line with our earlier observations and inferences (WAXRD and TEM sections).

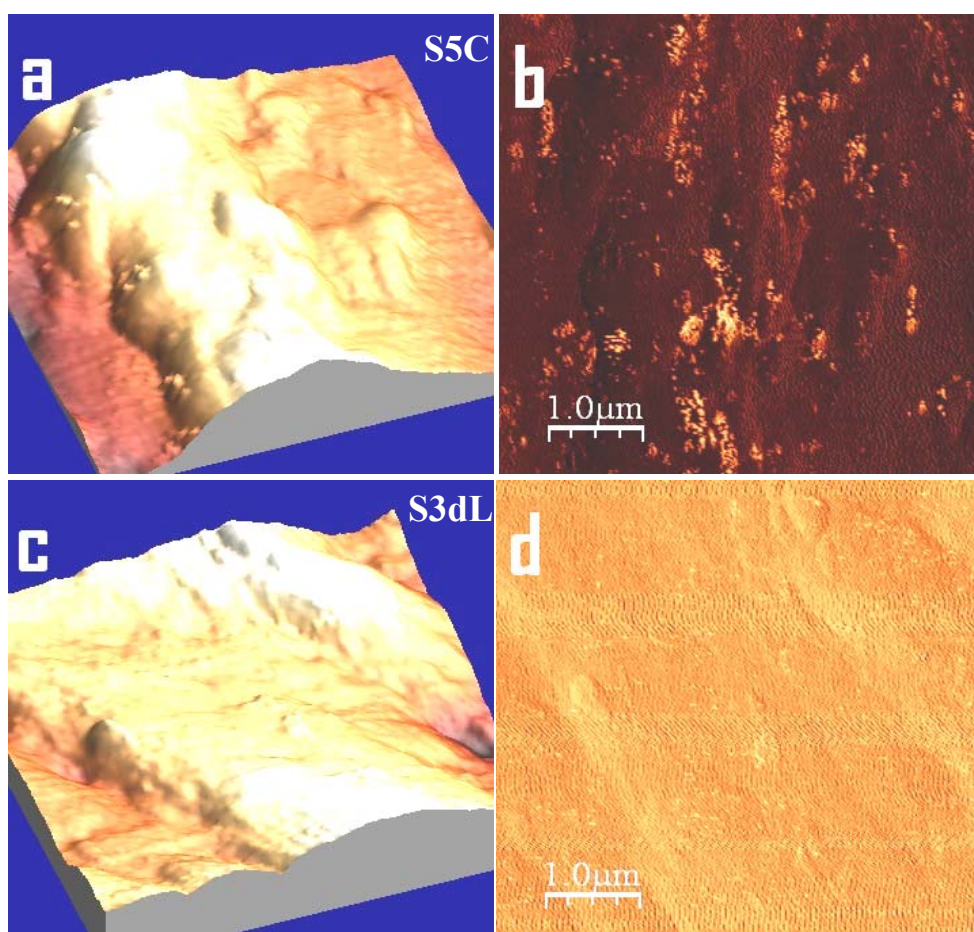


Figure 4A.6: AFM photomicrographs of TPUCN (a & c) Height images and (b & d) corresponding Phase images

4A.6 Differential Scanning Calorimetry (DSC)

Figure 4A.7 represents the DSC thermograms of the nanocomposites for second heating cycles. The thermogram exhibits the soft segment T_g, two endotherms followed by an exotherm. The soft segment T_g appears nearly at -40 °C. The endothermic peaks appear near about 98 °C and 170 °C, respectively, corresponding to the destruction of the short range and long range ordered hard domain (or semicrystalline melting) resulting from enthalpy relaxation [Chen et al. (1998); Seymour and Cooper (1973); Shu et al. (2001); Tsen et al. (2006)]. Due to the quicker evaporation of the solvent, hard segments do not get enough time to rearrange properly and hence the endotherm from 98 to 170 °C is quite broad. After the endotherm an exotherm is observed nearly at 200 °C corresponding to the degradation of the TPU. Hard segment T_g is not clearly seen because of the dominance of the amorphous soft segments over the hard domains and the presence of imperfect crystalline order.

There is no significant change in soft segment T_g of the nanocomposites as compared to the neat TPU (Table 4A.1). This may be due to the fact that the expected increment in T_g due to the incorporation of clay is being compensated by the plasticizing effect of the unreacted amines present in the modified clays. However, addition of clay increases the sharpness of the endothermic peaks at 98 and 170 °C. These endotherms are more clearly visible in case of SC and ScL (especially at higher clay content). But SdL does not exhibit any particular order and the semicrystalline ordering is destroyed at lower clay content. *This again may be an indication of the affinity of dL towards the hard domain.* But the order reappears for 5 and 7% clay content which can be seen from the sharpness of the melting endotherms. This supports our earlier hypothesis put forward under WAXRD section.

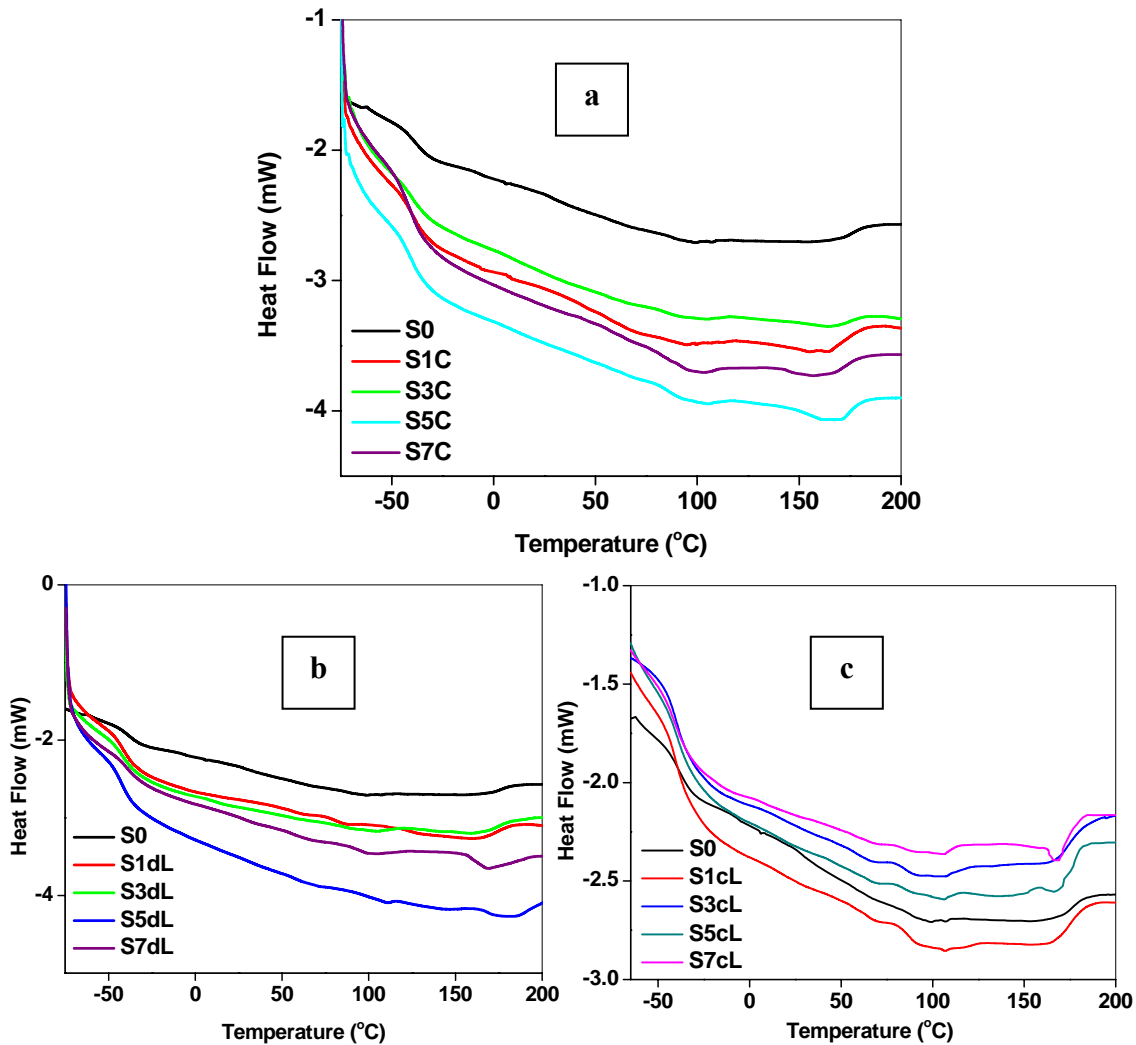


Figure 4A.7: DSC thermograms of (a) SC, (b) SdL and (c) ScL

4A.7 Dynamic Mechanical Analysis (DMA)

Figure 4A.8 displays the storage modulus vs. temperature plot of the TPUCNs. Table 4A.1 represents the change in storage modulus at different temperatures, T_g and the $\tan \delta_{\max}$ values. The percentage changes in those values are given in Table 4A.2.

Figure 4A.8a depicts the storage modulus of SC with varying clay content. S5C exhibits greater storage modulus value in the glassy state whereas, S7C shows the maximum value in the rubbery region. However, the maximum storage modulus is observed for S3dL and S3cL in both glassy and rubbery regions, among the dL and cL based TPUCN, respectively (as shown in Fig. 4A.8b and 4A.8c). It is observed that

clay content in excess of 5% for C and 3% for dL and cL deteriorates the storage modulus. It is well known that in glassy region, polymer becomes stiff and when the temperature raises it gradually softens. On the other hand for a filled system in the glassy state, polymer matrix becomes stiffer as compared to the filler aggregates. It is a general perception that at higher clay content the filler-filler interaction dominates over the polymer-filler interaction decreasing the storage modulus in both glassy and rubbery region.

In spite of these, there is not much change in the soft segment T_g which supports our earlier observation from DSC thermogram as well (Table 4A.1). However, the loss factor ($\tan \delta_{\max}$) decreases with the increase in clay content in all the cases. This shows the reinforcing effect (at least partly for Laponite) of fillers in the TPU matrix and the decrease in damping behavior with the increase in filler content at the glass transition region (Fig. 4A.9). In the rubbery region it can be seen that, with filler content damping behavior increases in all the cases. Rubbery plateau involves larger scale of segmental motion where filler-polymer and filler-filler interactions gradually contribute to the overall loss.

Table 4A.2 shows the percentage improvement in storage modulus and percentage change in $\tan \delta_{\max}$ values. It can be seen that increase in the storage modulus value is optimum for 5% C at $-60\text{ }^\circ\text{C}$, whereas, it is optimum for 7% C at $-20\text{ }^\circ\text{C}$, $+20\text{ }^\circ\text{C}$ and $+80\text{ }^\circ\text{C}$. But in case of Laponite filled systems optimum storage modulus is obtained with 3% clay content (in both dL and cL) in all the temperatures considered here ($-60\text{ }^\circ\text{C}$, $-20\text{ }^\circ\text{C}$, $+20\text{ }^\circ\text{C}$ and $+80\text{ }^\circ\text{C}$, respectively).

Laponite and Cloisite® differ in their platelet size and the CEC value. CEC value of Laponite RD and Cloisite® Na are ~ 60 and $\sim 100\text{-}150$ mequ/100g, respectively. Hence, the surfactant content vary in the clays proportionally (surfactant

content in C, dL and cL are reported in Chapter 3, Table 3.2). Expectedly, hydrophobicity of C is also higher compared to both dL and cL. Hence, the compatibility with the polymer, especially with the amorphous portion is also better with C compared to dL and cL.

Table 4A.1: Dynamic mechanical properties of TPUCNs

Sample ID	Storage Modulus (MPa)				T _g (°C)		tan δ _{max}
	-60 °C	-20 °C	+20 °C	+80 °C	by DMA	by DSC	
S0	1586.0	99.4	13.0	7.7	-22	-39	0.59
S1C	2185.0	186.1	36.0	13.7	-23	-39	0.57
S3C	2303.7	244.4	51.8	19.8	-23	-40	0.50
S5C	2622.3	250.4	57.7	21.7	-22	-40	0.46
S7C	2556.6	250.0	58.1	22.8	-22	-40	0.45
S1dL	1752.0	106.4	14.7	7.9	-22	-40	0.59
S3dL	1830.0	131.2	20.0	13.3	-21	-40	0.57
S5dL	1734.0	101.0	17.1	9.8	-21	-40	0.53
S7dL	1569.1	100.7	13.9	7.9	-21	-40	0.52
S1cL	1775.0	120.0	15.0	9.2	-22	-40	0.58
S3cL	1874.9	155.8	21.1	14.3	-23	-40	0.56
S5cL	1834.5	144.6	18.5	11.9	-22	-40	0.55
S7cL	1750.6	120.5	15.7	10.6	-22	-41	0.53

Table 4A.2: Percentage change in Dynamic mechanical properties of TPUCNs

Sample ID	% increase in Storage Modulus (MPa) of PUCN w.r.t. pure TPU			
	-60 °C	-20 °C	+20 °C	+80 °C
S1C	37.8	87.2	176.9	77.9
S3C	45.2	145.9	298.5	157.1
S5C	65.3	151.9	343.8	181.8
S7C	61.2	151.5	346.9	196.1
S1dL	10.5	7.0	13.0	2.6
S3dL	15.4	32.0	53.8	72.7
S5dL	9.3	1.6	31.5	27.3
S7dL	-1.1	1.3	6.9	2.6
S1cL	11.9	20.7	15.4	19.5
S3cL	18.2	56.7	62.3	85.7
S5cL	15.7	45.5	42.3	54.5
S7cL	10.4	21.2	20.8	37.7

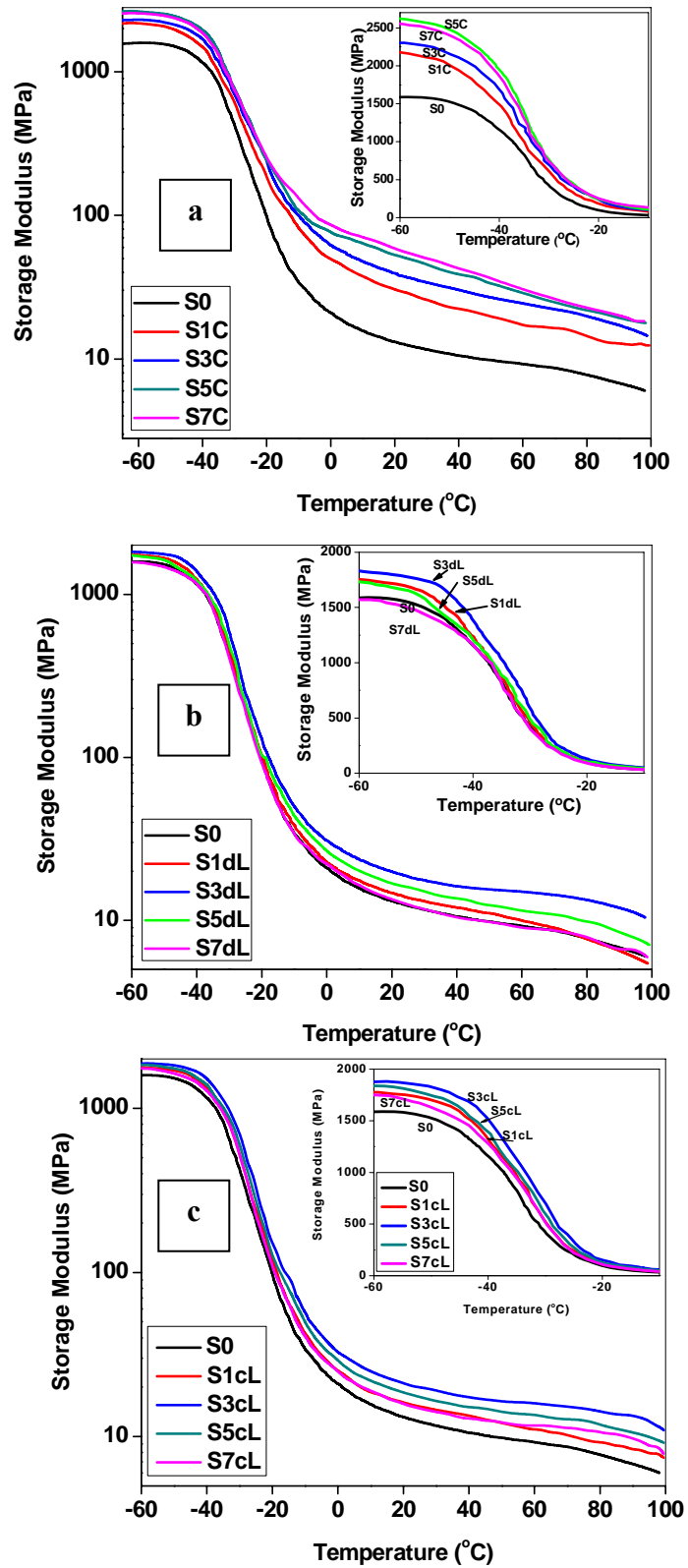


Figure 4A.8: Storage Modulus vs. temperature for (a) SC, (b) SdL & (c) ScL
(Inset in all the figures represents change in storage modulus from -60 °C to +30 °C)

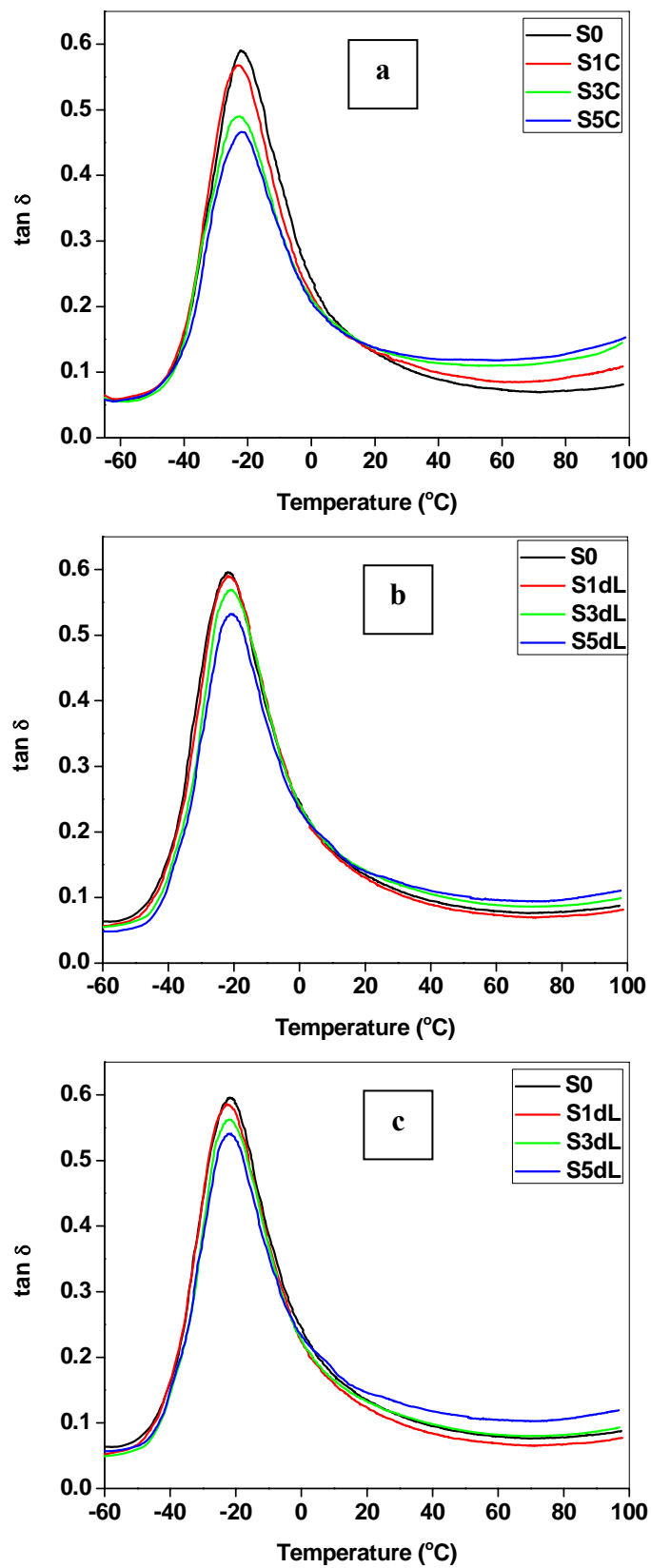


Figure 4A.9: $\tan \delta_{\max}$ vs. temperature for (a) SC, (b) SdL & (c) ScL

Due to higher hydrophilic nature and less percent of modification in case of modified Laponites, aggregation tendency is more compared to C and they tend to reaggregate, if higher amount is loaded in the polymer matrix. This may be the reason for optimum concentration of Laponite clay to be at 3%, whereas, for Cloisite® it turns out to be 5%.

4A.8 Thermogravimetric Analysis (TGA)

Figure 4A.10 and 4A.11 show the TGA and DTG thermograms of the nanocomposites, respectively. Table 4A.3 reveals the onset degradation temperature (T_i), temperature corresponding to the first (T_{1max}) and second maximum degradation (T_{2max}). The maximum increase in T_i is found to be 17.5, 8.3 and 11.4 °C, respectively for SC, SdL and ScL with 1% clay content. However, T_i decreases marginally (but steadily) with the increase in clay content. T_{1max} , which corresponds to the degradation of hard segment [Petrovic et al. (1994); Shieh et al. (1999)] also follows nearly the same trend like the T_i (except for S7cL) but T_{2max} , which corresponds to the degradation of soft segment [Petrovic et al. (1994); Shieh et al. (1999)] follows a reverse trend (it increases with the increase in clay content).

From Table 4A.3 it is evident that the T_i value decreases with the increase in clay content in all the three composites but interestingly it comes down below that of the neat TPU with S5dL and S7dL as well as with S7cL. This may be attributed to the decomposition of excess alkyl ammonium ion left over in the clay gallery. However, T_{1max} is always higher than that of the neat TPU. It is also interesting to observe that, T_{2max} for SC is always higher than that of the neat TPU (Fig. 4A.11a) but it is less for SdL (Fig. 4A.11b) and ScL (Fig. 4A.11c) upto 5% clay content. The higher thermal stability of SC as compared to SdL and ScL can be ascribed to the higher degree of dispersion of C as compared to dL and cL in the TPU matrix. Greater thermal stability

of ScL as compared to that of SdL is possibly due to improved (slightly) dispersion of cL in the TPU matrix as compared to that of dL.

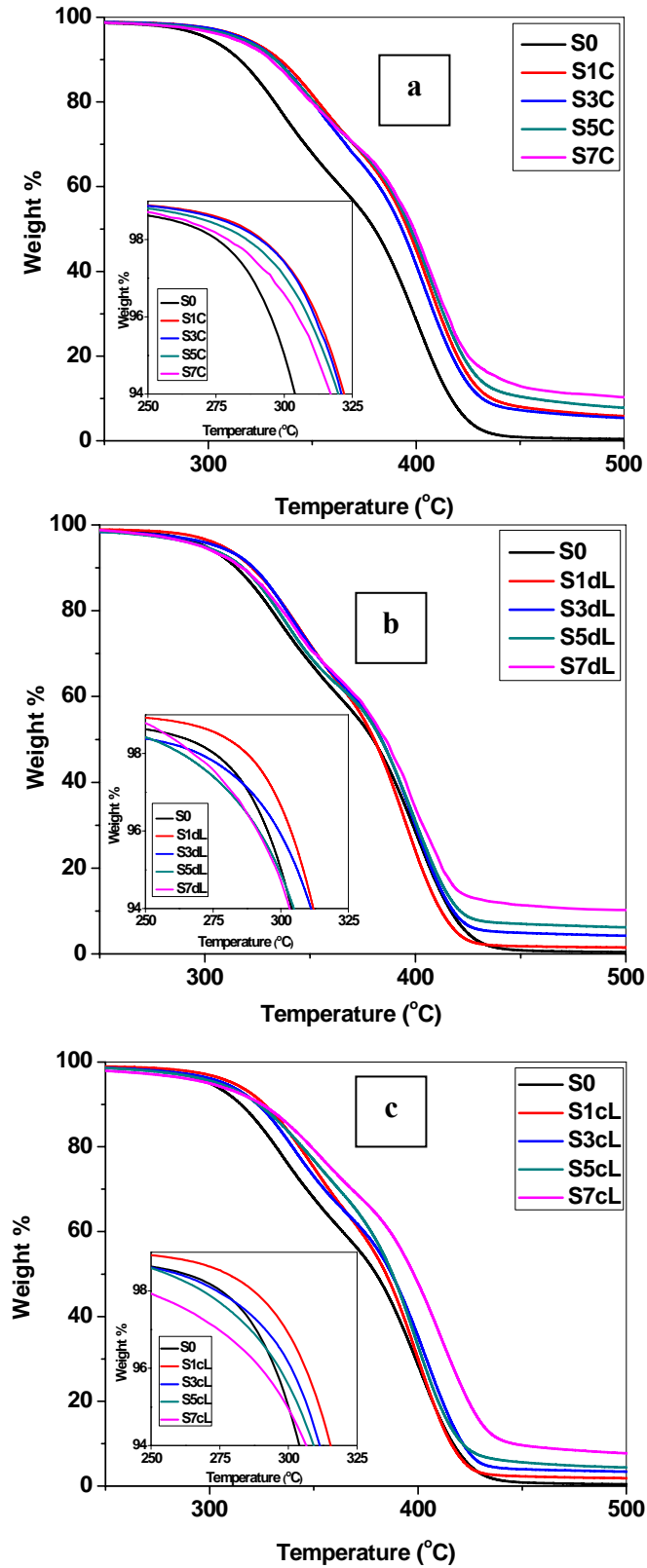


Figure 4A.10: TGA thermograms for (a) SC, (b) SdL and (c) ScL
(*Insets in all temperatures represent the TGA in the temperature range of 250-325 °C*)

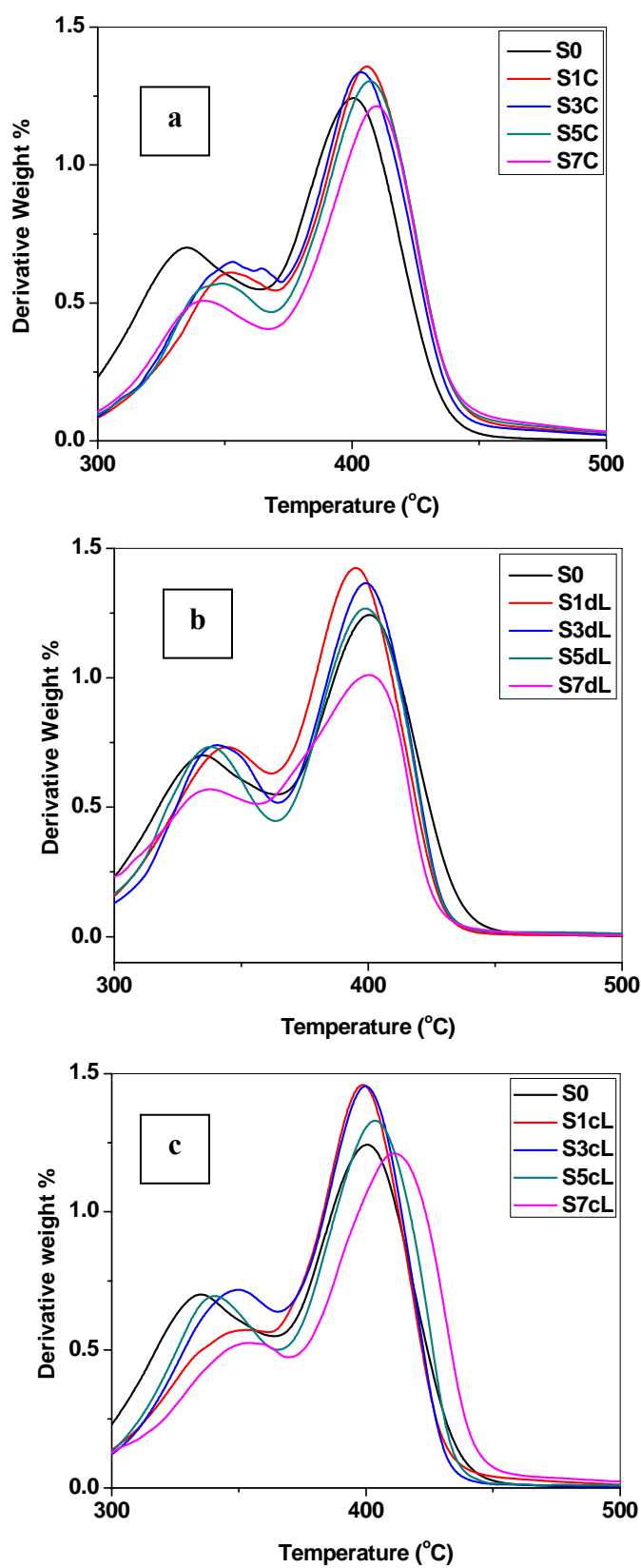


Figure 4A.11: DTG thermograms for (a) SC, (b) SdL and (c) ScL

Table 4A.3: TGA results of TPU-clay nanocomposites

Sample ID	T _i (°C)	T _{1max} (°C)	T _{2max} (°C)
S0	300.0	335.1	401.6
S1C	317.5	353.3	406.0
S3C	316.7	353.3	403.3
S5C	314.8	348.6	407.7
S7C	311.4	341.9	409.8
S1dL	308.3	344.3	395.8
S3dL	306.0	340.2	398.6
S5dL	299.2	337.9	399.1
S7dL	296.5	337.4	400.2
S1cL	311.4	353.3	398.5
S3cL	307.0	350.0	400.0
S5cL	303.7	340.7	403.2
S7cL	299.6	354.1	411.2

4A.9 Isothermal TGA

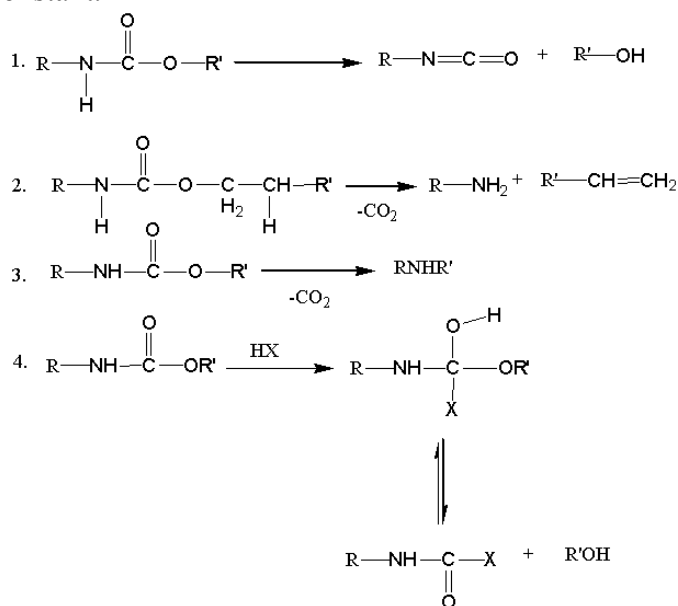
The activation energy of degradation for unfilled and filled polymeric systems can be calculated by using both isothermal and dynamic methods [Fambri et al. (2001); Lu et al. (2002); Nam and Seferis (1992); Zonga et al. (2004)]. An attempt is made in this work to carefully look into the effect of modifier and type of clay on the degradation behavior of TPUCN under isothermal conditions. For this study three different temperatures (300, 325 and 350 °C) have been selected based on the degradation behavior of TPU via TGA experiment (with dynamic heating) as depicted earlier (Section 4A.8). Figure 4A.12 shows the isothermal TGA thermogram of S0, S1C, S1dL and S1cL at different temperatures. The nanocomposites are represented here in as Sxy_z, where, x stands for weight % of clay, y stands for types of clay and z represents the corresponding temperatures at which isothermal experiment was carried out. Plausible mechanisms of degradation of TPU are shown in Scheme 4A.1.

In absence of any external stimuli it is expected to follow a first order rate equation and the equation is represented below:

$$\ln C = -kt + \ln C_0 \quad \dots\dots\dots (4A.1)$$

$$\text{or } \ln (C / C_0) = -kt \quad \dots\dots\dots (4A.2)$$

A plot of $\ln (C/C_0)$ vs. 't' should yield a straight line passing through origin with a slope of -k. In this case, C is the weight after time 't', 'C₀' is the initial weight and 'k' is the rate constant.



Scheme 4A.1: Degradation mechanisms of polyurethane

The increase in 'k' value at higher temperatures indicates the increased rate of degradation with the increase in temperature.

According to Arrhenius equation, the temperature dependent rate of degradation can be related to the activation energy as:

$$k = A e^{-E/RT} \quad \dots\dots\dots (4A.3)$$

$$\text{or } \ln k = \ln A - E/RT \quad \dots\dots\dots(4A.4)$$

Hence, the plot of $\ln k$ vs. $1/T$ results in a straight line with a slope of $-E/R$, where, 'E' is the activation energy, 'R' the universal gas constant (8.314 J/mol-K), 'T' the absolute temperature and 'A' is the pre-exponential factor. From the slope of

the curve, activation energy 'E' can be calculated. The rate constants and activation energy of the neat TPU, S1C, S1dL and S1cL have been calculated and presented in Table 4A.4.

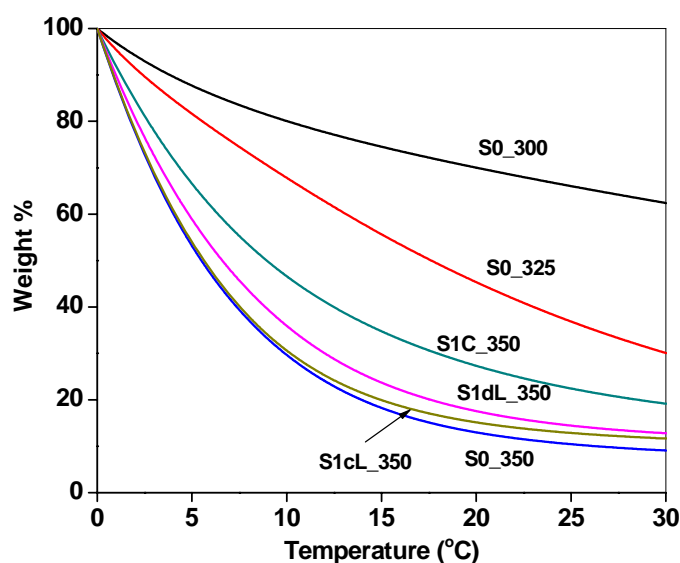
Figure 4A.12 shows the isothermal TGA thermogram of S0, S1C, S1dL and S1cL at different temperatures. The nanocomposites are represented here in as S_{xy_z}, where, 'z' represents the corresponding temperatures at which isothermal experiment is carried out. Two factors mostly contribute to the isothermal degradation process (i) polymer decomposition and (ii) physical stabilization. It is observed that at 300 °C, the rate constant 'k' remain indifferent for the neat TPU, S1C, S1dL and S1cL. At 325 °C, 'k' value of the neat TPU is marginally higher than those of S1C and S1dL ('k' value remaining indifferent for S0 and S1cL). At this temperature 'k' value follows the order S0~S1cL>S1C>S1dL. However, at 350 °C, 'k' value follows the order S0>S1cL>S1dL>S1C (Table 4A.4). In all the cases, 'k' value increases with the increase in temperature (i.e., 'k' value follows the order $k_{300} < k_{325} < k_{350}$). From the 'k' values it is quite obvious that S1C is providing better thermal stability to the TPU. Although the same is not reflected at 325 °C but it is quite clear at higher temperatures.

However, the activation energy follows the order S0>S1cL>S1dL>S1C. As observed in earlier section, thermal stability follows the order S0<S1dL< S1cL<S1C. In all the cases, the activation energy is found to decrease as compared to the neat TPU although an increase in thermal stability is observed by TGA with the dynamic temperature ramp. Similar results have been reported recently by Fambri et al. (2001) by adopting similar techniques.

Table 4A.4: Rate constants at different isothermal degradations

Sample ID	$k_{300} (\text{sec}^{-1}) \times 10^{-3}$	$k_{325} (\text{sec}^{-1}) \times 10^{-3}$	$k_{350} (\text{sec}^{-1}) \times 10^{-3}$	Activation Energy (J/mole)
S0	0.3 (0.95)	0.7 (1.00)	1.5 (0.92)	95.54
S1C	0.3 (1.00)	0.5 (0.97)	1.0 (0.96)	71.27
S1dL	0.3 (0.95)	0.6 (1.00)	1.3 (0.93)	86.92
S1cL	0.3 (0.95)	0.7 (0.96)	1.4 (0.91)	91.51

(* Values given inside parenthesis indicate the correlation coefficient)


Figure 4A.12: Isothermal TGA thermograms of TPUCN

The increase in thermal stability is due to the non-conducting barrier effect of inorganic clay platelets. Although, the exact reason for the decrease in activation energy is not known but there may be two reasons as speculated below:

- (i) one may be due to the complex mechanism followed at different temperatures (as degradation of the TPU follows a complex mechanism) and
- (ii) the second may be due to the contribution of the initial thermal history (10 °C ramp from room temperature to 300, 325 and 350 °C).

4A.10 Conclusions:

Cloisite® 20A exhibits better dispersion as compared to their modified Laponite based counterparts when dispersed in the TPU. Modified Laponite has a distinct affinity to be associated with the hard domain of the TPU. These differences in morphologies are quite reflected in the properties of the TPUCN.

4A.11 References:

Carrado K. A. (2000) Synthetic organo-and polymer-clays: preparation, characterization, and materials applications, *Applied Clay Science* 17, 1-23

Chen T. K., Shieh T. S., Chui J. Y. (1998) Studies on the First DSC Endotherm of Polyurethane Hard Segment Based on 4,4'-Diphenylmethane Diisocyanate and 1,4-Butanediol, *Macromolecules* 31, 1312-1320

Fambri L., Pegoretti A., Gavazza C., Penati A. (2001) Thermooxidative stability of different polyurethanes evaluated by isothermal and dynamic methods, *Journal Applied Polymer Science* 81, 1216-1225

Korley L. T. J., Liff S. M., Kumar N., McKinley G.H., Hammond P.T. (2006) Preferential Association of Segment Blocks in Polyurethane Nanocomposites, *Macromolecules* 39, 7030-7036

Liff S. M., Kumar N., McKinley G. H. (2007) High-Performance elastomeric nanocomposites via solvent exchange processing, *Nature Material* 6, 76-83

Lu M. G., Lee J. Y., Shim M. J., Kim S. W. (2002) Thermal degradation of film cast from aqueous polyurethane dispersions, *Journal Applied Polymer Science* 85, 2552-2558

Nam J. D., Seferis J. C. (1992) Generalized composite degradation kinetics for polymeric systems under isothermal and nonisothermal conditions, *Journal of Polymer Science Part B: Polymer Physics* 30, 455-463

Petrovic Z. S., Zavargo Z., Flynn J. F., Macknight W. J. (1994) Thermal degradation of segmented polyurethanes, *Journal Applied Polymer Science* 51, 1087-1095

Seymour R. W., Cooper S. L. (1973) Thermal analysis of Polyurethane block copolymers, *Macromolecules* 6, 48-53

Shieh Y. T., Chen H. T., Liu K. H., Twu Y. K. (1999) Thermal degradation of MDI-based segmented polyurethanes, *Journal Polymer Science Part A: Polymer Chemistry* 37, 4126-4134

Shu Y. C., Lin M. F., Tsen W. C., Chuang F. S. (2001) Differential scanning calorimetry analysis of silicon-containing and phosphorus-containing segmented polyurethane. I - Thermal behaviors and morphology, *Journal Applied Polymer Science* 81, 3489-3501

Tsen, W. C., Chuang, F. S. (2006) Phase transition and domain morphology of siloxane-containing hard-segmented polyurethane copolymers, *Journal of Applied Polymer Science* 101, 4242-4252

Zonga R., Hua Y., Wang S., Song L. (2004) Thermogravimetric evaluation of PC/ABS/montmorillonite nanocomposite, *Polymer Degradation and Stability* 83, 423-428

CHAPTER 4B

**RHEOLOGICAL CHARACTERISTICS OF TPUCN BASED
ON MODIFIED LAPONITE AND CLOISITE®**

A part of this chapter has been published in:

Rheologica Acta 49 (2010) 865

4B.1 Introduction

Rheology is an important tool to assess the processing characteristics of polymers and polymer composites. Flow behavior of polymer melts depends basically on molecular characteristics [Brydson (1981)], flow geometry [Ma et al. (1985); Yoo and Han (1981)] and processing conditions [Ferry (1980); Williams et al. (1955)] such as, temperature, shear rate or frequency.

The rheological behavior becomes more complex in case of filled polymer systems, because of the interactions between the polymers and the reinforcing fillers. ‘Payne effect’ plays an important role in determining mechanism of reinforcement of filled polymeric systems [Payne and Whittaker (1971)]. It is basically attributed to the breakdown of filler–filler networks at lower dynamic strain levels. Linear and non-linear viscoelastic properties in the molten state are generally useful to determine the degree of polymer–filler interactions and the structure-property relation of the polymeric materials. As a result, rheology appears to be a unique technique for the study of polymer nanocomposites. Rheometry is the measuring arm of rheology and its basic function is to quantify the rheological parameters of practical importance. Rheology of nanocomposites filled with organically modified nanoclays has been reviewed by Ray (2006).

Owing to its two-phase morphology, TPU is a very complex system. Addition of nanoclay adds further complexity to the system. Hence, the contemporary literature is scanty on the complete rheological analysis of the TPU-clay nanocomposite systems.

This chapter deals with the detailed rheological analysis of the TPUCNs based on Cloisite® 20A and two varieties of modified Laponites (dL and cL). Different experimental modes like Strain sweep, Temperature sweep, Time sweep, Frequency

sweep and Stress relaxation have been used to monitor the flow behavior of the nanocomposites and the results are presented in the subsequent sections of the present chapter.

4B.2 Strain Sweep

The amplitude dependent decrement of the dynamic storage modulus of filled polymers (at low dynamic strain levels) is often referred as the ‘Payne effect’ [Payne (1965)]. In case of the neat TPU, storage modulus shows considerable strain dependency even at lower strains (non-linearity due to polymer structure). Whereas, several factors like, polymer-filler interaction, filler-filler interaction, available surface area of filler in the matrix etc. can affect the strain dependencies of the TPUCN [Fröhlich et al. (2005)]. Percentage drop in modulus values at different dynamic strain percent (1, 7, 20, 70 and 100%) are compared with the initial modulus for the neat TPU and TPUCNs, respectively (Table 4B.1).

The modulus decreases monotonously with respect to the strain %, irrespective of the type of filler used. SC registers higher decrement in modulus over % strain as compared to Laponite based nanocomposites. ScL exhibit stronger ‘Payne effect’ as compared to their SdL counterparts (Table 4B.1). The greater amount of drop in modulus in case of SC as compared to those of SdL and ScL can be ascribed to the soft segment preference of C in combination with its greater platelet size. However, the stronger ‘Payne effect’ of the ScL as compared to those of SdL is probably due to their random distribution in both hard and soft domains as depicted in the earlier chapter.

A schematic representation explaining the decrement in modulus of the neat TPU at different strain levels is shown in Scheme 4B.1. Accordingly, the effect of strain for various nanocomposites is represented in Scheme 4B.2. Increase in the level

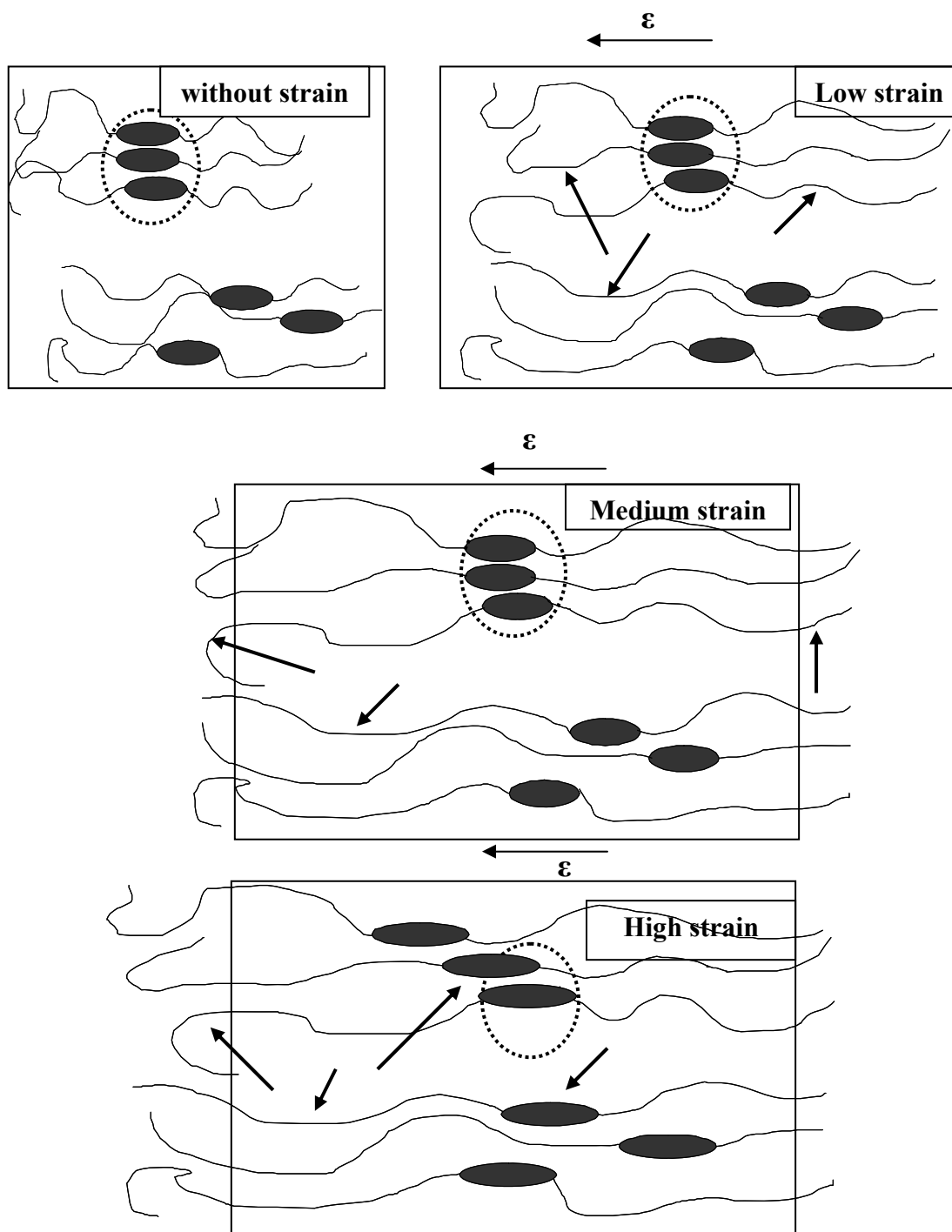
of strain from low to high mainly transfers the stress from soft segment to the hard domain (Scheme 4B.1). In case of SC, application of strain results in breakage of the secondary forces within the hard domain, between filler-filler and filler-polymer. Whereas, in case of SdL, application of strain results in breaking the secondary forces within the hard domain (which are already weak due to the hard domain preference of dL), filler-filler and filler-polymer interactions. Similarly, in case of ScL, application of strain results in breaking the secondary forces between the hard domain (which is partly preserved due to distribution of cL in both the segments), filler-filler (its contribution is supposed to be more than that of dL) and filler-polymer interaction (Scheme 4B.2).

Table 4B.1: Percentage decrease in modulus value as compared to the initial modulus at different strain levels

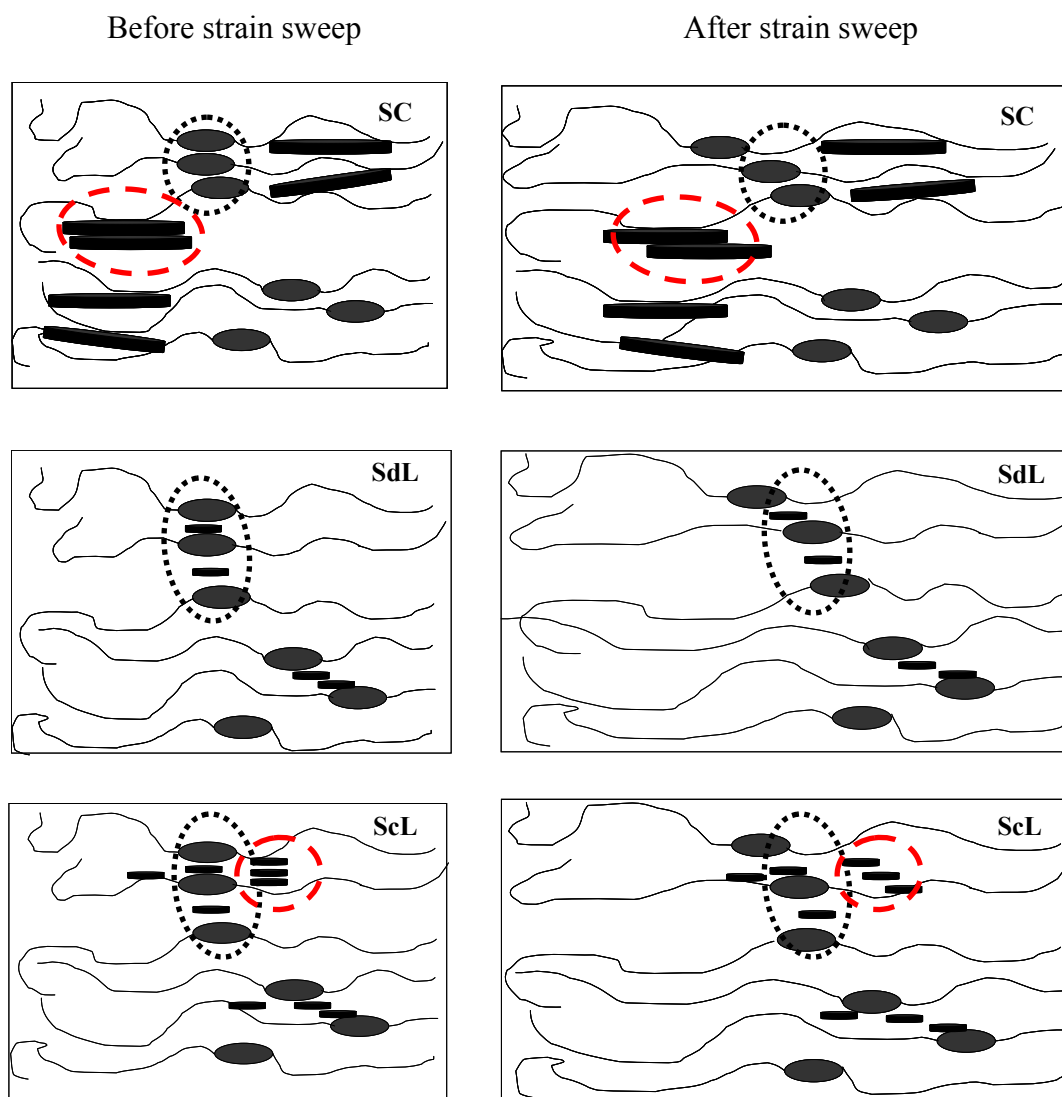
Sample ID	% drop in modulus value at different strain levels				
	1%	7%	20%	70%	100%
S0	7.8	13.9	28.0	60.7	68.6
S1C	6.2	23.9	43.1	71.0	79.0
S3C	17.5	29.7	48.3	71.0	81.3
S5C	22.5	48.3	57.1	78.1	83.6
S1dL	8.2	12.2	18.2	44.9	57.2
S3dL	9.3	16.0	25.2	54.9	63.7
S5dL	5.7	9.6	16.9	45.1	54.4
S1cL	13.1	24.9	40.7	69.5	75.7
S3cL	12.8	27.3	39.3	66.4	74.5
S5cL	12.4	26.4	38.1	64.3	72.2

Drop in modulus increases with the increase in C content in the TPU matrix and the percentage drop in modulus is independent of strain at higher levels (>20%). The maximum decrease in modulus value is observed with S5C. The decrease in modulus with an increase in amount of filler is a quite obvious phenomenon that has been observed by many researchers [Lion et al. (2004); Payne (1962); Zhong et al. (2005)]. A gradual increase in % decrement in modulus at higher strain levels for all

samples indicates that other mechanisms of deformation as mentioned above gradually contributes over filler structure breakdown.



Scheme 4B.1: Schemetic illustration of deformation of TPU against applied strain
(*The encircled portion indicate the hard domain region and the arrows indicate the deformed region due to the application of strain)



Scheme 4B.2: Speculative depiction of deformation of TPUCN by applied strain
 (*The encircled regions indicate the original position of the hard domains and nanoclays)

For dL, maximum decrement in modulus is observed with S3dL. It is due to the greater amount of filler-filler and polymer-filler interaction at this particular clay content. The decrement in modulus value in case of S5dL is even less than that of the neat TPU. This is possibly due to the combined accomplishment of the ball bearing action (spherical aggregate formation, which can lead to rolling effects on polymer chains in shear deformation) and the hard domain preference of dL (due to the hard domain preference the clay aggregate destroys the partial crystallinity in the hard

domain, as revealed from the WAXRD diffractograms depicted in Section 4A.2 of the previous chapter). In case of ScL the decrement in modulus value remains nearly same uncaring of the clay content. This is due to the similar size scale of aggregation at lower and higher clay contents and the random distribution of cL in hard and soft domains (as it was observed in the equilibrium bulk morphology of such composites).

4B.3 Temperature Sweep

A temperature range of 130 to 220 °C was chosen to understand the effect of clay on the modulus-temperature behaviors at higher temperature regions. The study was carried out at a heating rate of 6 °C/min. In all the cases, there is a drastic reduction in both storage (G') and loss (G'') modulus values from 140 to 170 °C followed by a comparatively slower and monotonous reduction upto 220 °C (Fig. 4B.3). The drastic reduction in modulus value is ascribed to the transition from the rubbery plateau to flow behavior and the terminal plateau corresponds to the restriction in flow. It is observed that all the nanocomposites possess lower storage modulus compared to the neat TPU for 1% clay content (Table 4B.2) at the range of temperatures studied here (130-220 °C). This is possibly due to the change in molecular relaxation due to which shear thinning events dominates at lower clay content. However, an increasing trend in modulus values with the increase in clay content in all the cases is also noticed.

Figure 4B.3 shows the storage and loss modulus values of the neat TPU and TPUCN with 3 weight % of various clays. Overall, SC possess higher storage and loss modulus values as compared to their Laponite counterparts at the whole range of temperatures. Highest modulus value of S3C at lower temperature region is possibly due to the longer platelet size, greater exfoliated structure (resulting in a greater polymer filler interaction) and soft domain preference of C (due to the combined

effect of inorganic and organic hard domains). Amongst the Laponite based nanocomposites, S3cL registers higher storage modulus values as compared to S3dL at low temperature regions (upto 170 °C). This is again due to the combined effect of organic and inorganic hard domains present in case of ScL (which is absent in case of SdL due to the destruction in crystallinity of the hard domain). However, at higher temperature region, no significant change in modulus is observed. This is due to the complete melting of the hard domain as a result of which TPU loose its stiffness.

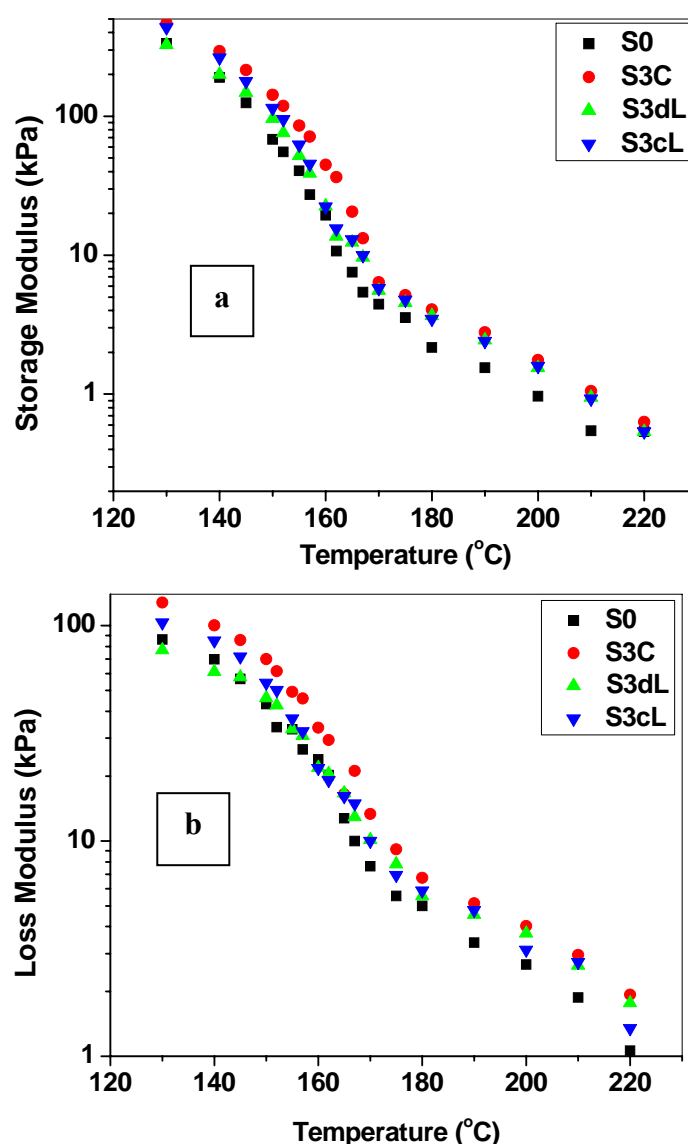


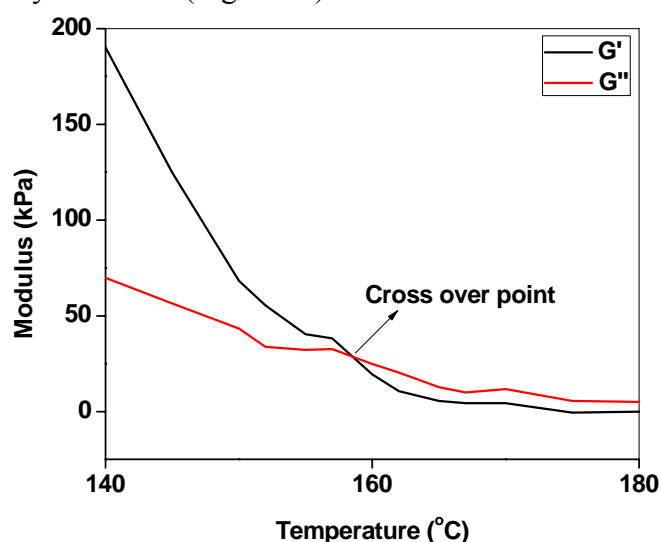
Figure 4B.3: Change in (a) Storage and (b) Loss modulus with respect to temperature of neat TPU and TPUCNs with 3% clay content

Table 4B.2: Storage modulus at four different temperatures for neat TPU and TPUCN with 1% clay content

Temperatures (°C)	Storage Modulus value (kPa)			
	S0	S1C	S1dL	S1cL
130	334.6	324.6	308.9	309.7
150	68.2	65.4	66.1	66.6
170	4.4	3.1	2.9	3.0
190	1.5	1.0	0.9	0.9

4B.4 Frequency Sweep

The changes in dynamic storage moduli and complex viscosity values with angular frequency were monitored. A monotonous decrease in complex viscosity (η^*) and a monotonous increase in dynamic storage modulus (G') is observed with the increase in frequency, independent of the temperatures studied here (140 and 170 °C), as it will be elaborated later. In general, two different sorts of behavior are encountered at two different temperatures. At 140 °C, $G' > G''$ whereas, at 170 °C, $G'' > G'$, for all the nanocomposites (independent of the types of clay). Accordingly, a crossover between G' and G'' has been observed in the temperature sweep experiment at a constant frequency of 0.5 Hz (Fig. 4B.4).

**Figure 4B.4:** Crossover point of the storage and loss modulus with respect to temperature

4B.4.1 Effect on Complex Viscosity at 140 °C

From the time sweep experiment of S0, S3C, S3dL and S3cL at 140 °C (Fig. 4B.5a), it is evident that the modulus values of S0 remain nearly same with respect to time. However, the modulus values increase upto an order of 30-40 kPa for the filled systems. The effect is more prominent in case of S3C as compared to S3dL and S3cL. This is possibly because of the mutual reorganization of nanoclays and TPU molecules thereby enabling optimum secondary interactions between the filler and polymer. However, time sweep above 150 °C (not shown), shows nearly marginal change in the modulus values with respect to time. Thus beyond 150 °C (Fig. 4B.5b) equilibrium reorganization is subdued.

Figure 4B.6 (a-d) displays the complex viscosity vs. frequency plots at 140 °C. It is observed that the complex viscosities (η^*) of SC, SdL and ScL are of the similar order of magnitude with that of the neat TPU upto 3% clay content (Fig. 4B.6 (a-d)). However, it is always higher than the neat TPU for 5% clay content independent of frequency range studied here (0.033 to 30 Hz). The lower η^* value at lower clay content is ascribed to the contribution of the shear thinning event due to the change in molecular relaxation (this is in agreement with our earlier observations in Section 4B.3). However, greater η^* value at 5% clay content is due to the increased state of aggregation. At higher clay content, the extent of intercalated structures possibly diminishes and the shear thinning events are restricted by preponderance of larger scale aggregated structures [Ray (2006)]. The slight increase in complex viscosity value in case of S3C as compared to the neat TPU at higher frequency region may be due to the mutual reorganization of nanoclays and TPU molecules, thereby enabling optimum secondary interactions between the filler and polymer in case of C (as seen in the time sweep experiment).

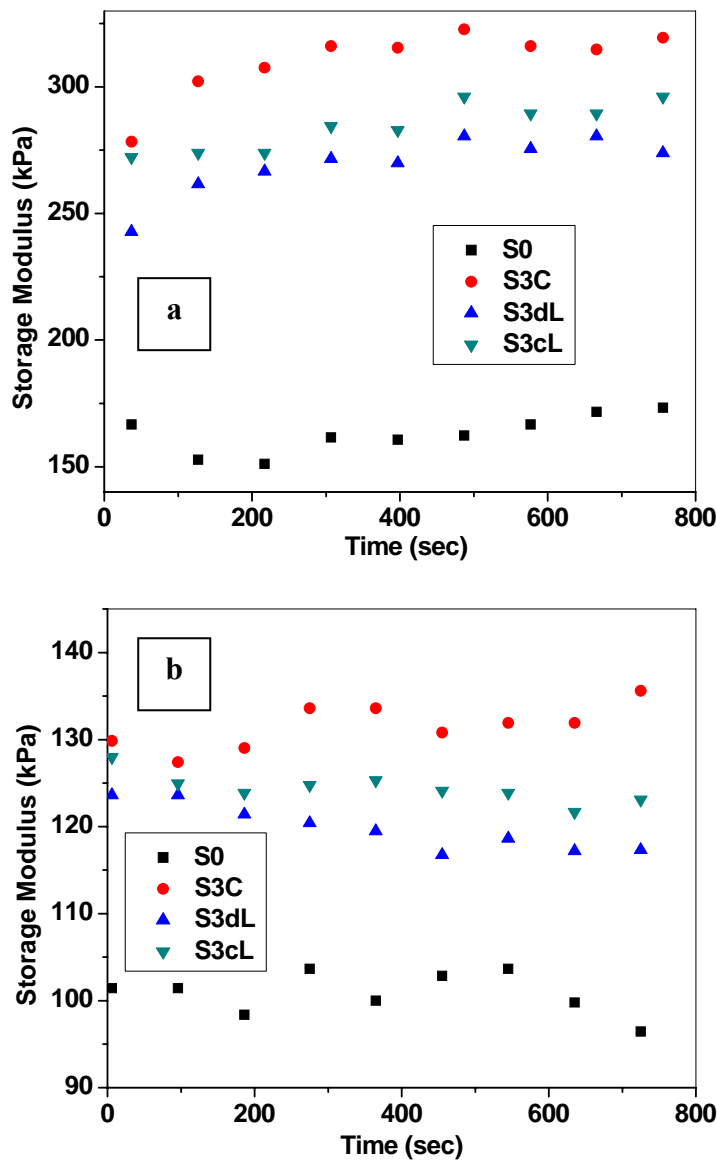


Figure 4B.5: Storage modulus vs. time at (a) 140 °C and (b) 170 °C

η^* values of S1C is always greater than those of S1dL and S1cL (e.g., η^* values of S1C, S1dL and S1cL at 3.33 Hz are 14917 Pa-s, 12263 Pa-s and 13134 Pa-s, respectively). However, at 3 and 5 % clay content, η^* values of SC are lower than that of SdL upto a frequency of 1.67 Hz and the corresponding values are greater at higher frequencies. Similarly, η^* values of SC at 3 and 5% clay content are lower than that of ScL upto 3.33 Hz and the values are greater at higher frequencies. The greater η^* value of S1C as compared to S1dL and S1cL are mainly due to the more exfoliated

morphology of clays (also due to soft segment preference and greater size) resulting in higher polymer-filler interaction. However, the frequency dependent decrease of initial viscosity also stems from the local segmental dynamics. But the increased modulus values at higher frequency region are due to the mutual reorganization of C and the TPU macromolecules. The increased η^* value at higher clay content is mainly due to the greater aggregation tendency of dL and cL as compared to that of C.

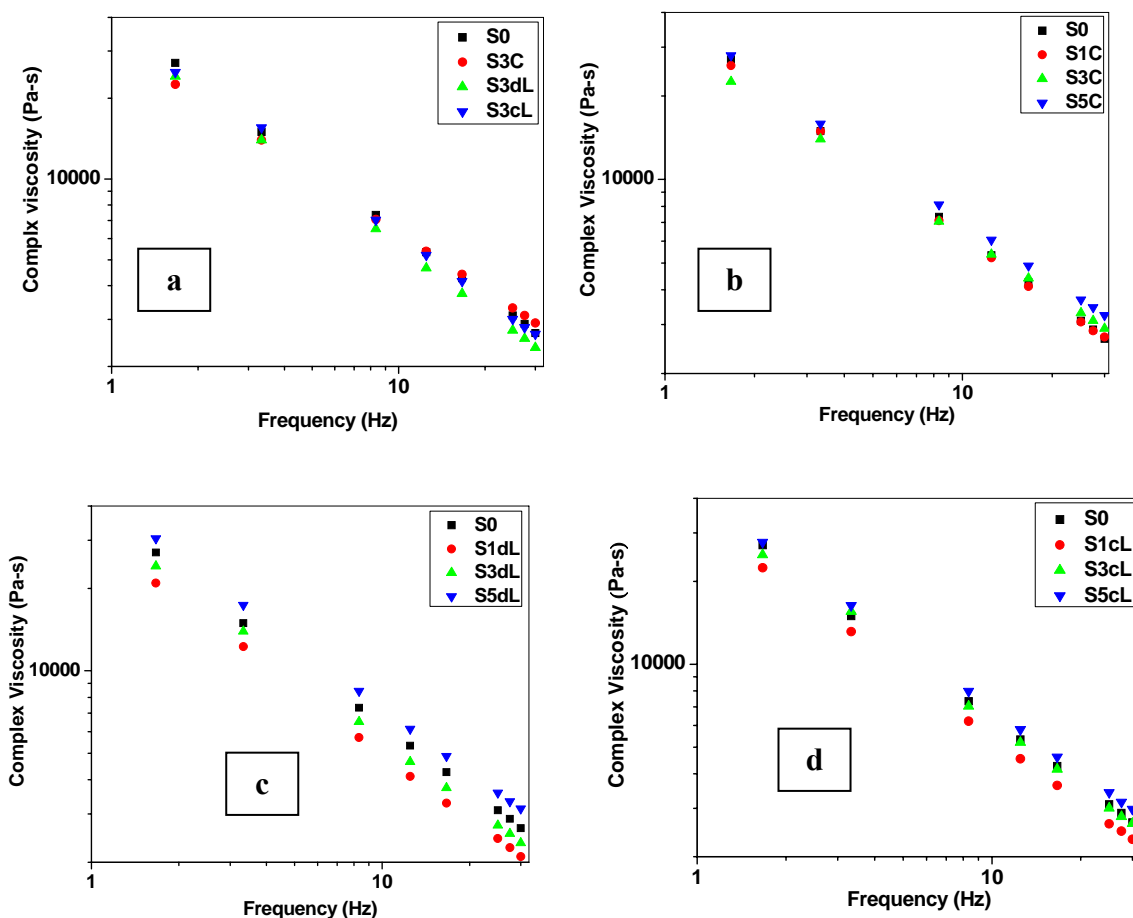


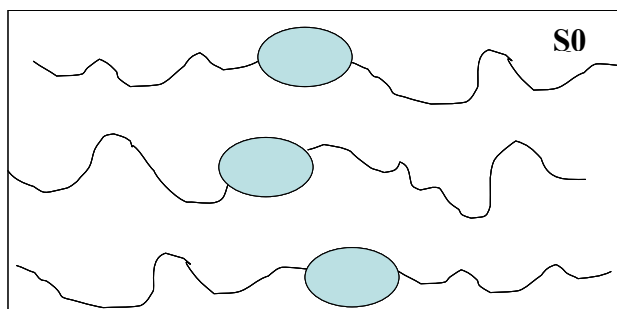
Figure 4B.6: Complex viscosity vs. frequency plots of (a) TPUCNs with 3% clay content (b) SC (c) SdL (d) ScL

The η^* values of ScL are greater as compared to their SdL counterparts at lower clay content (upto 3%). But the reverse is true at 5% clay content. The effect at lower clay content is ascribed to the hard domain preference of dL. But the increased

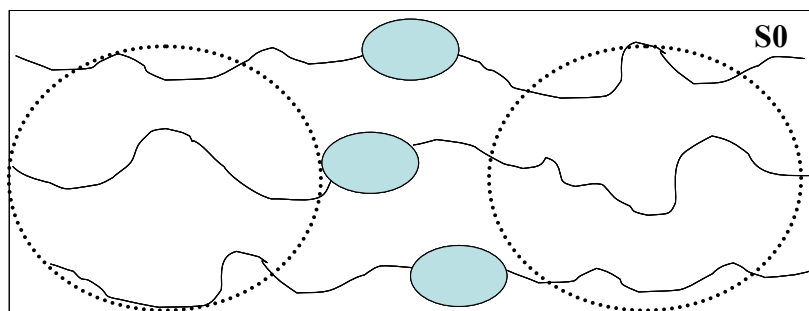
η^* value at higher clay content is possibly due to the reduced degree of preference of dL to hard segments at higher clay content.

Scheme 4B.3 represents the effect of frequency on the neat TPU at 140 °C. At low frequency region, sufficient time is allowed for the external force to elongate the soft domain to a maximum extent. However, at high frequency region, due to unavailability of time, stress gets concentrated mostly on the hard domain regions.

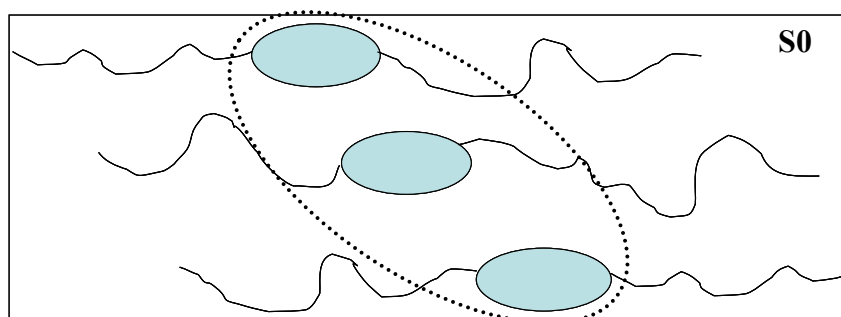
Before Experiment



Low Frequency region



High Frequency region



Scheme 4B.3: Deformation of TPU chains with respect to frequency
(*Encircled regions indicate the deformed portion of the neat TPU due to the applied dynamic stress)

Similarly, for the nanocomposites, at low frequency region, sufficient time is allowed for the stress to elongate the soft domain to a maximum extent (Scheme

4B.4). At high frequency region, due to paucity of time, stress gets concentrated mostly on the hard domain region and on the clay aggregates. Thus, a frequency dependent spectrum has been obtained especially at 140 °C. The shear thinning events especially at lower clay content can be explained based on the presence of more exfoliated structure and presence of the modifier on the clay surface. SC registers higher η^* value as compared to its Laponite based counterparts possibly due to the greater platelet size of clay and restoration of the hard domain ordering to maximum extent. However, lowest complex viscosity in case of SdL can be ascribed to the destruction of the hard domain ordering (due to the hard domain preference of clays).

4B.4.2 Effect on Complex Viscosity at 170 °C

Figure 4B.7 (a-d) displays the complex viscosity vs. angular frequency plots at 170 °C of the nanocomposites. At 170 °C, η^* values of TPUCNs follow an increasing trend with the increase in clay content independent of the type of clay used. At 170 °C, the long range ordering in the hard segment softens. Hence, most of the contributions towards the viscosity and modulus are attributed to the amount of fillers present in the matrix; following the Guth-Gold equation ((Equation 4B.1) hard or soft domain preference should not matter anymore).

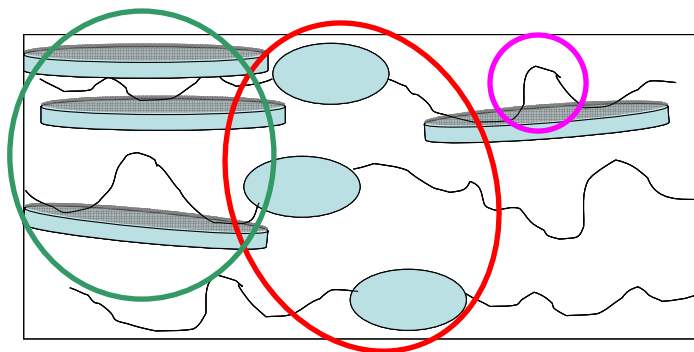
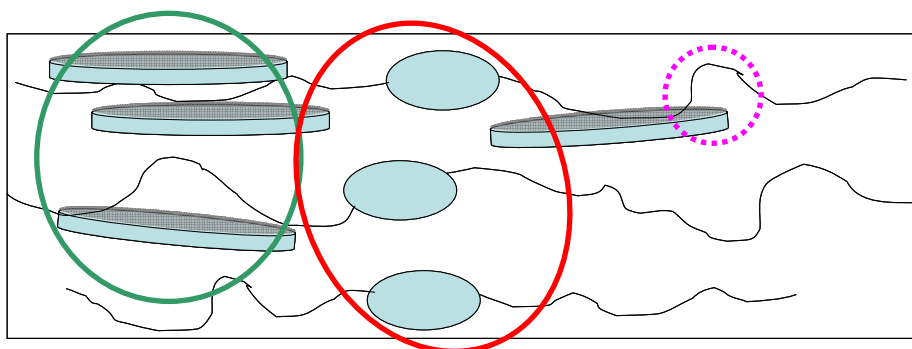
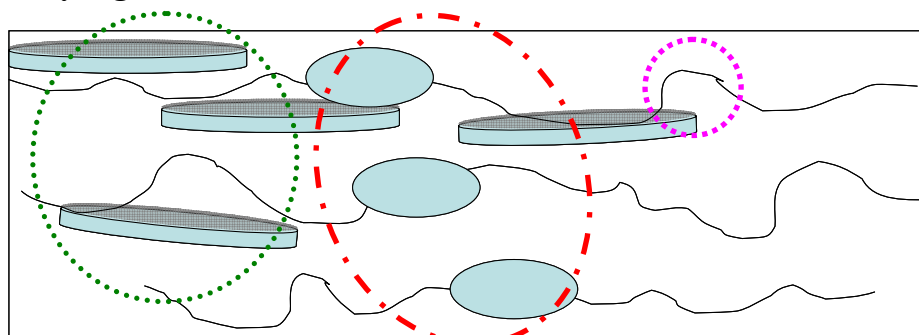
$$\eta_c = \eta_0(1 + 2.5\phi_r + 14.1\phi_r^2) \dots\dots\dots (4B.1)$$

where, η_c = Coefficient of viscosity of filled polymer

η_0 = Coefficient of viscosity of unfilled polymer

f = shape factor, related to l/d ratio of the particle

and ϕ_r = particle volume fraction

Before Experiment**Low Frequency region****High Frequency region****Scheme 4B.4:** Effect of frequency on SC

(*The solid circles indicate the original position and the dotted portion indicate the regions under deformation due to the applied dynamic stress)

Thus hard or soft domain preference should not influence the resultant viscosity at this temperature. At this temperature, η^* values of SC are higher than those of Laponite based nanocomposites with equivalent clay content. This can be ascribed to the greater size of individual platelet of C as compared to Laponite. On an average, the η^* values for ScL are higher as compared to SdL at this temperature. This is possibly because of the greater state of aggregation of dL as compared to cL.

At 170 °C, polymer chains are much labile and the presence of hard domain is also diminished. Application of even small amount of stress would enable the clay particles to move closer to each other. Thus the size of clay particles and their mutual degree of affinity are much more influential at this temperature.

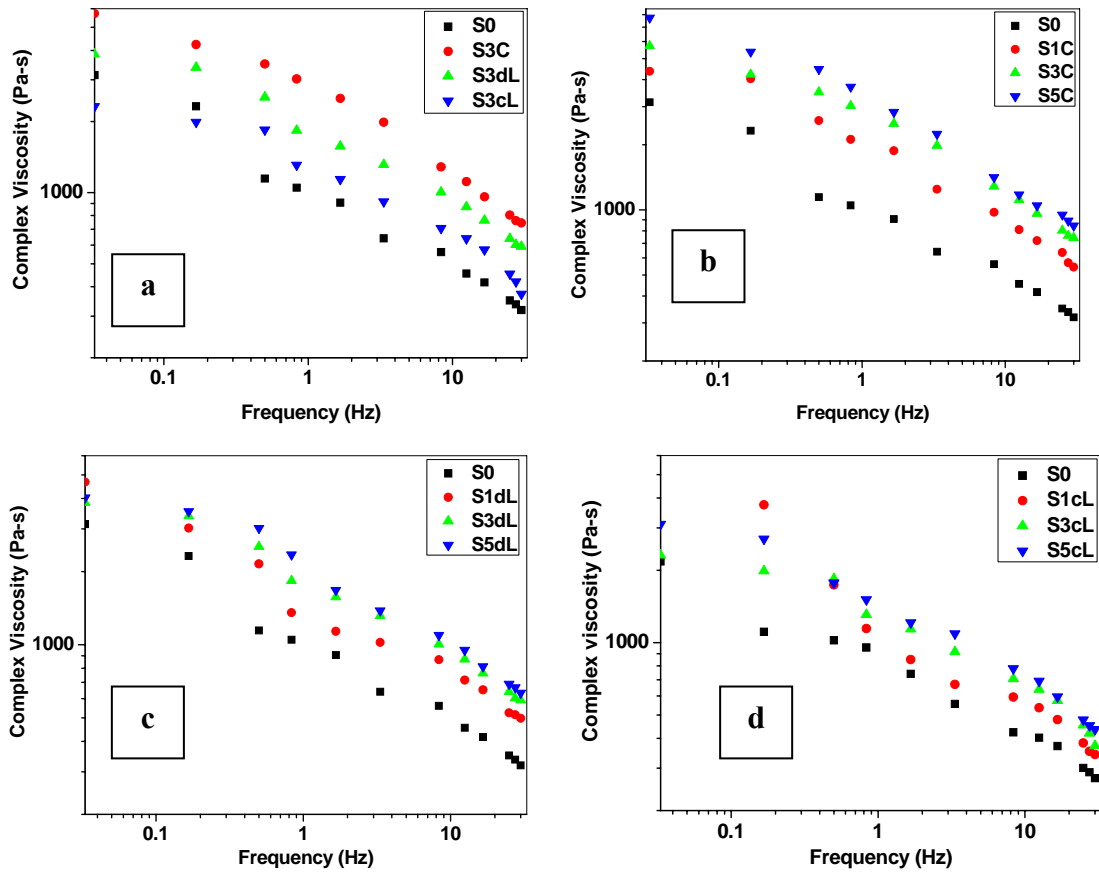


Figure 4B.7: Complex viscosity vs. frequency plot of (a) TPUCNs with 3% clay content (b) SC (c) SdL (d) ScL at 140 °C

The flow behavior index (*n*) was calculated by using the power law model, as:

$$\eta^* = k' \dot{\gamma}^{n-1} \dots\dots\dots (4B.2)$$

where, η^* is the complex viscosity, ‘*k*’ is the consistency index and $\dot{\gamma}$ is the shear rate.

Therefore Equation 4B.2 can be rewritten as:

$$\log \eta^* = \log k' + (n-1) \log \dot{\gamma} \quad \dots\dots\dots (4B.3)$$

The slope of $\log \eta^*$ vs. $\log \dot{\gamma}$ plot gives the value of ‘n’. The values of ‘n’ and ‘k’ are given in Table 4B.3.

A pseudoplastic behavior is observed in all the cases. The ‘n’ value is always higher than the neat TPU in all the nanocomposites irrespective of the type of clay and amount of clay used. This shear thinning behavior can be ascribed to the assistance in relaxation due to the presence of modifiers on the clay surface. Similar trend in shear thinning behavior is already mentioned earlier. ‘n’ value is found to follow the order SC>ScL>SdL at 140 °C. This can be ascribed to the hydrophobicity of the modifiers present on the clay surface. However, ‘n’ values of the nanocomposites are comparable at 170 °C. The consistency index ‘k’ is found not to follow any particular trend at both the temperatures.

Table 4B.3: Flow behavior index (n) and consistency index (k’) at 140 and 170 °C

Sample ID	140 °C		170 °C	
	n	k' x 10 ⁴ (Pa.s ⁿ)	n	k' x 10 ² (Pa.s ⁿ)
S0	0.18	19.05	0.66	19.49
S1C	0.20	17.38	0.67	34.67
S3C	0.26	13.80	0.68	44.66
S5C	0.23	17.38	0.67	56.23
S1dL	0.19	14.13	0.67	28.18
S3dL	0.19	16.22	0.70	30.19
S5dL	0.18	21.88	0.70	33.88
S1cL	0.21	14.12	0.67	51.28
S3cL	0.20	16.98	0.72	19.49
S5cL	0.21	18.62	0.69	23.98

4B.4.3 Effect on Modulus at 140 and 170 °C

Figure 4B.8a and b show the storage modulus vs. frequency plots of the 3% clay filled nanocomposites at 140 and 170 °C, respectively. It is observed that the storage moduli of SC, SdL and ScL, at 140 °C are lower or at the same order of

magnitude than that of the neat TPU upto 3% clay content (Figure 4B.8a). However, it is always higher than the neat TPU for 5% clay content independent of frequency range studied here (0.033 to 30 Hz). Overall, at 170 °C, the value of storage modulus of the nanocomposites is higher than the neat TPU (Figure 4B.8b). An increasing trend in the storage modulus value is observed with the increase in the clay content and this behavior is independent of the temperature. Here also similar reasons are applicable as already mentioned in earlier sections (Section 4B.4.1 and 4B.4.2).

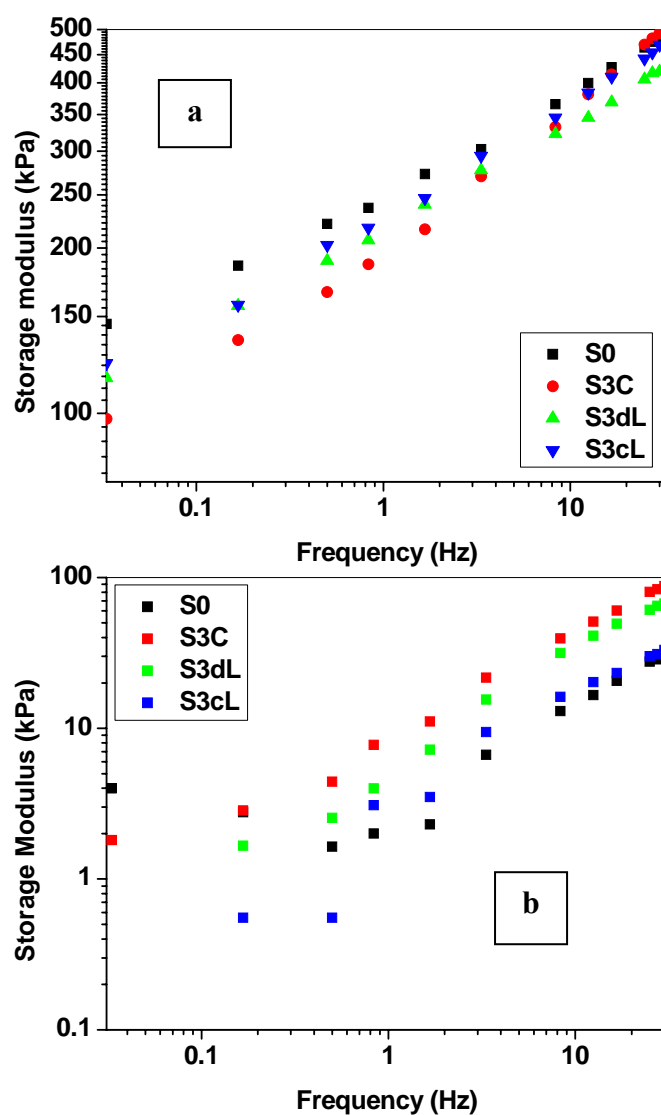


Figure 4B.8: Storage modulus vs. frequency plot of TPUCNs at (a) 140 and (b) 170 °C

4B.5 Stress Relaxation

Stress relaxation experiment was carried out at 120 °C (the temperature close enough for the destruction of the short range ordering in the hard domains).

4B.5.1 A Brief Theoretical Background on Stress Relaxation

To realize the behavior of stress relaxation, the Maxwell model - a spring of modulus ‘G’ and a dashpot of viscosity ‘η’ in serial combination, are frequently used. However, this model is not adequate to describe the molecular relaxations (e.g., glass transition or Brownian motion etc.), especially in case of a system like TPU, because of complex combinations of the several contributing units.

The Maxwell model describes the stress relaxation behavior of simple amorphous polymers qualitatively (for a singular relaxation). The expression for the stress relaxation in shear using simple Maxwell model is:

$$G = G_0 e^{-tv} \dots\dots\dots (4B.4)$$

where, G = Storage modulus at time ‘t’ s, G₀ = Initial storage modulus and

$$v = \frac{1}{\tau} \dots\dots\dots (4B.5)$$

where, ‘τ’ is the characteristic relaxation time and ‘v’ is the relaxation frequency.

Even a particular relaxation process of a simple amorphous polymer does not occur at a singular time but it happens over a distribution of time. The Generalized Maxwell model (as depicted below) can be applied to such systems for qualitative analyses as:

$$G = \sum_{i=1}^n G_i e^{-t/\tau_i} \dots\dots\dots (4B.6)$$

Various G_i’s can be replaced by a continuous function, G(τ) of the relaxation time (to

integrate the process), where this function is called a distribution of relaxation times.

In addition to the distribution $G(\tau)$, one often refers to $H(\tau)$, which is defined as:

$$H(\tau) = \tau G(\tau) \quad \dots\dots\dots (4B.7)$$

However, for this study simple Maxwell model has been used to capture the instantaneous stress relaxation time only (due to poor R^2 value at longer time).

4B.5.2 Instantaneous (0.1 s) and 30 s Stress Relaxation time at 120 °C

The ‘ τ ’ value was calculated from the plot of time vs. modulus (Fig. 4B.9), by using Equation 4B.4. A very good correlation coefficient (R^2 value >0.90) is observed upto 0.1 s time of relaxation. For longer time of relaxation, equation could not be fitted with the experimental results. Hence, ‘ τ ’ value was calculated upto 0.1 s and given in Table 4B.4. Although the ‘ τ ’ value within the fraction of a second (0.1 s) does not provide a clear picture of the flow behavior of the TPU as a whole, rather it gives insight about the instantaneous relaxation (equivalent to the running extrudate swell in steady state capillary rheology). However, to study the effect upon prolonged time (equivalent to the equilibrium extrudate swell) [Hui et al. (2009)], ‘ τ ’ value at 30 s was calculated. The values so obtained are given in Table 4B.4. The regression coefficient (R^2) values of the relaxation time at 30 s is not tabulated as the values are calculated directly by using Equation 4B.6 considering the initial modulus to be G_0 and the modulus value at 30 s to be G . It is observed that both instantaneous relaxation time and the relaxation time after 30 s are higher with the neat TPU as compared to the nanocomposites (Table 4B.4). This suggests that addition of nanoclay increases the elastic component of viscoelastic behaviors at 120 °C. ‘ τ ’ values are marginally lower in case of Cloisite® based nanocomposites as compared to their Laponite based counterparts. However, the values are nearly similar in case of SdL and ScL. Relaxation time at 30 s also follows a similar trend. The higher ‘ τ ’

values for the Laponite based TPU nanocomposites as compared to SC can be ascribed to the longer length scale of aggregation. This phenomenon is in accordance with the precedent results on longer time dependent mechanisms of relaxation of Laponite based nanocomposites [de Bruyn et al. (2008); Pignon et al. (1998)], which have been ascribed to aggregation phenomena at different length scales (from nanometer to micrometer length scales). For SC, its preference to the soft segments and more exfoliated morphology in the TPU matrix increase the elastic component of relaxation leading to diminished ' τ ' values.

Table 4B.4: Instantaneous relaxation time and relaxation time at 30 s at 120 °C

Sample ID	Instantaneous Relaxation time (s) (fitted upto 0.1 s)	Equilibrium Relaxation time (s) (at 30 s)
S0	0.27 (0.91)	24.9
S1C	0.22 (0.93)	21.9
S3C	0.20 (0.93)	20.0
S5C	0.19 (0.92)	19.3
S1dL	0.24 (0.93)	22.0
S3dL	0.24 (0.93)	22.5
S5dL	0.25 (0.92)	21.8
S1cL	0.24 (0.93)	23.4
S3cL	0.23 (0.94)	21.9
S5cL	0.23 (0.93)	21.8

* Values given in the parenthesis represent the respective correlation coefficients

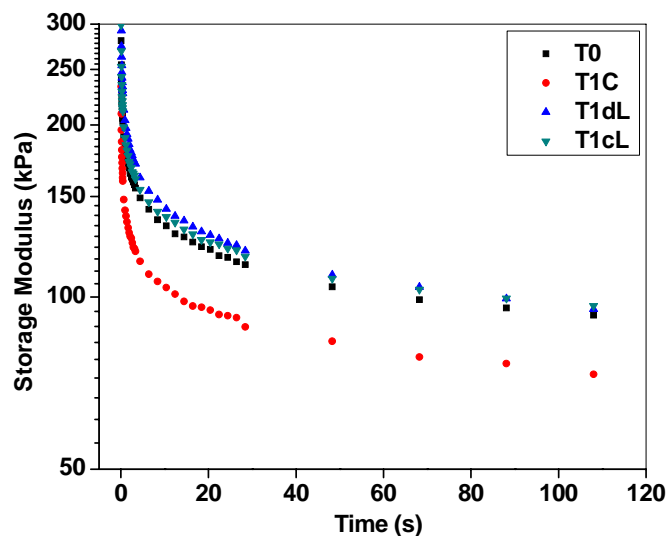


Figure 4B.9: Storage modulus vs. Time plot of TPUCN with 1% clay content at 120 °C

4B.6 Conclusions

Dynamic storage modulus and Complex viscosities of the Cloisite® based TPU-clay nanocomposite are higher than those of the Laponite based counterparts. This is because of the inferior dispersion of the modified Laponites in the TPU matrix. Hard/Soft domain preference of the nanoclays also plays a vital role to alter the dynamic rheological properties.

4B.7 References

- Brydson J. A. (1981) Flow Properties of Polymer Melts, Godwin: London
- de Bruyn J. R., Pignon F., Tsabet E., Magnin A. (2008) Micronscale origin of the shear-induced structure in Laponite–poly(ethylene oxide) dispersions, *Rheologica Acta* 47(1), 63-73
- Ferry J. D. (1980) Viscoelastic Properties of Polymers, John Wiley & Sons. Inc.: New York
- Fröhlich J., Niedermeier W., Luginsland H. D. (2005) The effect of filler–filler and filler–elastomer interaction on rubber reinforcement, *Composites: Part A* 36, 449-460
- Hui S., Chaki T. K., Chattopadhyay S. (2009) Dynamic and capillary rheology of LDPE-EVA-based thermoplastic elastomer: Effect of silica nanofiller, *Polymer Composites* 31, 377-391
- Lion A., Kardelky C. (2004) The Payne effect in finite viscoelasticity: constitutive modelling based on fractional derivatives and intrinsic time scales, *International Journal of Plasticity* 20, 1313-1345
- Ma, C. Y., White, J. L., Weissert F. C., Isayev A. I., Nakajima N., Min K. (1985) Flow Patterns in Elastomers and Their Carbon Black Compounds During Extrusion through dies, *Rubber Chemistry and Technology* 58, 815-829
- Payne A. R. (1965) Reinforcement of elastomers, Interscience: New York
- Payne A. R. (1962) The dynamic properties of carbon black-loaded natural rubber vulcanizates. Part I, *Journal of Applied Polymer Science* 6, 57-63
- Payne A. R., Whittaker R. E. (1971) Low Strain Dynamic Properties of Filled Rubbers, *Rubber Chemistry and Technology* 44, 440-478

Pignon F., Magnin A., Piau J. -M. (1998) Thixotropic behavior of clay dispersions: Combinations of scattering and rheometric techniques, *Journal of Rheology* 42, 1349-1373

Ray S. S. (2006) Rheology of Polymer/Layered Silicate Nanocomposites, *Journal of Industrial Engineering Chemistry* 12, 811-842

Williams M. L., Landel R. F., Ferry J. D. (1955) The Temperature Dependence of Relaxation Mechanisms in Amorphous Polymers and Other Glass-forming Liquids, *Journal of the American Chemical Society* 77, 3701-3707

Yoo H. J., Han C. D. (1981) Stress Distribution of Polymers in Extrusion through a Converging Die, *Journal of Rheology* 25, 115-137

Zhong Y., Zhu Z., Wang S. Q. (2005) Synthesis and rheological properties of polystyrene/layered silicate nanocomposite, *Polymer* 46, 3006-3013

CHAPTER 5

TPUCN BASED ON MODIFIED LAPONITE RDS

A part of this chapter has been published in:

Journal of Applied Polymer Science 115 (2010) 558

5.1 Introduction

It has been observed in earlier chapters that modification of the Laponite RD with dodecyl ammonium chloride and cetyltrimethyl ammonium bromide lead to inferior dispersion of the clay platelets as compared to that of Cloisite[®] 20A. Hence, another grade of Laponite series called Laponite RDS possessing similar dimension with additional site for ionic modification (the sodium pyrophosphate adsorbed on the clay surface) is chosen. The empirical formula of Laponite RDS is $\text{Na}_{0.7}(\text{Si}_8\text{Mg}_{5.5}\text{Li}_{0.3})\text{O}_{20}(\text{OH})_4 \cdot \text{Na}_4\text{P}_2\text{O}_7$ in contrast to $\text{Na}_{0.7}(\text{Si}_8\text{Mg}_{5.5}\text{Li}_{0.3})\text{O}_{20}(\text{OH})_4$ in case of Laponite RD. For Laponite RDS (LS) also same surfactants 'c' and 'd' were used for modification. This chapter deals with the structure-property relationship of the TPU-modified Laponite RDS based nanocomposites.

5.2 Wide Angle X-ray Diffraction (WAXRD)

WAXRD diffractograms of the neat TPU and TPUCN are shown in Figure 5.1. As explained earlier in Chapter 3, modification of LS with 'd' leads to a broad band in the angular range from 4.8 to 6.5° along with a peak corresponding to 2.6° 2θ value (d spacing of 3.4 nm). The broad band present in dLS registers a relatively sharp peak corresponding to ~5.4° 2θ value (d spacing of 1.6 nm) upon addition of dLS into the TPU matrix. Interestingly, the peaks retain nearly in the same position for all the clay contents studied here. However, the sharpness of the peaks gradually increases with the increase in clay content.

Similarly, modification of LS with 'c' shows a broad band ranging from 4.5 to 6.0° 2θ value (comprising of local peaks corresponding to 4.5, 5.1, 5.6 and 6.0° 2θ values) in the diffraction pattern. It is observed that the TPUCNs register different type of diffraction pattern at lower clay content than those with higher clay contents. TPUCN with 1% cLS displays a small peak at 5.4° 2θ (d spacing of 1.6 nm).

However, at higher clay content (especially at 5 and 7% of clay), the diffraction pattern resembles closely to that of pristine cLS.

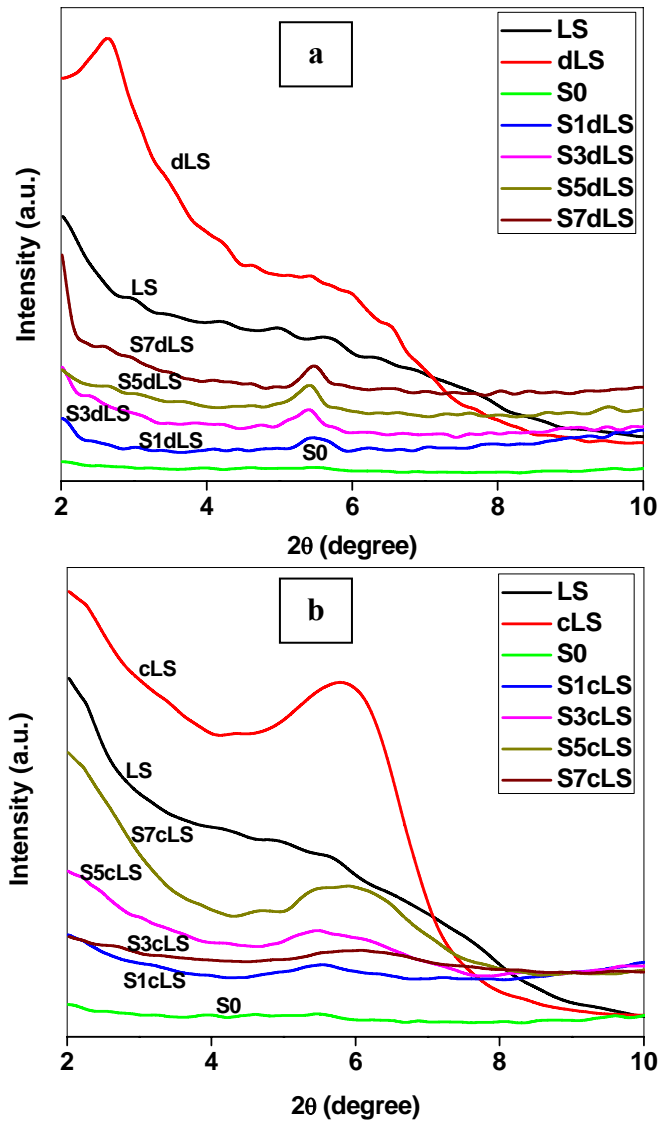


Figure 5.1: WAXRD diffractograms of TPUCNs with (a) dLS and (b) cLS from $2-10^\circ 2\theta$

Figure 5.2 shows the WAXRD diffractograms of the TPUCNs at higher angular ranges. It is observed that the neat TPU (shown earlier in Chapter 4A) consists of some semicrystalline features along with the broad hallow due to the amorphous soft domain. However, the smaller peaks are retained by and large in case of ScL. Similarly, in case of SdLS and ScLS, the smaller peaks corresponding to the

semicrystalline features are found to be partly retained. This is because of the greater extent of modification leading to increased dispersion. This results in a decreased destruction of the ordered hard domains.

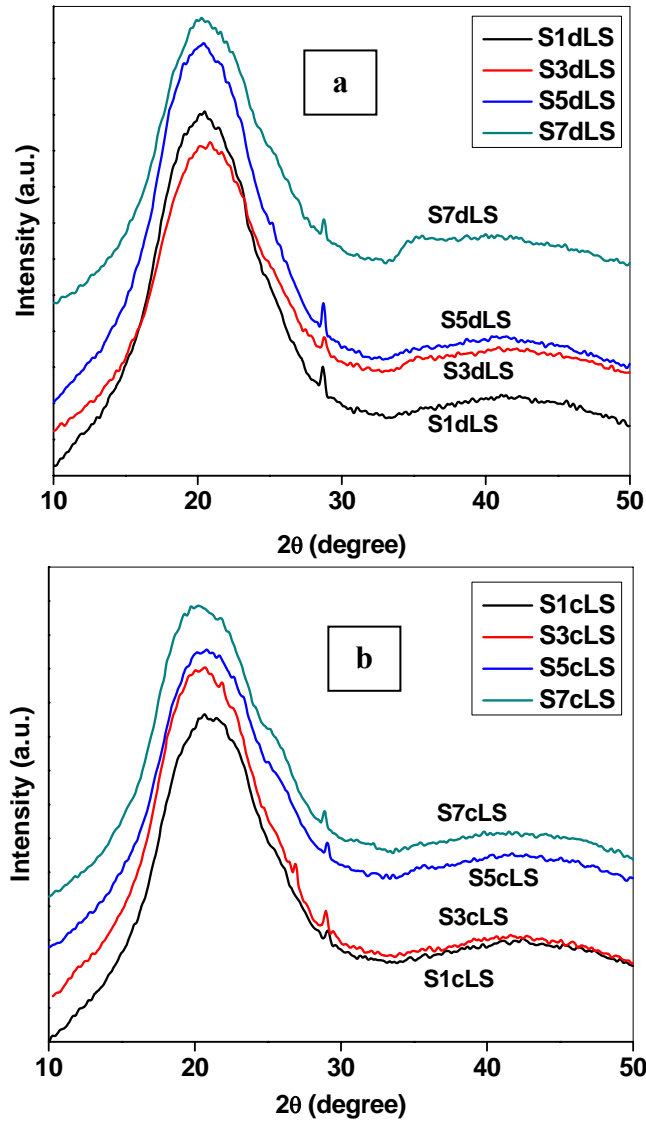


Figure 5.2: WAXRD diffractograms of TPUCNs with (a) dLS and (b) cLS from 10-50° 2θ

5.3 Transmission Electron Microscopy

Figure 5.3 (a-d) displays the TEM photomicrographs of solution cast nanocomposites (S1dLS, S5dLS, S1cLS and S5cLS, respectively). It is observed that both S1dLS and S5dLS (Fig. 5.3a and b) form nearly similar type of localized

spherical aggregations (aggregate size ranging from 150 to 300 nm). This is because of the preferential association of dLS to the hard domain (similar to that of dL as already explained in Chapter 4A). A magnified view of one of such spherical clusters in S5dLS reflects a loose structure accompanied by some comparatively tightly packed aggregates. Presence of the loose structures reveals the fact that the TPU is effectively penetrated into the clay galleries. The tightly packed aggregates possibly correspond to the peak at $5.6^\circ 2\theta$ value in the X-ray diffractogram (earlier section).

However, a different type of morphology is observed in case of cLS based nanocomposites. S1cLS (Fig. 5.3c) indicates a cylindrical pattern of clay distribution in the TPU matrix. A combination of aggregated, intercalated and partly exfoliated distribution of clay platelets is also seen. Orientations of clay platelets are nearly unidirectional, along with a few randomly oriented contributors. However, at 5% clay content (Fig. 5.3d), cLS forms a network type of structure with increased state of aggregation. It is interesting to note that, the inter-platelet distance within the intercalated structure or within loose aggregates, ranges from 8 to 12 nm for dLS and from 1.7 to 6.0 nm for cLS, respectively.

Figure 5.3 (e-f) displays the TEM photomicrographs of the annealed samples (annealing was performed following the similar procedure as explained earlier in Chapter 4A). The preferential association of dLS is further confirmed from the morphology of the annealed nanocomposites. It is found that in case of SdLS, not even a single clay platelet is exposed outside the hard domain. But in case of ScLS, part of it lies within hard domain and part of it are distributed in the soft domain regions as well.

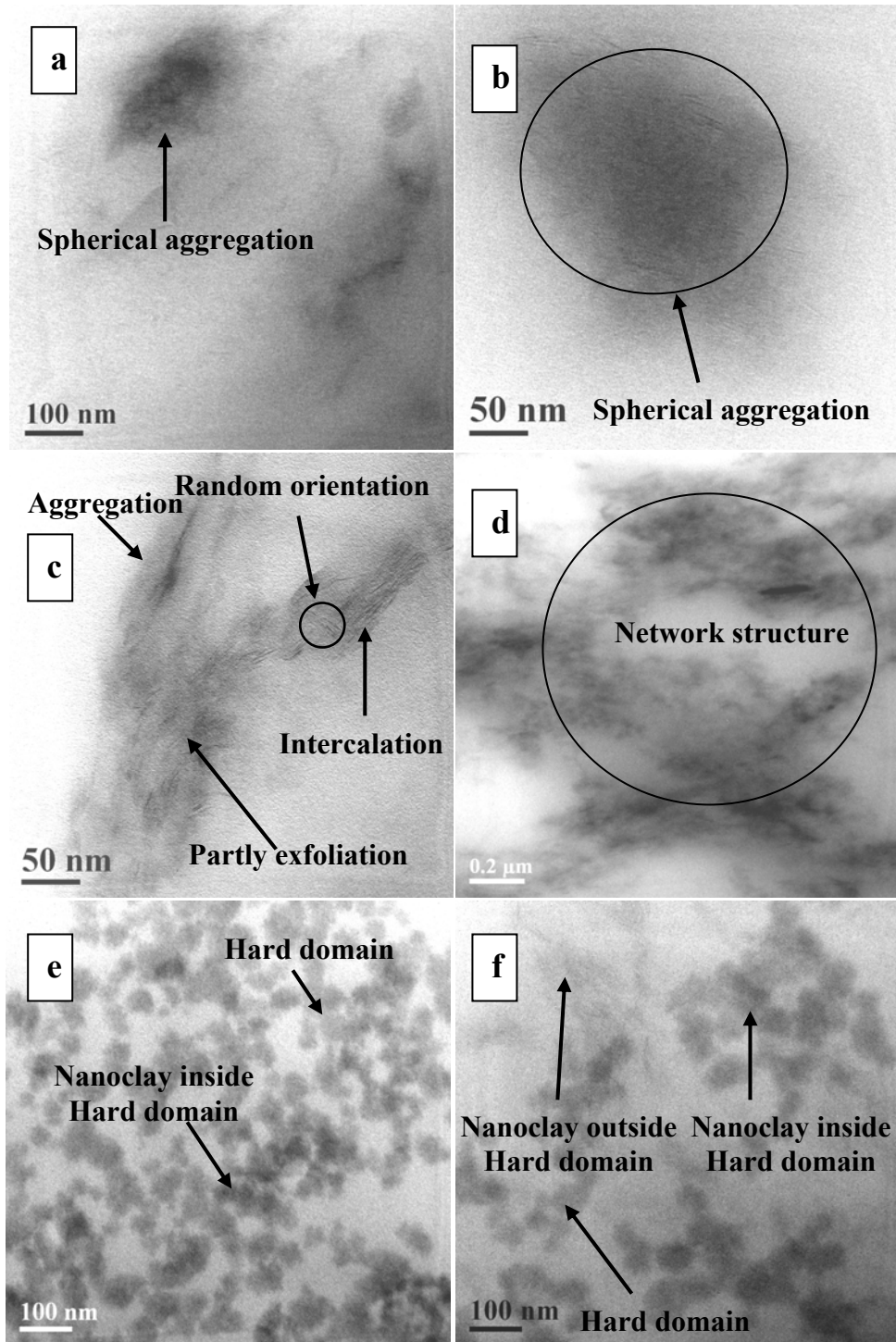


Figure 5.3: TEM photomicrographs of solution casted TPUCN, (a) S1dLS, (b) S5dLS, (c) S1cLS, (d) S5cLS and annealed TPUCN, (e) S3dLS (f) S3cLS

Therefore, from TEM analysis it is apparent that dLS exhibits a preferential association with the hard domains (as the spherical aggregate size matches well with

the average size scale of the TPU as reported in literature [Liff et al. (2007)]. However, cLS does not show any preference. The higher degree of such preference of dLS as compared to cLS can be ascribed due to the more hydrophobic character of cLS as compared to dLS (alkyl chain length of 'c' is 16 and that for 'd' is 12 as described in Chapter 4A for dL and cL).

5.4 Field Emission Scanning Electron Microscopy (FESEM)

Figure 5.4 (a-d) displays the FESEM photomicrograph of S1dLS, S7dLS, S1cLS and S7cLS, respectively. The small cracks are visible (in all the photomicrographs) due to the nonuniform gold coating and it has been confirmed for all other samples as well. The clay aggregate size varies from 30 to 250 nm for S1dLS (Fig. 5.4a) and 30 nm to 300 nm for S7dLS (Fig. 5.4b). Similarly, the aggregate size varies from 30 to 200 nm for S1cLS (Fig. 5.4c) and 30 to 800 nm for S7cLS (Fig. 5.4d).

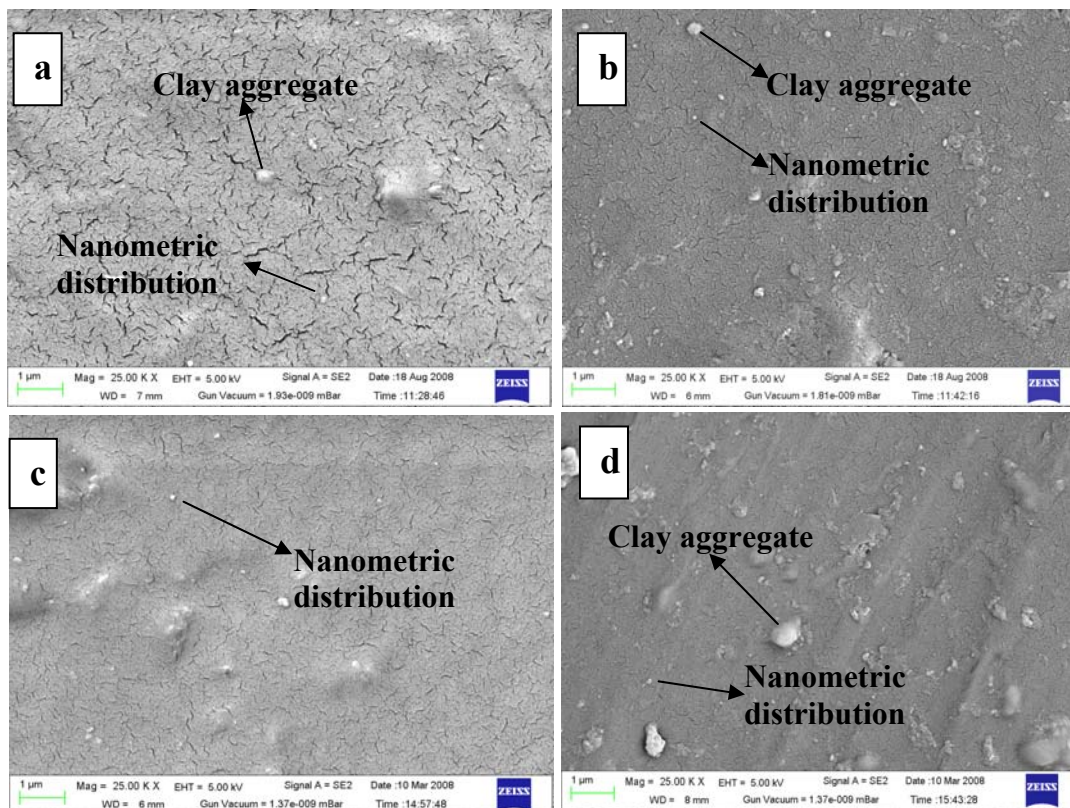


Figure 5.4: FESEM photomicrographs of (a) S1dLS, (b) S7dLS, (c) S1cLS & (d) S7cLS

Hence, increase in clay content increases the size of aggregation in case of cLS based nanocomposites. However, it remains nearly indifferent in case of dLS based nanocomposites. This supports our earlier observations in WAXRD and TEM. More uniform and nano-scale distribution of clay is observed in case of S1cLS as compared to that of S1dLS. However, with increase in clay content, more uniform distribution is noticed in case of S7dLS as compared to that with S7cLS.

5.5 Differential Scanning Calorimetry (DSC)

Figure 5.5a and b display the DSC thermograms of the TPU and TPUCN with different clay contents. The thermograms exhibit a distinct soft segment T_g, two endotherms followed by an exotherm. The soft segment T_g appears nearly at -40 °C. The endothermic peaks appearing nearly at 98 °C and 170 °C, corresponds to the destruction of the short range and long range ordered hard domain (or semicrystalline melting) resulting from enthalpy relaxation [Chen et al. (1998); Seymour and Cooper (1973) ; Shu et al. (2001); Tsen and Chuang (2006)]. Due to the quicker evaporation of the solvent, hard segments are not getting enough time to arrange properly and hence the endotherm ranging from 98 to 170 °C is quite broad. After the endotherm, an exotherm is observed nearly at 200 °C corresponding to the degradation of TPU. Hard segment T_g is not clearly seen because of the dominance of the amorphous soft segment over the hard domains and the presence of imperfect crystalline orders. There is no significant change in soft segment T_g with the incorporation of nanoclay (Table 5.1). This may be due to the fact that the expected increment in T_g due to the incorporation of clay is being compensated by the plasticizing effect of the unreacted amines present in the modified clays. However, addition of clay increases the sharpness of the endothermic peaks at 98 and 170 °C. This suggests that clay modifies the crystalline order in the TPU matrix. The endotherms are more distinct and clear in

case of cLS based nanocomposites as compared to that of dLS based nanocomposites. The preferential association of dLS with the hard domain (which destroys the crystalline ordering in hard domain to a greater extent) is possibly responsible for this.

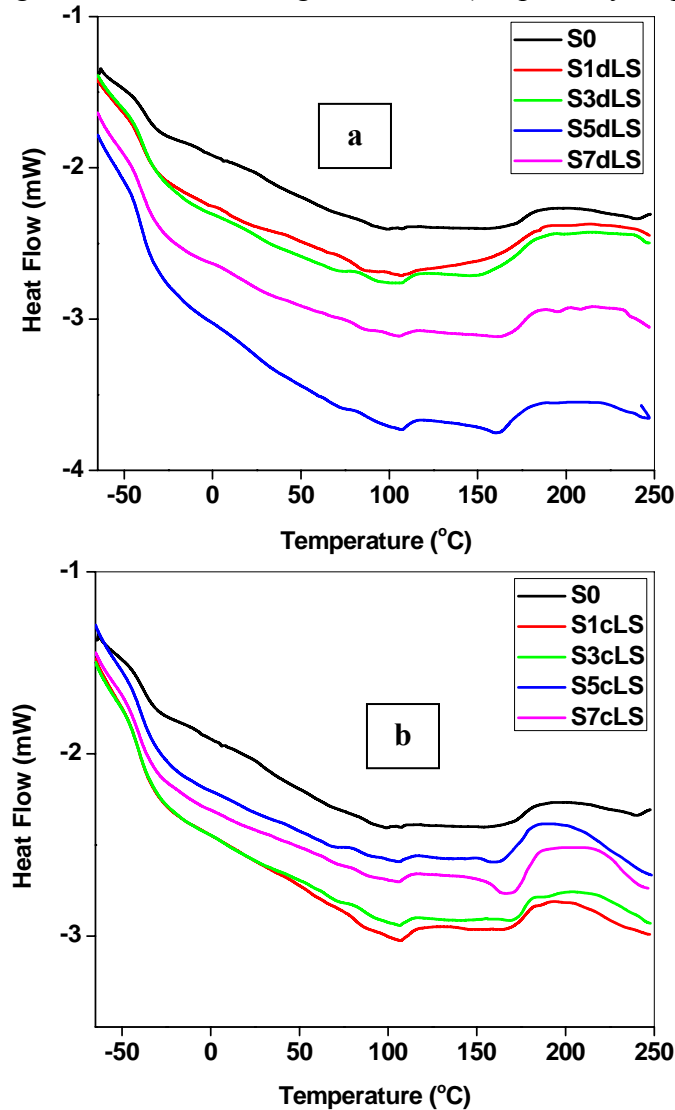


Figure 5.5: DSC thermograms of TPUCNs with (a) dLS and (b) cLS

5.6 Dynamic Mechanical Analysis (DMA)

The structure, concentration and organization of the hard segments and nano-scale distribution and dispersion of clays, have a dominant influence on the physical and mechanical properties of TPU. Figure 5.6a and b represent the change in storage modulus with respect to temperature for the neat TPU and TPUCN, respectively. For this study, the samples were subjected to a sinusoidal displacement of 0.1% strain at a

frequency of 1Hz from -80 to 100 °C and with a heating rate of 5 °C/min. The values of storage modulus at three different temperatures, the values of $\tan \delta_{\max}$ and T_g are presented in Table 5.1.

In case of dLS based TPUCNs, the storage modulus increases monotonously with the increase in clay content. The same trend is observed in both glassy and rubbery states. In the rubbery state nearly 2.5 fold increase in storage modulus as compared to the neat TPU is observed with 7% dLS filled composite (Table 5.1). However, a different trend is observed in case of ScLS. Nearly two times increase in storage modulus value is observed for S1cLS as compared to the neat TPU (both in glassy and in rubbery state). In the glassy state, the storage modulus is optimum with 1% clay content and thereafter the modulus gradually decreases with the increase in clay content. In the rubbery state, storage modulus of the resulting nanocomposite with 1 and 3% cLS is almost two times higher than that of the neat TPU (Table 5.1). However, thereafter the storage modulus gradually decreases with the increase in clay content.

Table 5.1: DMA and DSC results for TPU and TPUCN with dLS and cLS

Sample ID	Storage Modulus (MPa)			$\tan \delta_{\max}$	T_g (°C)	
	-60 °C	-20 °C	+20 °C		DMA	DSC
S0	1587.7	92.0	13.1	0.59	-21.9	-39
S1dLS	1877.8	108.0	23.8	0.55	-22.0	-40
S3dLS	2800.5	135.8	25.1	0.52	-23.8	-40
S5dLS	3015.3	177.1	29.9	0.49	-23.7	-40
S7dLS	3236.9	208.8	33.0	0.46	-22.0	-40
S1cLS	3039.6	149.0	26.0	0.55	-24.6	-40
S3cLS	2735.8	145.0	26.1	0.53	-24.5	-40
S5cLS	1772.7	120.4	21.3	0.49	-23.8	-40
S7cLS	1617.4	122.8	20.3	0.46	-23.5	-40

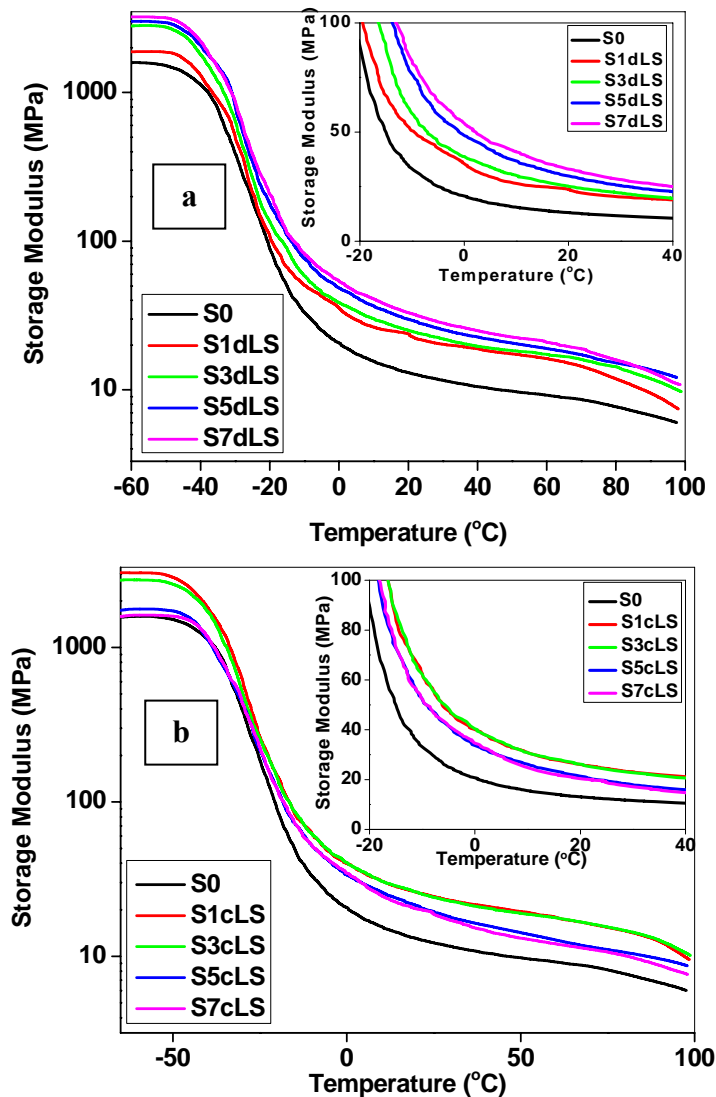


Figure 5.6: DMA thermograms of TPUCN with (a) dLS and (b) cLS

The increased storage modulus of TPUCN with the increase in dLS content can be ascribed to the preferential association of dLS with the hard segment (as explained earlier) with nearly constant aggregate size for all clay contents. The marginal increase in storage modulus at lower dLS content may be due to the loss of crystalline ordering. The initial loss of crystalline order (due to the penetration of dLS into the hard domain) at lower clay content is compensated largely by the reinforcement due to polymer-filler interaction at higher clay content. This is possible because of the similar size scale of aggregation at lower and higher clay content in

this case (Section 5.2 to 5.4). However, the decrease in storage modulus value of TPUCN with the increase in cLS content can be ascribed to the increased aggregation and network type of structure formation or due to the increase in plasticizing action of the surface alkyl ammonium moieties. The initial increase in storage modulus at lower clay content is due to the balance between intercalation and loose aggregation observed in morphology of the nanocomposites.

It is observed that the $\tan \delta_{\max}$ value gradually decreases with the increase in clay content implying (Fig. 5.7) lower damping characteristics. Nearly similar values are observed for SdLS and ScLS at similar clay contents (Table 5.1). This is due to the decrease in the fraction of TPU in the nanocomposite with the increase in clay content. Although not much change in T_g is found from DSC, but nearly 2-3 °C decrease is observed in DMA. This may be due to the plasticizing effect of a small amount of unreacted amine present inside the clay gallery or due to the segmental dynamics of the polymer inside the clay gallery which become more prominent in dynamic experiments [Anastasiadis et al. (2000); Xiong et al. (2004)].

5.7 Dynamic Rheological Analysis

5.7.1 Strain sweep

Percentage drop in modulus values at different strain levels (1, 7, 20, 70 and 100 %) are compared with the initial modulus for the neat TPU and TPUCN (Table 5.2). The modulus decreases monotonously with respect to the strain % irrespective of the type of clay used. The decrement in modulus value is lower in both SdLS and ScLS as compared to the neat TPU, except with S5cLS. This is probably due to the plasticizing effect of the surface alkyl ammine group (due to the modification of the surface $\text{Na}_4\text{P}_2\text{O}_7$). A gradual increase in % decrement in modulus at higher strain levels for SdLS indicates that other mechanisms of deformation gradually contributes

over filler structure breakdown. In case of ScLS longer length scale of aggregation supports the network structure (filler-filler) to sustain upto higher level of strains. In case of both SdLS and ScLS, 5% clay content grossly reveals higher decrement especially at higher % strain. Exceptionally high value of decrement in storage modulus with S5cLS is possibly ascribed to the network type of morphology present in S5cLS (Section 5.3).

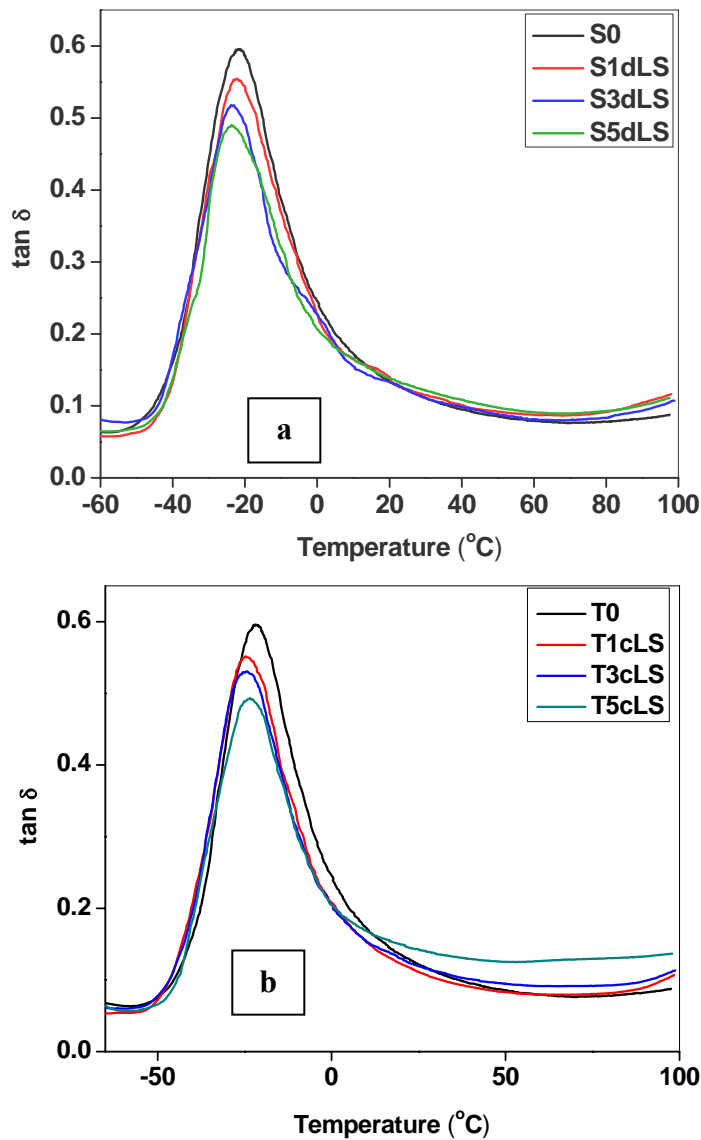


Figure 5.7: $\tan \delta_{\max}$ vs. temperature for (a) SdLS & (b) ScLS

Table 5.2: Percentage decrease in dynamic storage modulus value as compared to the initial modulus at different strain levels

Sample ID	% drop in modulus value at different strain levels				
	1%	7%	20%	70%	100%
S0	7.8	13.9	28.0	60.7	68.6
S1dLS	4.0	6.0	10.5	36.8	50.5
S3dLS	5.7	10.9	18.0	47.7	59.6
S5dLS	4.7	8.3	18.8	50.3	59.6
S1cLS	8.7	21.7	25.0	28.9	30.5
S3cLS	7.3	10.8	17.4	43.7	53.5
S5cLS	13.8	34.5	48.2	68.6	74.9

5.7.2 Temperature Sweep

Figure 5.8 (a-b) shows plots of the storage modulus vs. temperature with 3% clay content. In all the cases, there is a drastic decrease in both storage (G') and loss (G'') modulus values from 140 to 170 °C followed by a comparatively slower decrease (terminal plateau) upto 220 °C. The drastic decrease in modulus value is ascribed to the transition from the rubbery plateau to flow behavior and the plateau region afterwards corresponds to the extended terminal region (restricted flow). It is observed that all the nanocomposites possess lower storage modulus compared to the neat TPU for 1% clay content at the range of temperatures studied here (130-220 °C). This is possibly due to the change in molecular relaxation due to which shear thinning events dominates at lower clay content.

There is an increasing tendency in modulus values with the increase in clay content in case of SdLS but the reverse trend is observed in case of ScLS. The increasing tendency of modulus with the clay content can be described based on the Guth-Gold equation. However, the reverse trend with ScLS is possibly due to the plasticizing effect of the surface alkyl ammine group and greater hydrophobic nature of the modifier contributing to the decrease in modulus value (presence of tertiary alkyl ammonium pyrophosphate on the surface). S3dLS shows higher G' and G''

values as compared to that of S3cLS irrespective of temperatures studied here (130-220 °C). The plasticizing action and greater hydrophobicity of the surface alkyl ammonium ions associated with cLS reduces the modulus to a greater extent.

In Figure 5.8, it is observed that S3dLS grossly possess higher storage and loss modulus values as compared to its S3cLS counterpart. The plasticizing effect of the surface alkyl amine group is more reflected here in case of S3cLS.

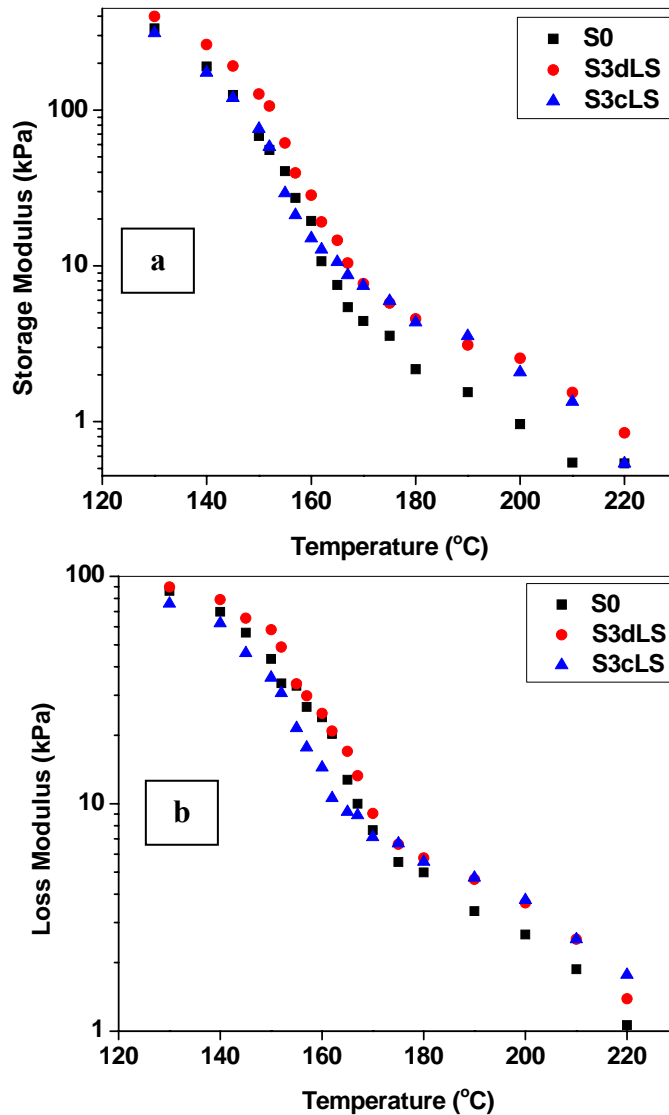


Figure 5.8: Changes in (a) Storage and (b) Loss modulus of TPUCNs with 3% clay content with respect to temperature

5.7.3 Frequency sweep

In this case also similar type of behavior is encountered as it was observed with the neat TPU and TPUCNs (Chapter 4B). At 140 °C, $G' > G''$ whereas, at 170 °C, $G'' > G'$, for all the composites (independent of the types of modified clay) and this behavior is also independent of frequency range studied here.

5.7.3.1 Effect on Complex Viscosity at 140 °C

Figure 5.9 displays the complex viscosity vs. frequency plots at 140 °C. The complex viscosity (η^*) of SdLS is always higher than the neat TPU irrespective of the clay content and an increase in η^* value is observed with the increase in clay content. However, the same (η^*) is lower than that of the neat TPU in case of ScLS and increase in clay content is found to bring down the values further.

The increase in complex viscosity with the increase in dLS content is mainly responsible for the increased entrapped TPU chains inside the loosely aggregated clay platelets. This is possible only because of the consistency in the spherical aggregate size in case of SdLS both at lower and higher clay contents (Section 5.3). However, the decreasing tendency of the η^* value is possibly due to the plasticizing action of the organic moieties on the surface resulted due to the modification of the $\text{Na}_4\text{P}_2\text{O}_7$.

5.7.3.2 Effect on Complex Viscosity at 170 °C

Figure 5.10 displays the complex viscosity vs. angular frequency plots at 170 °C. At 170 °C, η^* value of SdLS follows an increasing trend with the increase in clay content but a reverse trend is observed in case of ScLS. At 170 °C, the long range ordering in the hard segment breaks. Hence, most of the contributions towards the viscosity and modulus are attributed to the amount of fillers present in the matrix; following the Guth-Gold equation (hard or soft domain preference should not matter anymore). But the decrease in η^* value in case of ScLS is plausibly due to the slight

plasticizing effect of cLS or else the ball-bearing effect (due to the low aspect ratio of Laponite and its spherical aggregate structure, TPU chains can slip past on them).

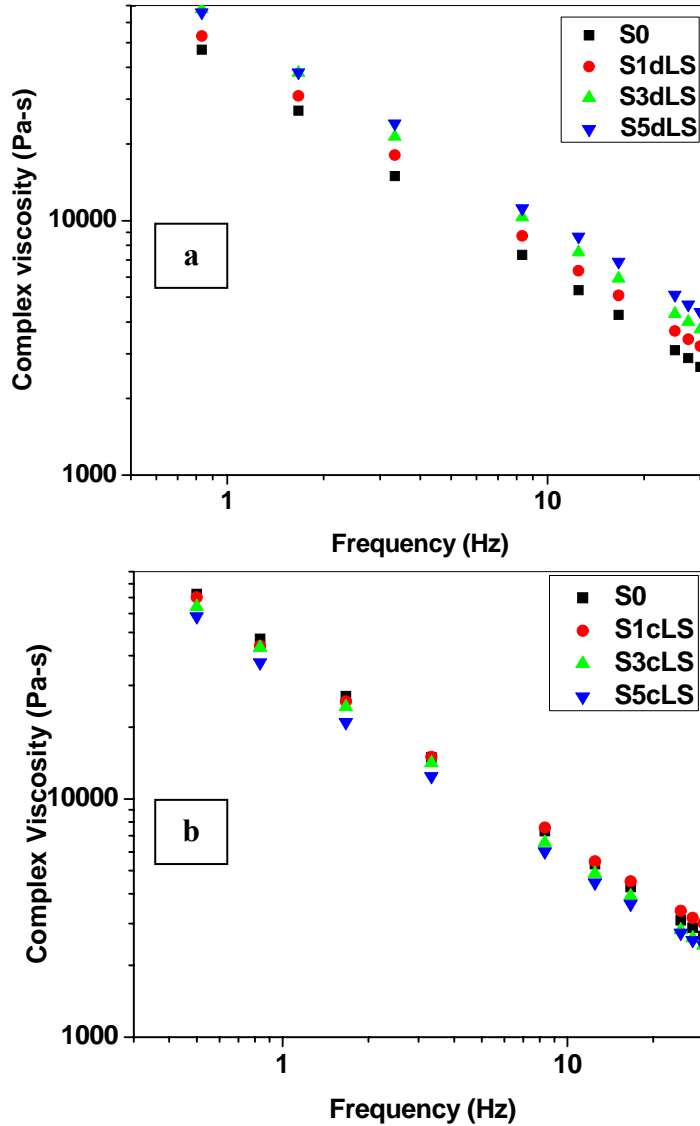


Figure 5.9: Complex viscosity vs. frequency plot of (a) SdLS and (b) ScLS at 140 °C

5.8 Thermogravimetric Analysis (TGA)

Figure 5.11a and b show the TGA thermograms of the TPUCN with dLS and cLS, respectively. Table 5.3 represents the temperatures corresponding to the onset degradation (T_i), 1st maximum degradation temperature (T_{1max}) and 2nd maximum degradation temperature (T_{2max}). Although the degradation has started nearly at 200 °C but in order to achieve a better comparison (avoiding the weight loss due to

the entrapped moisture and unreacted or free amine present inside the clay gallery) comparison is made on 5% weight loss basis.

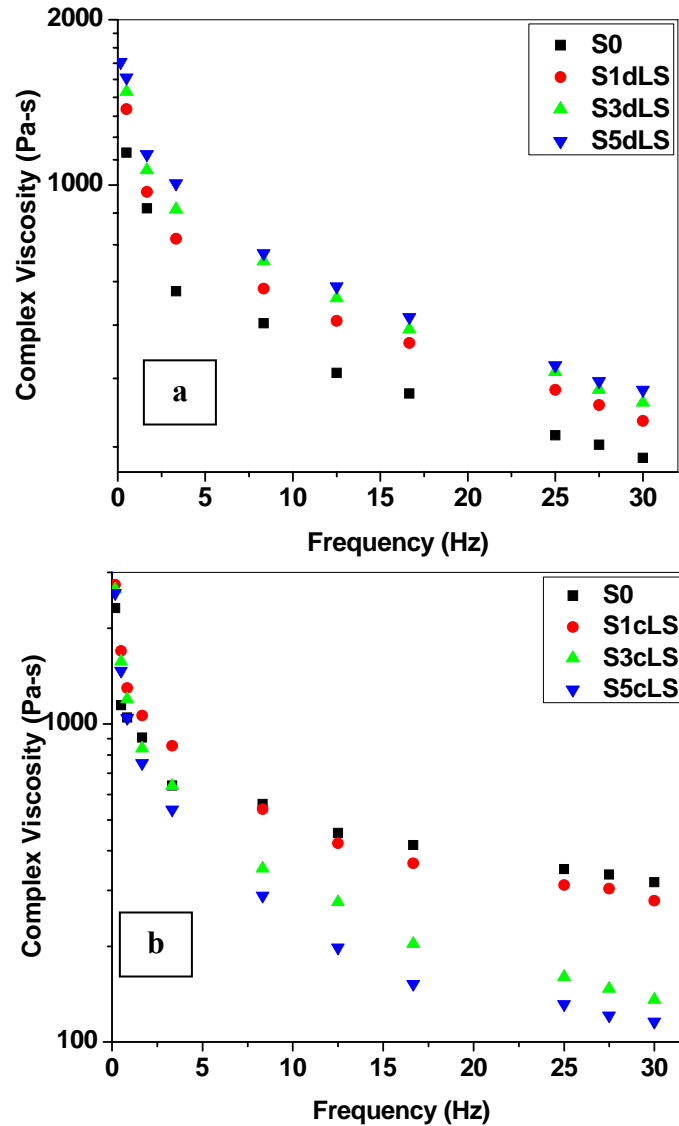


Figure 5.10: Complex viscosity vs. frequency plot of (a) SdLS & (b) ScLS at 170 °C

T_i is increased by 12.5 °C for S1dLS and then it follows a gradual decreasing trend with the increase in clay content. T_{1max} (which is due to the hard segment degradation) [Petrovic et al. (1994); Shieh et al. (1999)] also follows the same trend and a maximum increase of 7.3 °C is observed with 1% clay filled sample. However, T_{2max} of the nanocomposites (which is due to the soft segment degradation) [Petrovic et al. (1994), Shieh et al. (1999)] is always less than that of the neat TPU irrespective

of the clay content. Similar trend is followed for T_i , T_{1max} and T_{2max} in case of cLS based nanocomposites. An increase in 19.1 °C and 25 °C is observed in T_i and T_{1max} values, respectively for 1% cLS content as compared to the neat TPU. However, T_{2max} is lower than that of the neat TPU upto 3% cLS content. T_{2max} becomes higher than the neat TPU for more than 5% clay content. T_{2max} follows an increasing trend with the increase in clay content, unlike in T_{1max} .

Table 5.3: TGA results for TPU and TPUCN with dLS and cLS

Sample ID	Weight %		
	T_i (°C)	T_{1max} (°C)	T_{2max} (°C)
S0	300.0	335.1	401.6
S1dLS	312.5 (12.5)	342.4 (7.3)	397.9 (-3.7)
S3dLS	297.8	341.2	398.1
S5dLS	291.6	336.0	401.2
S7dLS	286.2	336.6	400.4
S1cLS	319.1 (19.1)	360.0 (24.9)	398.0 (-3.6)
S3cLS	310.1	353.0	398.0
S5cLS	301.5	346.4	404.3
S7cLS	294.5	345.1	407.3

(* Values given inside parenthesis indicate the increase in temperature compared to the neat TPU)

The decrease in T_i , with an increase in clay content in both the cases is due to the presence of excess/unreacted amine left over inside the clay galleries. Due to the presence of greater amount of surfactant in dLS compared to cLS (as mentioned earlier), T_{1max} of cLS based TPUCN is higher than that of dLS based TPUCN. A comparative study shows that, there is not much change in T_{2max} (Table 5.3) for the composites having lower cLS and dLS content. But T_{2max} value for S7cLS is 7 °C higher than that of S7dLS. This is possible only because of the network type of structures (distributed both in hard and soft segment) formed by cLS at higher clay content. On the contrary, due to the confined structure of dLS at the vicinity of hard segments, it is unable to interfere with the degradation process of the soft segment.

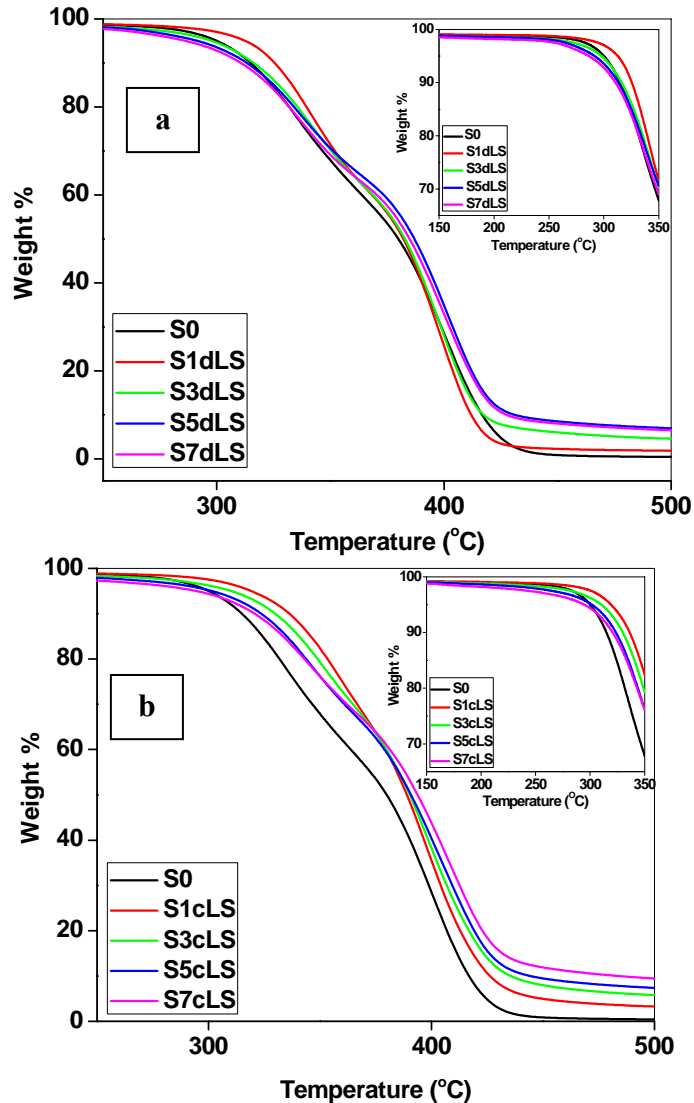


Figure 5.11: TGA thermograms of TPUCN with (a) dLS and (b) cLS

5.9 Isothermal TGA

An attempt is made in this section to carefully look into the effect of modifier on the degradation behavior of TPUCN under isothermal conditions. For this study three different temperatures (300, 325 and 350 °C) were selected based on the degradation behavior of TPU via TGA experiment with dynamic heating process (Section 5.8). Figure 5.12 shows the isothermal TGA thermogram of S0, S1dLS and S1cLS at different temperatures. The nanocomposites are represented here in as S_{xy}_z , where, z represents the corresponding temperatures at which isothermal

experiment is carried out. Based on the theory mentioned in Section 4A.9 (Chapter 4A), the rate constants and activation energy of the neat TPU, S1dLS and S1cLS were calculated and compiled in Table 5.4.

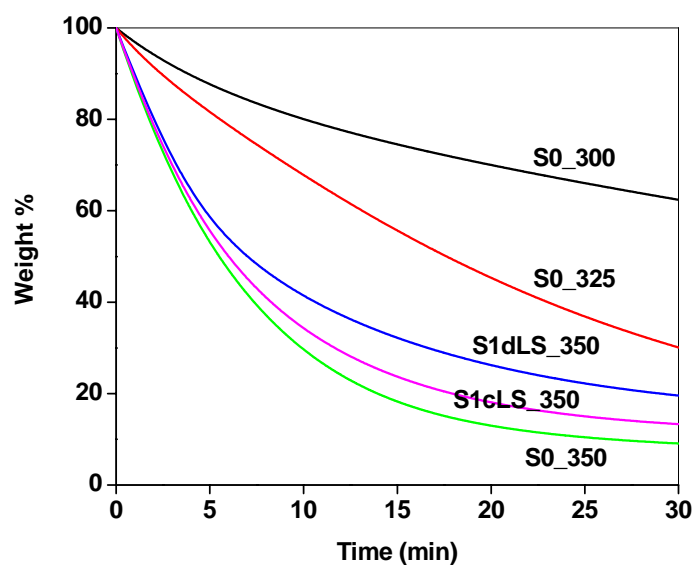
Isothermal degradation process is mostly contributed by two factors, namely, polymer decomposition and physical stabilization. It is observed that at 300 °C, the rate constant 'k' remains indifferent for the neat TPU, S1cLS and S1dLS. At 325 °C, 'k' value of the neat TPU is marginally higher than those of S1dLS and S1cLS (k value remaining indifferent for both S1dLS and S1cLS). However, at 350 °C, 'k' value follows the order S1cLS<S1dLS<S0 (Table 5.4). In all the three cases, 'k' value increases with the increase in temperature (i.e., 'k' value follows the order $k_{300} < k_{325} < k_{350}$). From the 'k' values it is quite obvious that S1cLS is providing better thermal stability to the TPU matrix. Although the same is not reflected at lower temperatures but it is quite clear at 350 °C.

However, the activation energy follows the order S0>S1dLS>S1cLS. As observed in earlier section, thermal stability follows the order S0<S1dLS<S1cLS, which is just the reverse of the trend in activation energy found here. Hence, the activation energy is found to decrease as compared to the neat TPU in this case as well (similar to Section 4A.9), although an increase in thermal stability is observed by TGA with the dynamic temperature ramp. Similar results are reported recently by Fambri et al. (2001) by following the similar technique. The increase in thermal stability is due to the non-conducting barrier effect of inorganic clay platelets. Although, the exact reason for the decrease in activation energy is not known but a similar reason can be corroborated as explained in Section 4A.9.

Table 5.4: Rate constants at different conditions of isothermal degradations

Sample ID	$k_{300} (\text{sec}^{-1}) \times 10^{-3}$	$k_{325} (\text{sec}^{-1}) \times 10^{-3}$	$k_{350} (\text{sec}^{-1}) \times 10^{-3}$	Activation Energy (J/mole)
S0	0.3 (0.95)	0.7 (1.00)	1.5 (0.92)	95.5
S1dLS	0.3 (0.93)	0.6 (1.00)	1.0 (0.90)	86.9
S1cLS	0.3 (0.97)	0.6 (0.98)	1.3 (0.91)	71.6

(* Values given inside parenthesis indicate the correlation coefficients)

**Figure 5.12:** Isothermal TGA diffractogram of the neat TPU and TPUCNs

5.10 Conclusions

Dispersion of the ionically modified Laponite RDS in the TPU matrix is improved as compared to the modified Laponite RD counterparts. As a result of this the onset of degradation is found to be enhanced even more as compared to the Cloisite[®] based nanocomposites. However, plasticizing action of the surface alkyl groups are highly reflected in thermal properties, especially, in the dynamic rheological characteristics.

5.11 References:

- Anastasiadis S. H., Karatasos K., Vlachos G., Manias E., Giannelis E. P. (2000) Nanoscopic-Confinement effects on Local Dynamics, *Physical Review Letter* 84, 915-918
- Chen T. K., Shieh T. S., Chui J. Y. (1998) Studies on the First DSC Endotherm of Polyurethane Hard Segment Based on 4,4'-Diphenylmethane Diisocyanate and 1,4-Butanediol, *Macromolecules* 31, 1312-1320
- Fambri L., Pegoretti A., Gavazza C., Penati A. (2001) Thermooxidative stability of different polyurethanes evaluated by isothermal and dynamic methods, *Journal Applied Polymer Science* 81, 1216-1225
- Liff S. M., Kumar N., McKinley G. H. (2007) High-Performance elastomeric nanocomposites via solvent exchange processing, *Nature Material* 6, 76-83
- Petrovic Z. S., Zavargo Z., Flynn J. F., Macknight W. J. (1994) Thermal degradation of segmented polyurethanes, *Journal Applied Polymer Science* 51, 1087-1095
- Seymour R. W., Cooper S. L. (1973) Thermal analysis of Polyurethane block copolymers, *Macromolecules*, 6, 48-53
- Shieh Y. T., Chen H. T., Liu K. H., Twu Y. K. (1999) Thermal degradation of MDI-based segmented polyurethanes, *Journal Polymer Science Part A: Polymer Chemistry* 37, 4126-4134
- Shu Y. C., Lin M. F., Tsen W. C., Chuang F. S. (2001) Differential scanning calorimetry analysis of silicon-containing and phosphorus-containing segmented polyurethane. I - Thermal behaviors and morphology, *Journal Applied Polymer Science* 81, 3489-3501
- Tsen W. C., Chuang F. S. (2006) Phase transition and domain morphology of siloxane-containing hard-segmented polyurethane copolymers, *Journal of Applied Polymer Science* 101, 4242-4252
- Xiong J., Liu Y., Yang X., Wang X. (2004) Thermal and mechanical properties of polyurethane/montmorillonite nanocomposites based on a novel reactive modifier, *Polymer Degradation and Stability* 86, 549-555

CHAPTER 6

**TPUCN BASED ON COVALENT AND DUAL MODIFIED
LAPONITE RD**

A part of this chapter has been accepted in:

Advanced Science Letters 4 (2011) 1 (to be published)

6.1 Introduction

In Chapter 5, it has been observed that Laponite RDS modified by cetyltrimethyl ammonium bromide provides better thermal stability (due to improved dispersion) into the TPU matrix. However, such modified nanoclays suffer from certain drawbacks like, plasticizing effect due to the excess surface alkyl groups as it has been apparent from the rheological experiments. Keeping in mind that the excess surface alkyl groups are just adsorbed on the surface of the Laponite RDS (as $\text{Na}_4\text{P}_2\text{O}_7$ is physically adsorbed on the surface of the clay), it is contemplated to improve the dispersion of Laponite RD by additionally modifying the surface $-\text{OH}$ groups covalently. These $-\text{OH}$ groups can be modified by using alkyl alkoxy silanes as reported by Wheeler et al. (2005, 2006). It has been observed earlier that among the two surfactants 'd' and 'c', clay modified by 'c' provided better properties as compared to the clay modified by 'd'. Hence, 'c' is chosen for ionic modification of the dual modified clay subsequently. Dual modification is carried out in two ways, (a) covalent followed by ionic and (b) ionic followed by covalent modification. This chapter deals with structure-property relationship of the TPU-clay nanocomposites based on octyl silane modified (covalently modified) and dual modified Laponite RD.

6.2 Wide Angle X-ray Diffraction (WAXRD)

Figure 6.1a and b shows the WAXRD diffractograms of the TPUCN at lower angular range (from 2 to 10° 2θ value) and wider angular range (from 10 to 50° 2θ value).

It is observed from the diffractograms (Fig. 6.1a) that broadness of the diffraction pattern still persists with SOSL (as observed with OSL, Chapter 3, Section 3.4.2). Increase in clay amount possibly leads to an increase in aggregation tendency (as evidenced by the increased intensity and shifting of the characteristic broad band

towards higher angular range). However, a similar type of feature is not present in TPUCN based on dual modified clays (SOScL and ScOSL). Although few hallows are observed but those possibly fall within the error limit of the measurement.

WAXRD diffractogram at higher angular range (Fig. 6.1b) reveals that the semicrystalline features initially present in the neat TPU is completely vanished with the addition of nanoclay. This behavior is independent of the types of clay used (covalent and dual modified).

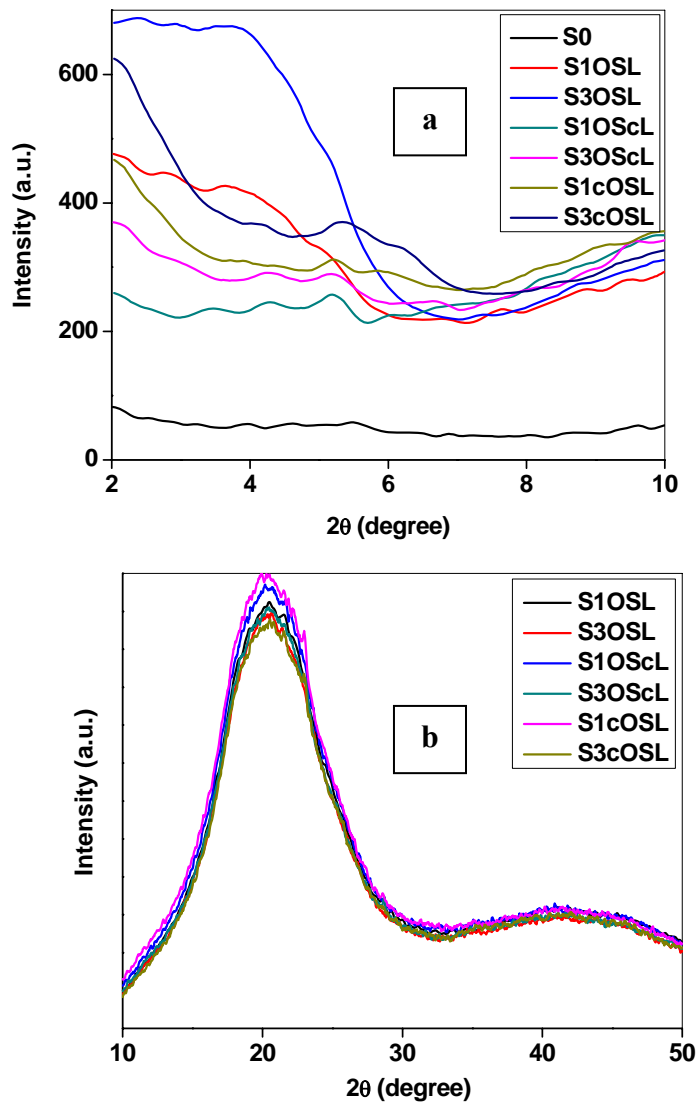


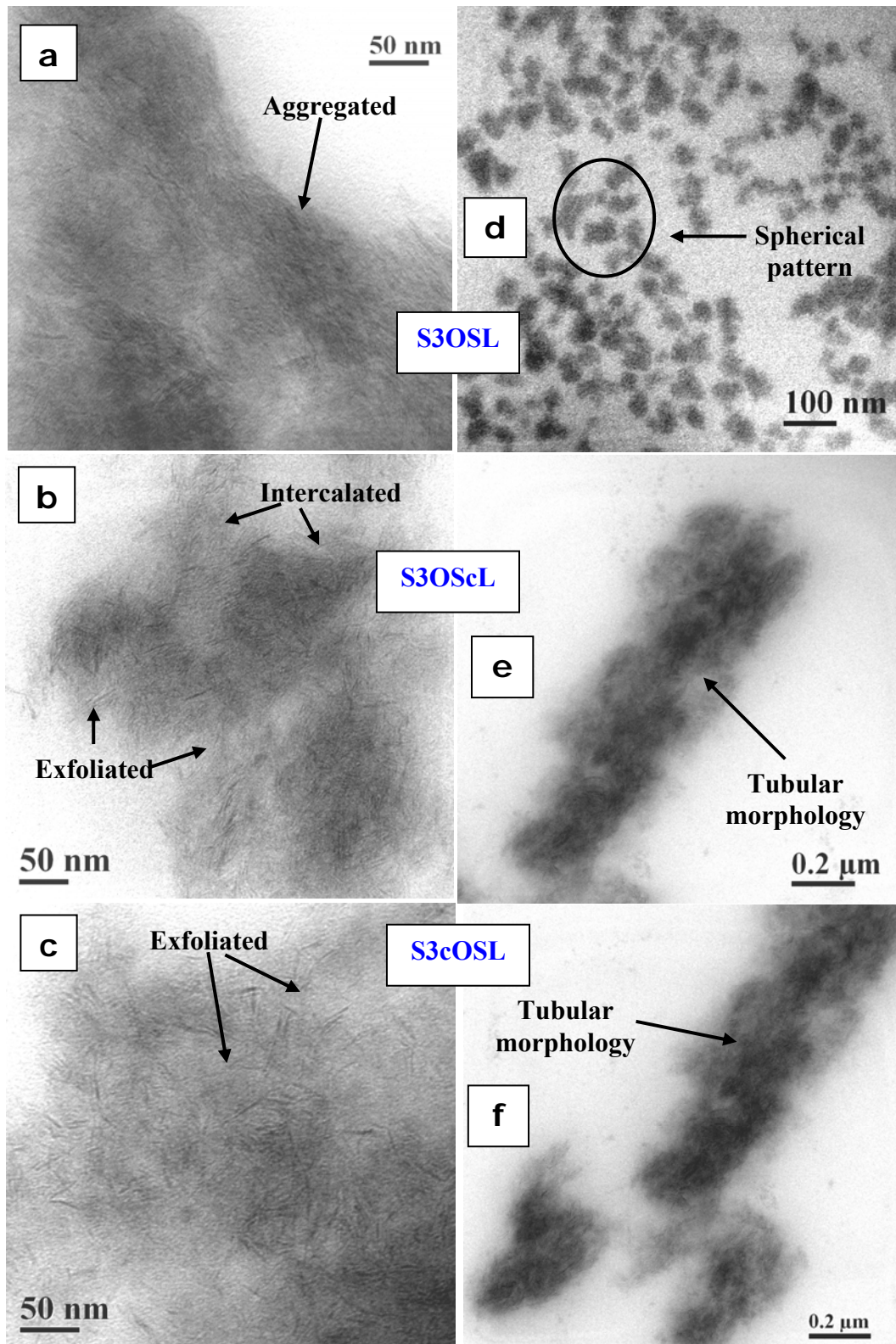
Figure 6.1: WAXRD of PUCNs (a) at lower and (b) at higher angular ranges

6.3 Transmission Electron Microscopy

Figure 6.2 (a-c) shows the representative TEM photomicrographs of the nanocomposites containing various modified clays at constant clay content of 3%. In the photomicrographs, the dark coloured spots and linings indicate clay platelets. The grey spots possibly indicate the hard domains whereas, lighter spots indicate the soft domains. It is observed that S3OSL shows an aggregated morphology with a small amount of intercalation (Fig. 6.2a). Mostly intercalated with slightly exfoliated structures persist with S3OScL (Fig. 6.2b), whereas, along with a few signatures of intercalated morphology, exfoliated structures are predominant with S3cOSL (Fig. 6.2c).

The existence of more exfoliated structure in case of 'cOSL' as compared to 'OScL' is due to the higher extent of modification in case of 'cOSL' (Table 3.2). Initial silane modification of Laponite with trimethoxy silane leads to the formation of crosslinked structure derived from the oligomeric siloxane chains (Chapter 3, Scheme 3.1). This crosslinked structure partly restricts the entrance of the cetyltrimethyl ammonium group to effectively utilize all the exchangeable Na^+ ions present inside the clay gallery. However, initial ionic exchange by the CTAB can effectively utilize the exchangeable Na^+ ions present inside the clay gallery. Hence, extent of modification (Table 3.2) and degree of exfoliation is higher in case of 'cOSL' as compared to 'OScL'.

Figure 6.2 (d-f) shows the TEM photomicrographs of the annealed samples. The grey features indicate the hard domain, bright region indicates the soft domain whereas, very dark regions correspond to the clay inside the hard domain. It is observed that in all the nanocomposites (S3OSL, S3OScL and S3cOSL), clay particles are found not to be distributed in the soft domain region.



Solution Cast

Annealed

Figure 6.2: TEM images of solution cast (left side) and annealed (right side) morphologies of TPUCNs

Interestingly, S3OSL clay retains the spherical pattern (as observed in the neat TPU), but both S3OScL and S3cOSL, give rise to tubular structures (Figure 6.2e and f). *This type of novel morphology of TPU-clay nanocomposites are not yet reported in the literature.* The formation of this tubular morphology can be explained based on the formation of arrays of H-bonding between the hard segment of TPU and the –OH groups present on the siloxane oligomer (covalently attached to clay platelets) in combination with the hindrance provided by the cetyltrimethyl ammonium ions (CTA⁺ ion) against the clay platelets to come closer. Presence of –OH group in siloxane oligomer is confirmed earlier from FTIR and NMR study (Chapter 3). Absence of the CTA⁺ ion may be responsible for the formation of spherical pattern in S3OSL. Modification of Laponite by simple cation exchange reaction has also been found to form spherical hard domains with clay platelets (Chapter 4A and 5). Thus, from these results it can be inferred that singly modified clay does not possess the capability to modify the phase separated morphology in TPU, which is in agreement with the results reported by Finnigan et al. (2005).

6.4 Differential Scanning Calorimetry

Figure 6.3 shows the DSC thermograms of the neat TPU and the TPUCN with 3% clay content. It is observed that the T_g of the TPUCN remain almost same or slightly lower than the neat TPU (similar to that already mentioned in Chapters 4A and 5). However, the melting endotherms due to the short range ordered hard domains and long range ordered hard domains become sharper as compared to that of the neat TPU. The endotherms remain in the same position or slightly lower than that observed in case of the neat TPU. This indicates that the modified nanoclay alters the crystalline order in the hard domain of TPU.

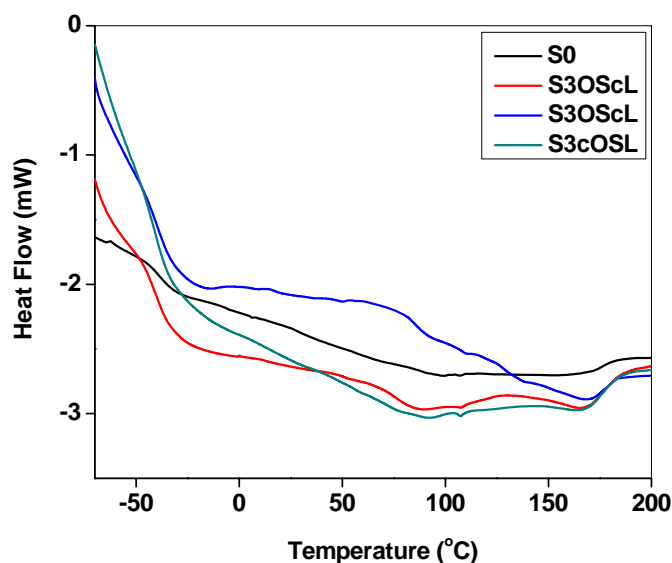


Figure 6.3: DSC thermograms of TPUCN with 3% clay content

Figure 6.4 represents a comparative study of the DSC thermograms of the solution cast and annealed samples. Here, S0an and S3cOSLan represent the annealed samples of S0 and S3cOSL, respectively. The T_g value of the annealed samples (both S0an and S3cOSLan) remains same. However, possibly due to additional quasicrystalline ordering, a sharp endotherm has been observed at +30 °C. However, this peak is not observed in S3cOSLan. Similarly, in both S0an and S3cOSLan, due to the formation of proper hard domain ordering, the sharpness of the melting endotherms is enhanced as compared to their solution cast counterparts. The temperatures corresponding to the destruction of the short range and long range ordered hard domains of the annealed samples are also lower than their corresponding solution cast counterparts.

6.5 Dynamic Mechanical Analysis (DMA)

Figure 6.5 displays the storage modulus vs. temperature plot of the TPUCN. Table 6.1 represents the magnitude of storage modulus at different temperatures, the glass transition temperature (T_g) and the $\tan \delta_{\max}$ values.

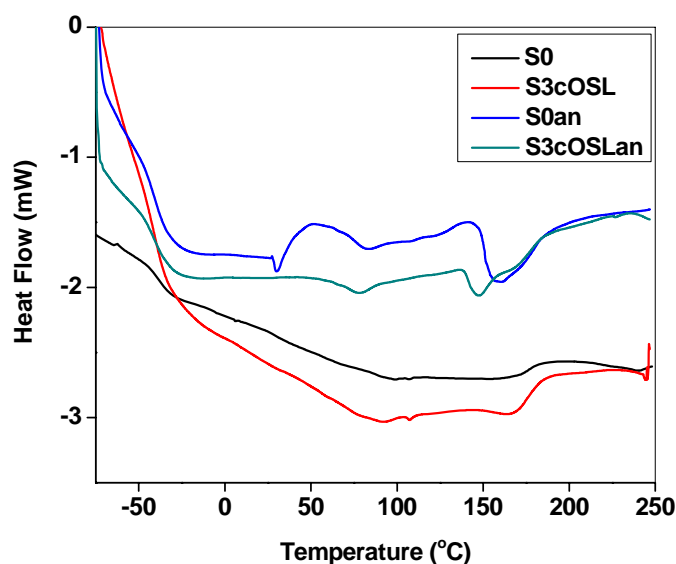


Figure 6.4: DSC thermograms of neat TPU and TPUCN (solution cast and annealed samples)

It is observed that in the glassy region, highest storage modulus (E') is imparted by S3OScL. But at -20 and $+20$ °C, S3OSL exhibits maximum E' and at higher temperatures ($+80$ and $+98$ °C) the storage modulus values are highest for S3cOSL. Hence, it can be inferred that the dual modified clay with a combined intercalated and exfoliated (OScL) structures provides better retention of modulus at lower temperature (glassy region). But the nanocomposite possessing highest degree of exfoliation (ScOSL), retains the modulus at higher temperatures. It is interesting to observe from Figure 6.5 (inset) that at a very high temperature ($+98$ °C) all the nanocomposites tend to register similar storage modulus values comparable to that of the neat TPU. However, S3cOSL exhibits exceptionally high storage modulus value at this temperature.

In case of SOSL series, S1OSL registers higher storage modulus value as compared to S3OSL. This is because of the increased aggregation tendency with the increase in clay content from 1 to 3%. This is also reflected from the WAXRD diffractogram as mentioned in earlier section (Fig. 6.1a). In case of SOScL, 3% clay

content is giving rise to the maximum storage modulus both in the rubbery and glassy state. But in case of ScOSL, nanocomposite containing 1% clay shows maximum storage modulus value below T_g whereas, above T_g , higher storage modulus value can be achieved with nanocomposite containing 3% clay.

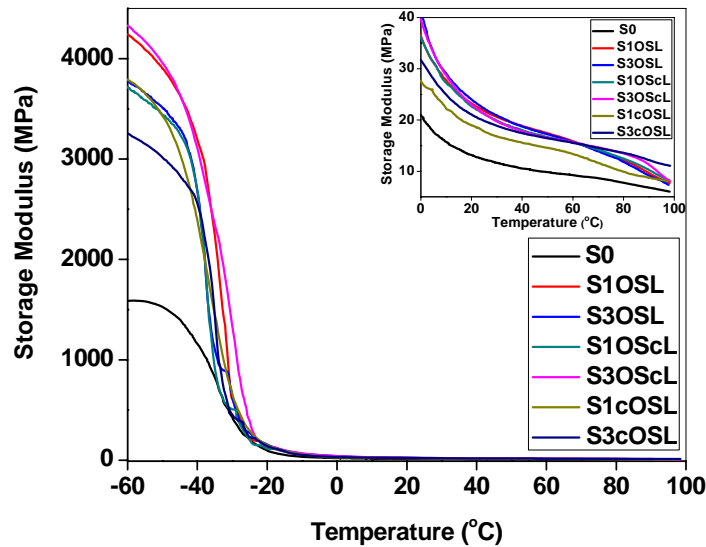


Figure 6.5: DMA thermogram of TPUCN

Table 6.1: Dynamic mechanical properties of TPU-clay nanocomposite

Sample ID	Storage Modulus (MPa)*					T _g (°C) by DMA	tan δ _{max}
	-60 °C	-20 °C	+20 °C	+80 °C	+100 °C		
S0	1586.0	99.4	13.0	7.7	6.0	-22.0	0.59
S1OSL	4241.3 (167.4)	132.6 (33.4)	23.2 (78.5)	12.1 (57.1)	7.7 (28.3)	-23.5	0.58
S3OSL	3778.4 (138.2)	155.5 (56.4)	24.0 (84.6)	11.8 (53.2)	7.4 (53.2)	-24.7	0.56
S1OScL	3709.3 (133.9)	117.2 (17.9)	22.7 (74.6)	12.5 (62.3)	8.2 (36.7)	-27.1	0.58
S3OScL	4327.3 (172.8)	141.2 (42.1)	23.0 (76.9)	13.5 (75.3)	8.2 (36.7)	-23.8	0.57
S1cOSL	3790.3 (140.0)	150.1 (51.0)	19.0 (46.1)	9.9 (28.6)	8.2 (36.7)	-23.9	0.59
S3cOSL	3254.2 (105.1)	142.1 (42.9)	21.0 (61.5)	13.6 (76.6)	11.1 (85.0)	-26.0	0.55

(*Values given inside parenthesis indicate the percentage increase in storage modulus of the nanocomposites as compared to S0)

Increase in the clay content leads to a decrease in $\tan \delta_{\max}$ value (Fig. 6.6). This infers that increasing clay content results in lowering the damping characteristic for all the nanocomposites. However, the damping characteristics of the nanocomposites are higher than the neat TPU at higher temperatures.

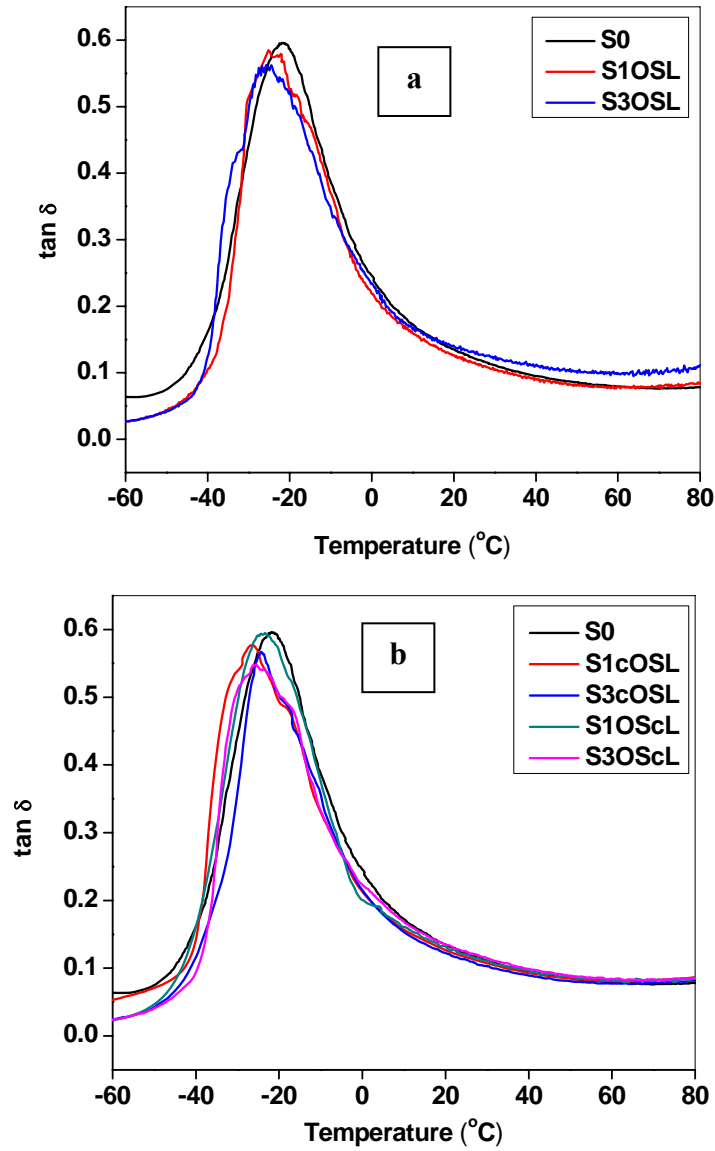


Figure 6.6: $\tan \delta_{\max}$ vs. temperature for nanocomposites based on (a) covalent and (b) dual modified clays

6.6 Dynamic Rheological Analysis

Dynamic rheological analysis (strain sweep and frequency sweep) were performed with the neat TPU and TPUCN with 3% clay content.

6.6.1 Strain Sweep

Percentage drop in modulus at different strain % (1, 7, 20, 70 and 100%) are compared with the initial modulus for the neat TPU and TPUCNs (Table 6.2).

An early drop in modulus is very sharp with respect to the initial storage modulus even in the neat TPU. This is due to the two-phase morphology and presence of hard domains in the TPU. The increase in drop in modulus values in case of TPUCN as compared to the neat TPU indicates the increased ‘Payne effect’. The effect is more pronounced especially at higher strain (7% strain onwards). However, as compared to the nanocomposites based on dual modified clays, SOSL possess more stable aggregates and it is not possible to capture the total breakdown of aggregate within the range of strain studied here (0.28 to 100%).

Among the nanocomposites based on dual modified clays, drop in modulus is highest with S3OScL as compared to S3cOSL. This is due to the better state of dispersion in combination with intercalated morphology and the formation of crosslinked siloxane structure in case of SOScL. But ScOSL possessing highly exfoliated morphology exhibits lesser ‘Payne effect’ as compared to the SOScL.

Table 6.2: Percentage drop in modulus value as compared to the initial modulus at different strain levels for the neat TPU and TPUCNs with 3% clay content

Sample ID	% drop in modulus value at different strain levels				
	1%	7%	20%	70%	100%
S0	7.8	13.9	28.0	60.7	68.6
S3OSL	7.5	23.5	48.0	71.7	76.1
S3OScL	10.2	28.4	53.8	77.2	82.9
S3cOSL	8.0	26.9	49.2	74.1	80.9

6.6.2 Temperature Sweep

Table 6.3 represents the changes in dynamic storage modulus values at different temperatures. It is observed that the dynamic storage modulus values of S3OSL and S3OScL are lower than the neat TPU. However, a significant increase in G' is noticed with S3cOSL. This again supports our earlier observation in DMA analysis that cOSL retains modulus at higher temperatures probably due to its highly exfoliated morphology.

Table 6.3: Dynamic Storage Modulus values at different temperatures

Sample ID	Storage Modulus (kPa) at different Temperatures		
	140 (°C)	150 (°C)	160 (°C)
S0	190.1	68.2	19.4
S3OSL	175.7	74.7	18.5
S3OScL	177.5	69.4	12.9
S3cOSL	231.3	93.2	25.9

6.6.3 Frequency Sweep

Figure 6.7a and b display the complex viscosity vs. frequency plot of TPUCNs at 140 °C and 170 °C, respectively. In this case also the similar type of crossover between the storage and loss modulus is observed (as shown in Chapter 4B, Fig. 4B.4 and Chapter 5).

6.6.3.1 Effect on Complex Viscosity at 140 °C

It is observed that at 140 °C, the complex viscosity (η^*) of all the nanocomposites are lower than the neat TPU within the frequency range studied here (0.033 to 30 Hz). This is due to the contribution of the shear thinning events due to the change in molecular relaxation. However, among the nanocomposites, η^* values grossly follow the order: S3cOSL>S3OScL>S3OSL. This is possibly because of the increase in the degree of dispersion leading to increased polymer-filler interaction thereby increasing the η^* values. In all the cases a pseudoplastic behavior is observed at this temperature.

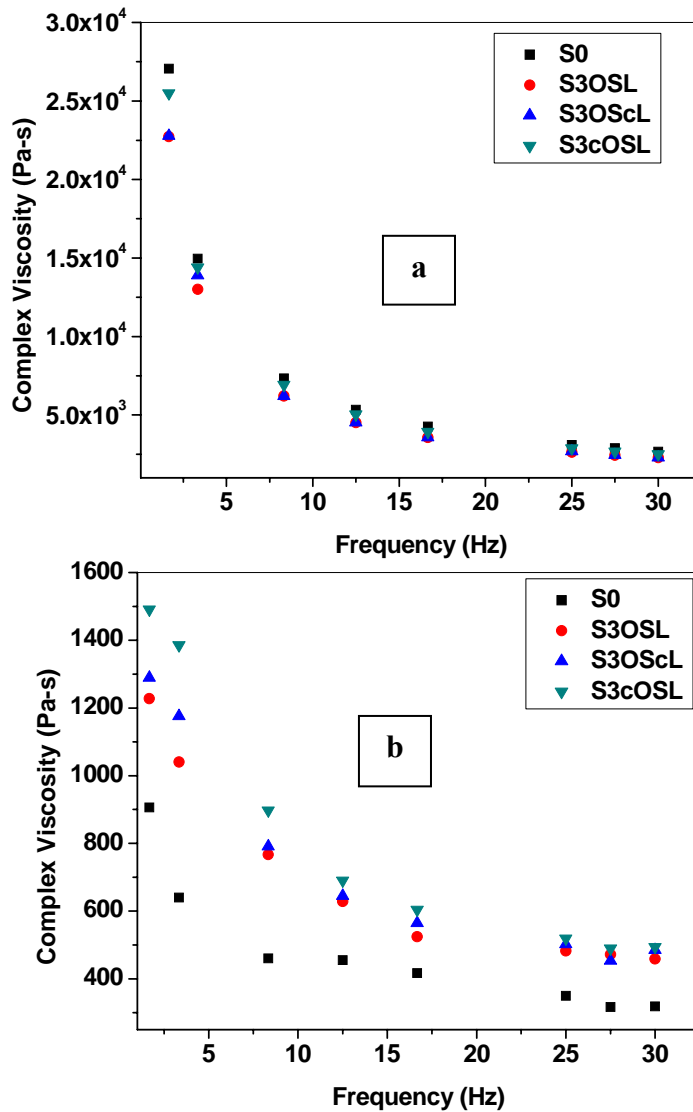


Figure 6.6: Complex viscosity vs. frequency plot of TPUCN at (a) 140 °C and (b) 170 °C

6.6.3.1 Effect on Complex Viscosity at 170 °C

Interestingly, at 170 °C, the complex viscosity (η^*) of all the nanocomposites are higher than that of the neat TPU within the frequency range studied (0.033 to 30 Hz). This may be due to softening of the hard domain (long range ordering) present in the neat TPU at this temperature. Hence, major contributions towards the η^* values are attributed to the presence of fillers. The trend in complex viscosity remains similar to that observed at 140 °C (S3cOSL>S3OScL>S3OSL). This is again due to the

greater degree of dispersion in cOSL as compared to other varieties of modified nanoclays.

6.7 Thermogravimetric Analysis

TGA thermograms of the neat TPU and nanocomposites with 1% clay content are shown in Figure 6.8. It is observed that maximum onset degradation (T_i) is observed with 1% clay content in all the nanocomposites. Improvements in thermal stability (with respect to T_i) of 17.1, 19.4 and 28.7 °C with S1OSL, S1OScL and S1cOSL, respectively are observed as compared to the neat TPU (Table 6.4). From the TEM photomicrographs (Fig. 6.2), it has been observed that the extent of dispersion follows the order ScOSL>SOScL>SOSL. Thus, it may be inferred that thermal stability of the nanocomposite is directly proportional to the extent of dispersion. As compared to the ionically modified clay (Chapter 4A, Section 4A.8), silane modified and dual modified clays offer enhanced thermal stability. This is because of the formation of more stable siloxane oligomer. However, increase in the amount of clay renders the decrement in thermal stability of the nanocomposites. This is because of the increased contribution from the decomposition of the excess modifiers present inside the clay galleries. However, at higher levels of degradation (e.g., 50% and 80%) nanocomposites containing 3 wt% clay offer higher thermal stability.

6.8 Isothermal TGA

For this study, three different temperatures (300, 325 and 350 °C) were selected based on the degradation behavior of TPU via dynamic TGA experiment. Based on the theory mentioned in Chapter 4A, Section 4A.9, the rate constants and activation energy of the neat TPU and S1cOSL were calculated and compiled in Table 6.5. In this case also (like in Chapter 4A and 5) the activation energy of the

nanocomposite is found to be lower than the neat TPU. The explanations remain same as mentioned in earlier chapters.

Table 6.4: Temperatures corresponding to 5, 50 and 80% degradation

Sample ID	T_i	T_{50}	T_{80}
S0	300.0	378.5	400.2
S1OSL	317.1 (17.1)	388.3 (9.8)	412.4 (12.2)
S3OSL	315.6	387.6	414.6
S1OScL	319.4 (19.4)	388.9 (10.4)	414.3 (14.1)
S3OScL	308.1	389.2	415.9
S1cOSL	328.7 (28.7)	389.3 (10.8)	412.2 (12.0)
S3cOSL	325.5	392.4	418.2

(* Values given inside parenthesis indicate the increase in corresponding temperatures compared to the neat TPU)

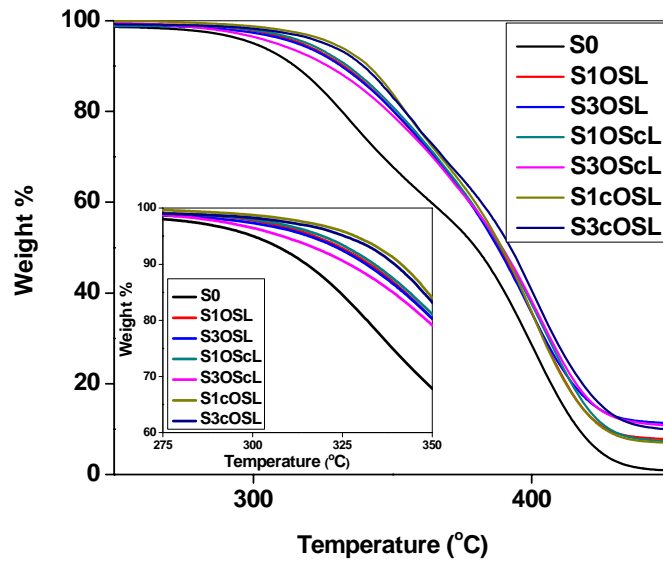


Figure 6.8: TGA thermograms of TPUCN

Table 6.5: Rate constants at different isothermal degradation conditions

Sample ID	$k_{300} (\text{sec}^{-1}) \times 10^{-3}$	$k_{325} (\text{sec}^{-1}) \times 10^{-3}$	$k_{350} (\text{sec}^{-1}) \times 10^{-3}$	Activation Energy (J/mole)
S0	0.3 (0.95)	0.7 (1.00)	1.5 (0.92)	95.5
S1cOSL	0.2 (0.98)	0.5 (0.97)	0.8 (0.97)	82.6

(* Values given inside parenthesis indicate the correlation coefficients)

6.9 Conclusions

Simple covalent modification leads to aggregated morphology of the modified Laponite in the TPU matrix. However, incorporation of dual modified clay is found to register exfoliated and intercalated morphology. The nanocomposites containing dual modified clay, especially cOSL exhibit better thermal, dynamic mechanical and rheological properties as compared to other varieties of nanoclays (OSL and OScL).

6.10 References

- Finnigan B., Jack K., Campbell K., Halley P., Truss R., Casey P., Cookson D., King S., Martin D. (2005) Segmented Polyurethane Nanocomposites: Impact of Controlled Particle Size Nanofillers on the Morphological Response to Uniaxial Deformation, *Macromolecules* 38, 7386-7396
- Wheeler P. A., Wang J., Baker J., Mathias L. J. (2005) Synthesis and Characterization of Covalently Functionalized Laponite Clay, *Chemistry of Materials* 17, 3012-3018
- Wheeler P. A., Wang J., Mathias L. J. (2006) Poly(methyl methacrylate)/Laponite Nanocomposites: Exploring Covalent and Ionic Clay Modifications, *Chemistry of Materials* 18, 3937-3945

CHAPTER 7

***EX-SITU AND IN-SITU PREPARED TPUCN
BASED ON DUAL MODIFIED LAPONITE RD***

A part of this chapter has been accepted in:

Polymer (2010)

7.1 Introduction

In Chapter 6, it has been observed that better dispersion of Laponite in the TPU matrix can be obtained and as a result improved thermal stability and increased high temperature modulus could be achieved with Laponite RD modified with CTAB followed by octyl trimethoxy silane (cOSL). Another interesting observation has been that the exfoliated Laponite form a tubular morphology along with the hard domain of the TPU matrix upon annealing. Association of Laponite with the hard domain has been found to destroy the proper hard domain ordering.

Hence, in order to counterbalance the effect diminished hard domain ordering, TPU having 42% hard domain has been synthesized. Two varieties of dual modified Laponite RD (modified by CTAB followed by octyl trimethoxy silane, cOSL and CTAB followed by 3-aminopropyl triethoxy silane, cAPL) are used. cAPL contains more number of active functional groups on its surface due to the presence of $-NH_2$ group in each silane unit. Hence, cAPL can provide sites for more number of H-bonding. In this chapter, TPU-clay nanocomposites are prepared by using both *ex-situ* and *in-situ* preparation techniques by using these two types of dual modified clays (cOSL and cAPL). A detailed study on the structure-property correlation of the resulting nanocomposites is described in this chapter.

7.2 Wide Angle X-ray Diffraction (WAXRD)

7.2.1 WAXRD at Lower Angular Range

Figure 7.1a and b show the diffractograms of the TPUCN prepared by *ex-situ* and *in-situ* techniques, respectively. It is observed that the neat TPU registers a peak at around $9-10^\circ 2\theta$ in the diffractogram (Fig. 7.1a and 7.1b) which possibly appears due to ordered hard domains. This peak almost diminishes upon incorporation of

nanoclays. However, in I3cAPL an exception is noticed where, the signature remains rather at a lower angle.

In case of *ex-situ* prepared nanocomposites, addition of cOSL does not increase the d-spacing of the clay gallery and it remains at $5.8^\circ 2\theta$ (d value of 1.5 nm). But an increase in clay content increases the broadness of the peak. This reflects the presence of a broad distribution of the size range of clay aggregates for cOSL based nanocomposites. However, E1cAPL does not exhibit any peak corresponding to the d-spacing in the clay gallery, whereas, E3cAPL shows a peak centered at $5.8^\circ 2\theta$ (d value of 1.5 nm) as a mark of the increased aggregation.

Similarly, in case of *in-situ* prepared nanocomposites, I1cOSL gives rise to a peak at $5.8^\circ 2\theta$ (d value of 1.5 nm). Although the peak position remains the same, but intensity of the peak increases with I3cOSL. However, I1cAPL and I3cAPL show peak centred at $6.0^\circ 2\theta$ (d value of 1.5 nm) having similar peak intensities, indicating the clay platelets to stay closer as compared to the parent modified clay, cAPL.

From these observations, it is apparent that the gallery spacing of the modified clay remains in the similar range except in case of cAPL based nanocomposites prepared by *in-situ* technique (where the clay platelets approach closer). This can be ascribed to the formation of siloxane oligomers during covalent modification, which are attached to two closely spaced platelets and do not allow the clay platelets to expand further. However, the interplatelet distance is slightly reduced in case of I1cAPL and I3cAPL. This is possibly due to the presence of greater number of active functional groups (like, $-\text{OH}$ and $-\text{NH}_2$ groups) in cAPL. Thus, greater number of sites on the clay surface from the modifier are available for the reaction with the $-\text{NCO}$ group of the prepolymer (Scheme 7.1). Possibly this leads to an increased H-bonding within the vicinity of the clay platelets. The schemes depicting the

intermolecular H-bonding in the polyurethane system has been shown by Dai et al. (2004).

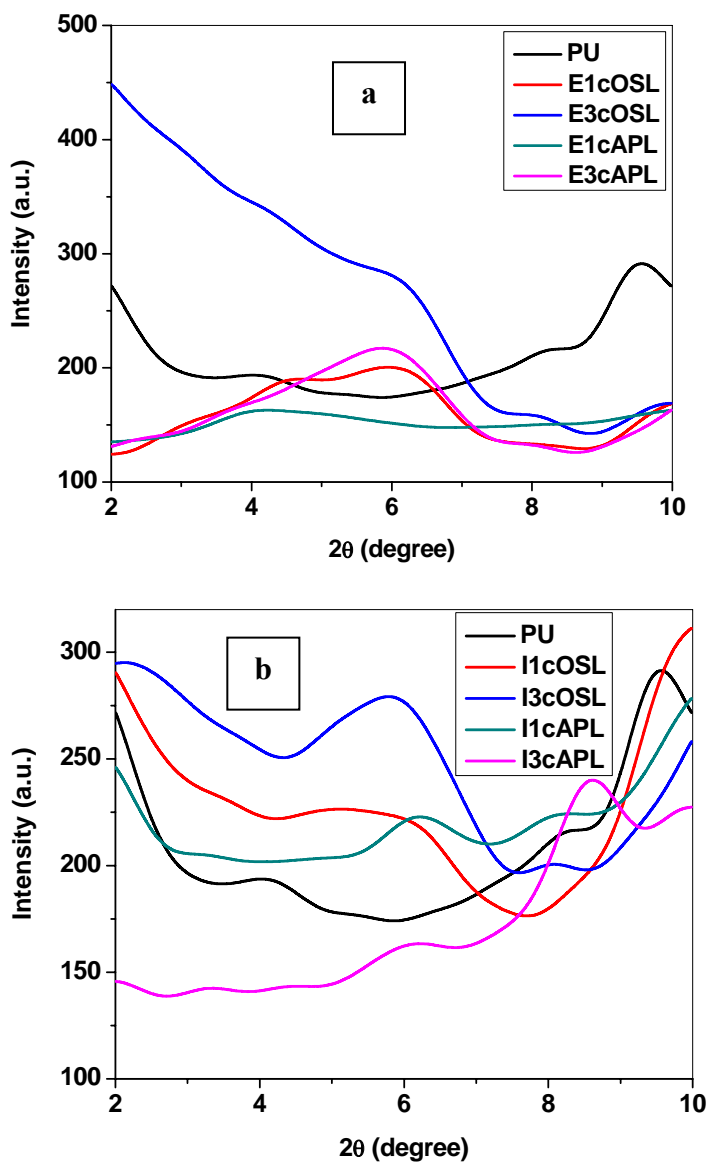
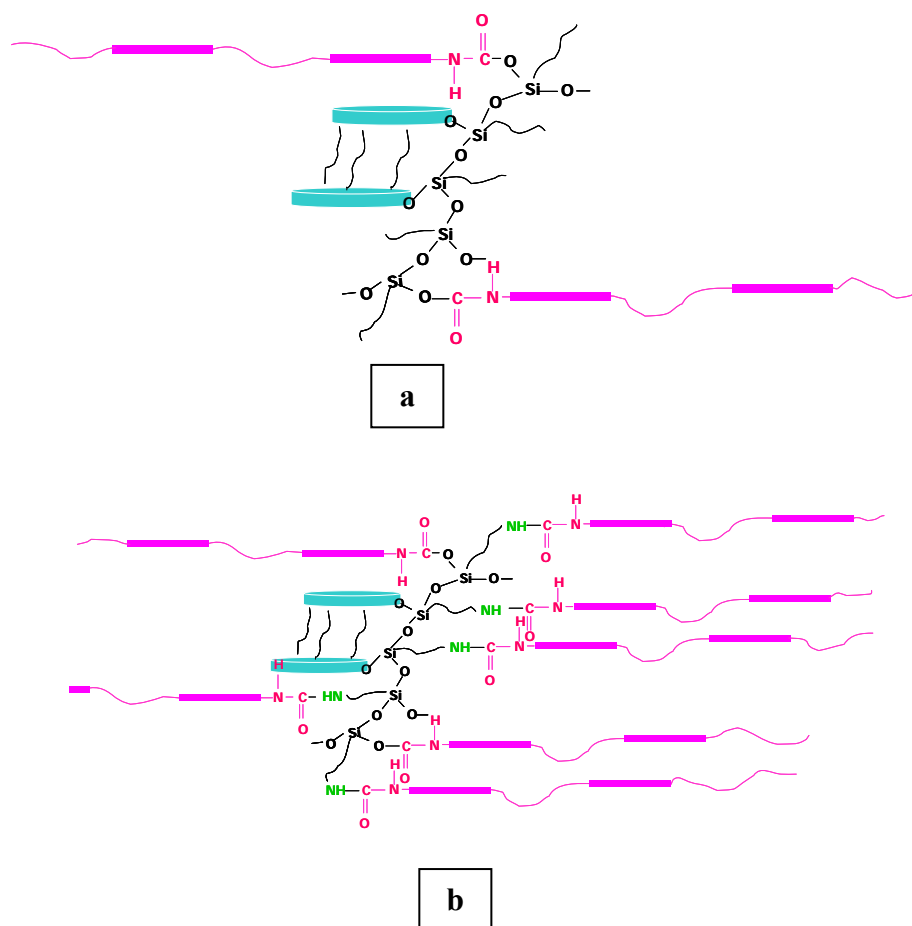


Figure 7.1: WAXRD diffractograms of TPU and TPUCN prepared by (a) *ex-situ* and (b) *in-situ* technique measured in the lower angular range



Scheme 7.1: Schematic representation of structure of (a) IcOSL and (b) IcAPL

7.2.2 WAXRD at Higher Angular Range

WAXRD in the higher angular range ($10\text{-}50^\circ 2\theta$) for the *ex-situ* and *in-situ* prepared nanocomposites and the neat TPU are presented in Figure 7.2a and b, respectively. It is observed that the neat TPU shows two broad hallows ranging from 12.6 to $33.2^\circ 2\theta$ and 34.5 to $50^\circ 2\theta$, respectively. The broad hallows in the range from 12.6 to $33.2^\circ 2\theta$ contains a sharp peak at $19.4^\circ 2\theta$ along with two shoulders. The presence of sharp (semicrystalline) peaks in the neat TPU is due to the self organization of the hard domains present in the TPU. The self organizations of the hard domains occur due to annealing and slow cooling process during molding. The sharp peak and shoulders remain preserved in all the nanocomposites prepared by

ex-situ technique with reduced intensity. Interestingly, these features completely disappear in case of the nanocomposites prepared by *in-situ* technique. Reduction in the peak intensities can be ascribed to the interference of the clay platelets with the ordering of the hard domain (Scheme 7.2). However, absence of these features in case of *in-situ* prepared nanocomposites can be explained on the basis of reaction between the isocyanates (–NCO group) of the prepolymer with the –XH groups (–X = –O in case of cOSL; –O and –NH in case of ‘cAPL’) of the modified clays. The extent of reaction is expected to be higher in case of ‘cAPL’ as compared to ‘cOSL’ (Scheme 7.1) due to the presence of greater number of active functional groups in cAPL (additional –NH₂ groups present in each silane units for cAPL).

The area under the crystalline peak and amorphous hallow regions were determined in arbitrary units and the degree of crystallinity was measured using the relation:

$$\chi = \frac{I_c}{I_c + I_a} \dots\dots\dots(7.1)$$

where, I_a and I_c are the integrated intensities corresponding to the amorphous and crystalline regions, respectively. 2θ values could be reproduced within ± 0.05° variation. Relative crystallinity of the neat TPU and the nanocomposites are reported by comparing a peak corresponding to the semicrystalline peak of the hard domain with that of the amorphous hallow region.

The crystallite sizes were calculated from the WAXRD data using the Scherrer’s equation, as:

$$C_s = \frac{0.9\lambda}{\beta \cos \theta} \dots\dots\dots(7.2)$$

where, C_s is the crystallite size, λ is the wave length of the incident X-ray beam (15.4 nm), β is the full width at half maximum (FWHM) of the most intense X-ray peak and θ is the angle corresponding the most intense peak (peak at 19.4° 2θ).

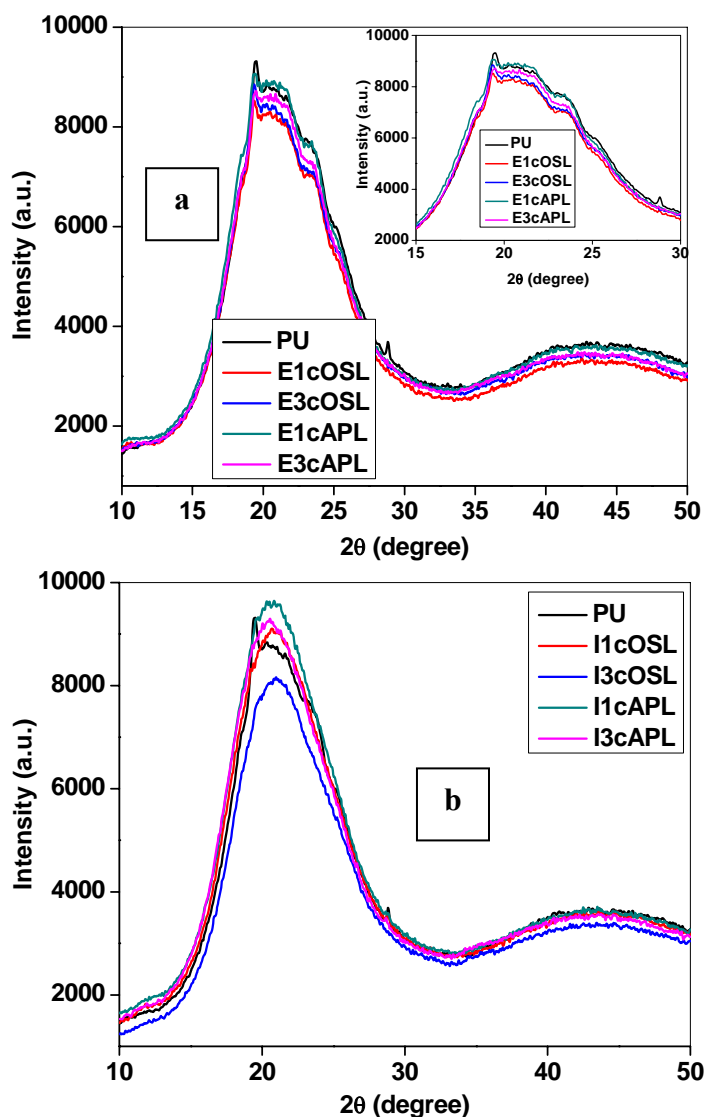
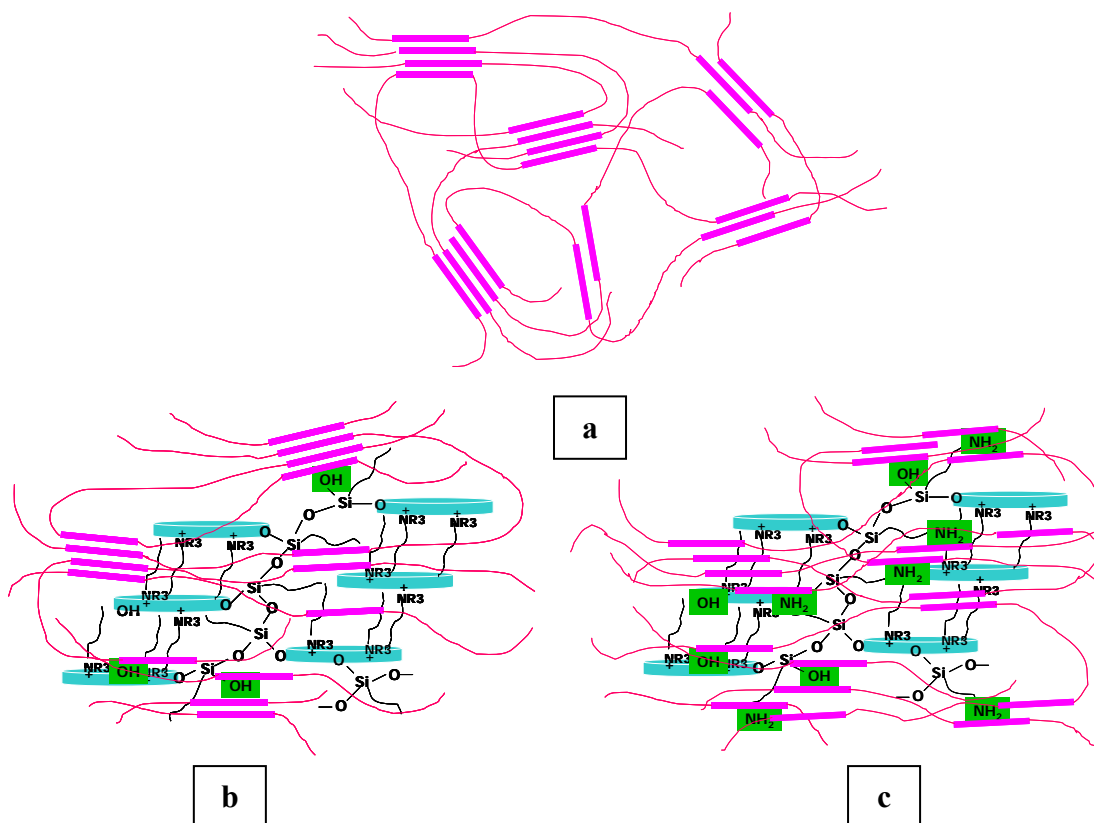


Figure 7.2: WAXRD diffractograms of TPU and TPUCN prepared by (a) *ex-situ* and (b) *in-situ* technique measured in the range 10 to 50° 2θ value

Relative crystallinity and crystallite size calculated from the WAXRD studies are presented in Table 7.1. It is observed that the relative crystallinity of all the nanocomposites is lower than that of the neat TPU, but the crystallite size of the nanocomposites stands higher than that of the neat TPU. Relative crystallinity follows an increasing trend with the increase in amount of clay (in both ‘cOSL’ and ‘cAPL’). Similar trend is observed in crystallite size with the addition of cOSL but interestingly, it follows a reverse trend upon addition of cAPL. The decreased relative crystallinity with the addition of clay is due to the interference of clay in the hard

domain ordering (Scheme 7.2). The increased crystallite size infers that the modified clays possess the capability to change the mode of organization of the hard domains due to the availability of the H-bonding sites (active functional groups) on their surface.



Scheme 7.2: Schematic representation of structures of (a) PU, (b) EcOSL, (c) EcAPL

Table 7.1: Relative crystallinity and crystallite size of the *ex-situ* prepared nanocomposites

Sample ID	Crystallinity* (%)	Crystallite Size (Å)
PU	33.9	19.8
E1cOSL	18.1	24.6
E3cOSL	18.9	25.5
E1cAPL	18.2	24.4
E3cAPL	22.0	21.6

(* Crystallinity values calculated represent the relative values with respect to the neat TPU rather than the exact values for the peak at $19.4^\circ 2\theta$)

7.3 Transmission Electron Microscopy

Figure 7.3 shows the representative TEM photomicrographs of the neat TPU and TPUCN containing 3% clay prepared by *ex-situ* and *in-situ* technique. The grey regions indicate the hard domains, lighter regions indicate the soft domains and the dark regions reveal the clay platelets distributed in the hard domains. Figure 7.3a shows the morphology of the phase separated (self organized) hard domains. In all the nanocomposites, clay platelets are found not to be distributed in the soft domain regions. This is in agreement with our deductions presented in the earlier section.

The self organized hard domains in the neat TPU forms a spherical pattern (Fig. 7.3a). Size of the individual spherical hard domains varies from 35 to 100 nm. Several such spherical hard domains join together, forming arrays of hard domains (with an average length of 200 nm and l/d ratio of 5). In case of E3cOSL, clay platelets along with the hard segment form a tubular type of structure (with an average length of the aligned clay to be 780 nm and l/d ratio of nearly 6.4, Fig. 7.3b). Similarly, in case of E3cAPL elliptical type of morphology (with an average length of 400 nm with l/d ratio of 2.4, Fig. 7.3c) is formed. The tubular type of morphology can be ascribed to the formation of arrays of H-bonding between the hard domain of TPU and the –OH groups of the siloxane oligomers (attached to the clay platelets). The hindrance offered by the cetyltrimethyl ammonium ions against the clay platelets (to approach closer) may also have roles to play for the evolution of such morphology. However, the increased number of active functional groups (tethering) on the surface of cAPL possibly leads to elliptical type of morphology (to minimize the surface energy with structural constraints).

In case of *in-situ* prepared nanocomposites, (I3cOSL and I3cAPL) spherically aggregated morphology is obtained in both the cases (Fig. 7.3d and e). The size range

of the individual aggregate varies from 100 to 150 nm in case of I3cOSL, whereas, it is of the order of 100 to 320 nm in case of I3cAPL. However, several such small spherical units form long arrays of micro-aggregates with approximately 600 nm length (with average l/d ratio of 4) in case of cOSL.

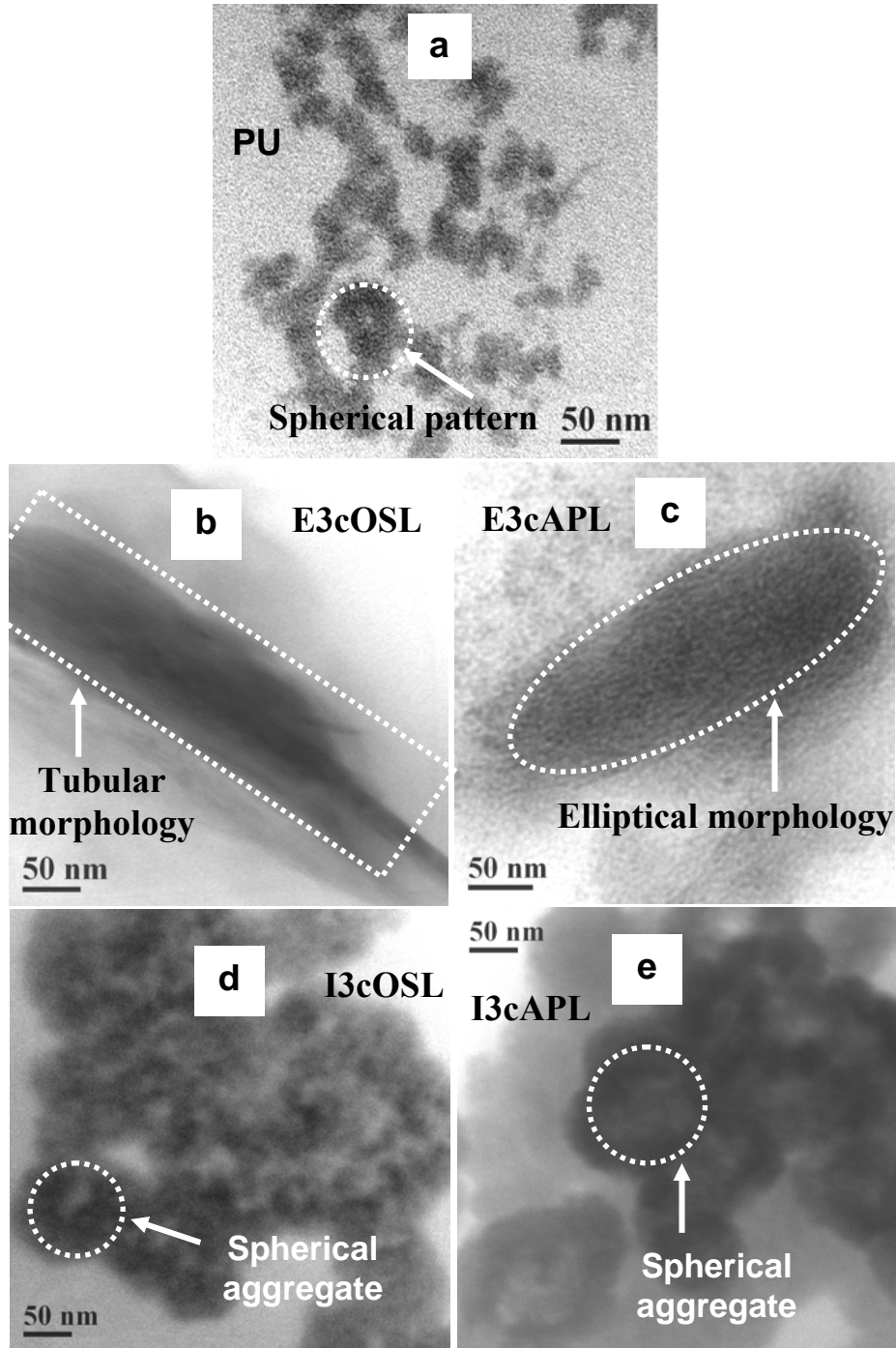
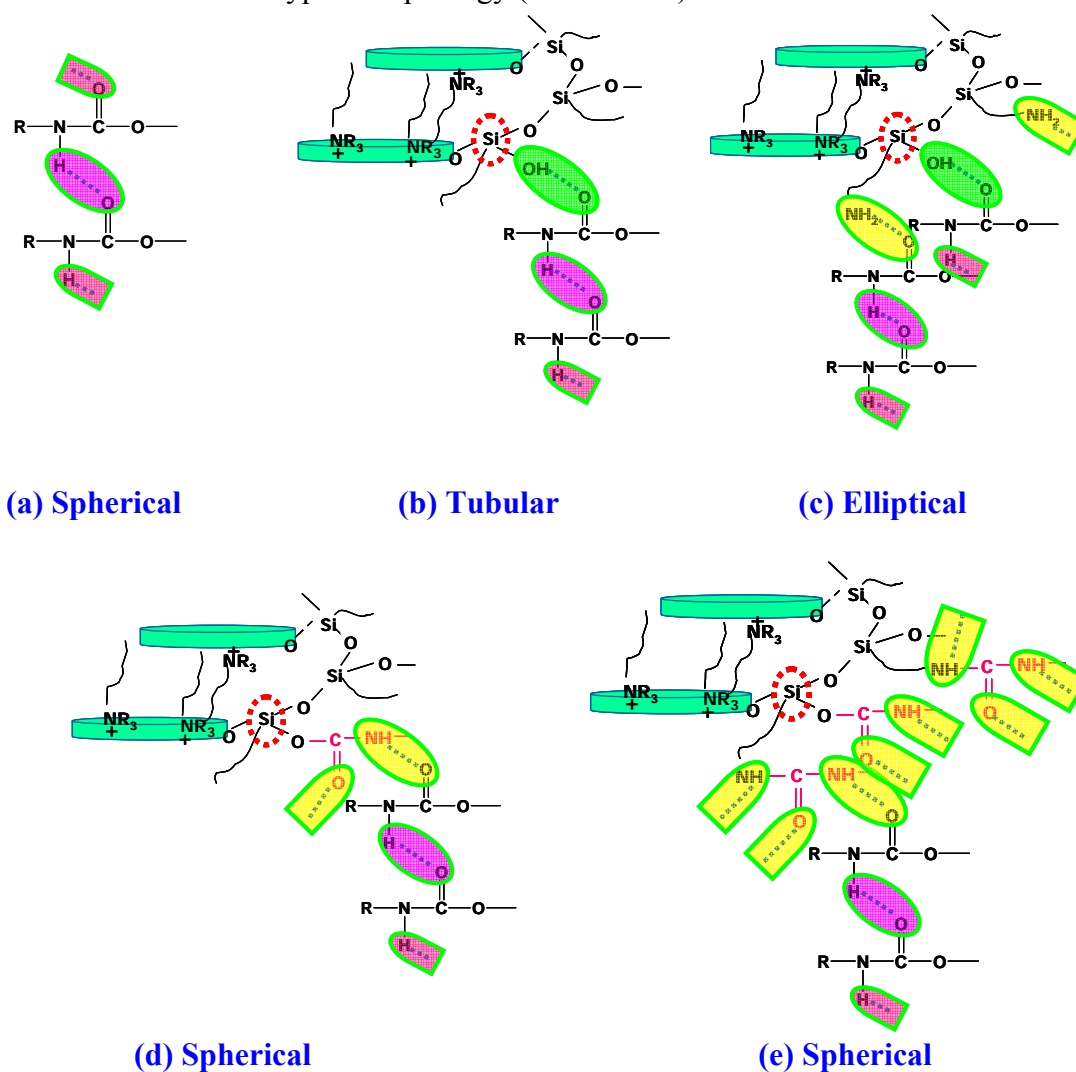


Figure 7.3: TEM photomicrographs of the neat TPU, *ex-situ* and *in-situ* prepared TPUCN

For cAPL the average size of micro-aggregates is 800 nm (with average l/d ratio of 4). Reaction between the $-NCO$ group of prepolymer with the $-XH$ group of the modified clay ($X = -O$ for cOSL and $-O$ and $-NH$ for cAPL) leads to a different type of molecular arrangement of the hard domain leading to the spherical structures. The spherical aggregates are relatively darker in case of I3cAPL as compared to that of I3cOSL. This may be due to the formation of a tight aggregate with I3cAPL because of the presence of more number of active functional groups. Based on the spectroscopic studies (Chapter 3), and the results obtained from WAXRD and TEM, a scheme has been proposed depicting the approximate structures responsible for the formation of different types morphology (Scheme 7.3).



Scheme 7.3: Mechanism for the development of different types of structures

Formation of these novel morphologies of the nanocomposites infers that the microphase separated morphology of the hard domain can be changed by changing the modifiers present in the dual modified Laponite RD.

7.4 Differential Scanning Calorimetry (DSC)

DSC thermograms of the *ex-situ* and *in-situ* prepared nanocomposites are shown in Figure 7.4a and b, respectively. The neat TPU shows two endotherms corresponding to the destruction of the short range (T_{m1}) and long range (T_{m2}) ordered hard domains (or semicrystalline melting) resulting from enthalpy relaxation [Chen et al. (1998); Seymour and Cooper (1973); Shu et al. (2001); Tsen and Chuang (2006)]. In case of the neat TPU and nanocomposites prepared by *ex-situ* method, the relaxations due to short range ordering are very less prominent as compared to that of the long range ordering (Fig. 7.4a). Both T_{m1} and T_{m2} decrease with the addition of clay as compared to those of the neat TPU (Table 7.2). Increase in the amount of clay further decreases the corresponding values. This is possibly due to the interference of the clay platelets in the molecular arrangement of the hard domains (as reflected from WAXRD Section 7.2.2). Presence of more number of active functional groups on the surface of cAPL leads to further decrement in T_m values of the resulting nanocomposites as compared to their cOSL counterparts (at a fixed clay content). This is possibly due to the change in molecular arrangement (Scheme 7.2). However, a different kind of relaxation behavior is encountered with *in-situ* prepared nanocomposites. This is because of the difference in molecular arrangement and hard domain ordering in case of *in-situ* prepared nanocomposites (Scheme 7.1). Pattnaik and Jana (2005) have already reported that a complete disappearance of the hard domain melting peak occurs, when tethered clay is used as a pseudo chain extender.

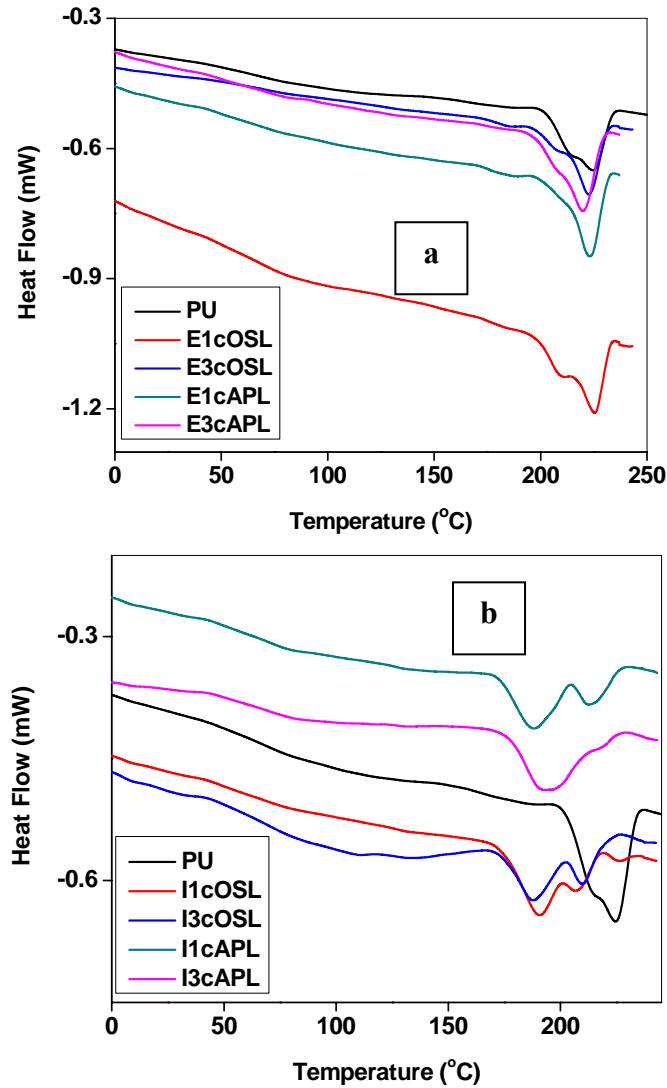


Figure 7.4: DSC thermograms of (a) *ex-situ* and (b) *in-situ* prepared TPUCN

Table 7.2: Temperature corresponding to the melting of the hard domains of TPU and TPUCN as obtained from DSC thermograms

Sample ID	T_{m1} (°C)	T_{m2} (°C)
PU	214.2	224.7
E1cOSL	209.7	225.3
E3cOSL	208.4	222.7
E1cAPL	broad	223.4
E3cAPL	206.5	219.8
I1cOSL	190.4	206.8
I3cOSL	187.9	209.2
I1cAPL	188.2	213.3
I3cAPL	194.2	217.7

Both the melting endotherms (T_{m1} and T_{m2}) are drastically reduced in case of *in-situ* prepared nanocomposites as compared to the neat TPU and their *ex-situ* based

counterparts. T_{m2} of the *in-situ* prepared nanocomposites are very close to that of the T_{m1} of the *ex-situ* prepared nanocomposites. This is possibly due to the increased fraction of short range ordered hard domain in case of the *in-situ* based nanocomposites. However, the formation of new endotherm (T_{m1}) in case of *in-situ* based nanocomposite is possibly due to the presence of different type of molecular arrangement (as already mentioned).

7.5 Dynamic Mechanical Analysis

Figure 7.5a and b show the change in storage modulus with respect to temperature for the nanocomposite prepared by *ex-situ* and *in-situ* preparation techniques, respectively. Table 7.3 shows the storage modulus at different temperatures, T_g and $\tan \delta_{\max}$ values.

In case of the *ex-situ* prepared nanocomposites E' is found to be higher with cOSL based nanocomposites as compared to their cAPL counterparts with a similar amount of clay. This is possibly due to the tubular morphology of the cOSL based nanocomposites as against the elliptical morphology of the cAPL based nanocomposite. Increase in clay content increases the storage modulus values in both cOSL and cAPL based nanocomposites. This is due to the increase in reinforcing effect due to the increase in clay content.

However, increase in clay content is found to be detrimental to the E' value of the *in-situ* prepared nanocomposites. The E' values of the *in-situ* prepared nanocomposites are also lower than their corresponding E' values of the nanocomposites prepared by *ex-situ* technique. Increase in clay content increases the possibility of side reactions during *in-situ* preparation, giving rise to further reduction in the E' values. Lowest E' values in case of cAPL based nanocomposites is due to

increased active functional groups present in the clay macrounits, leading to increased side reaction during the process of polymerization.

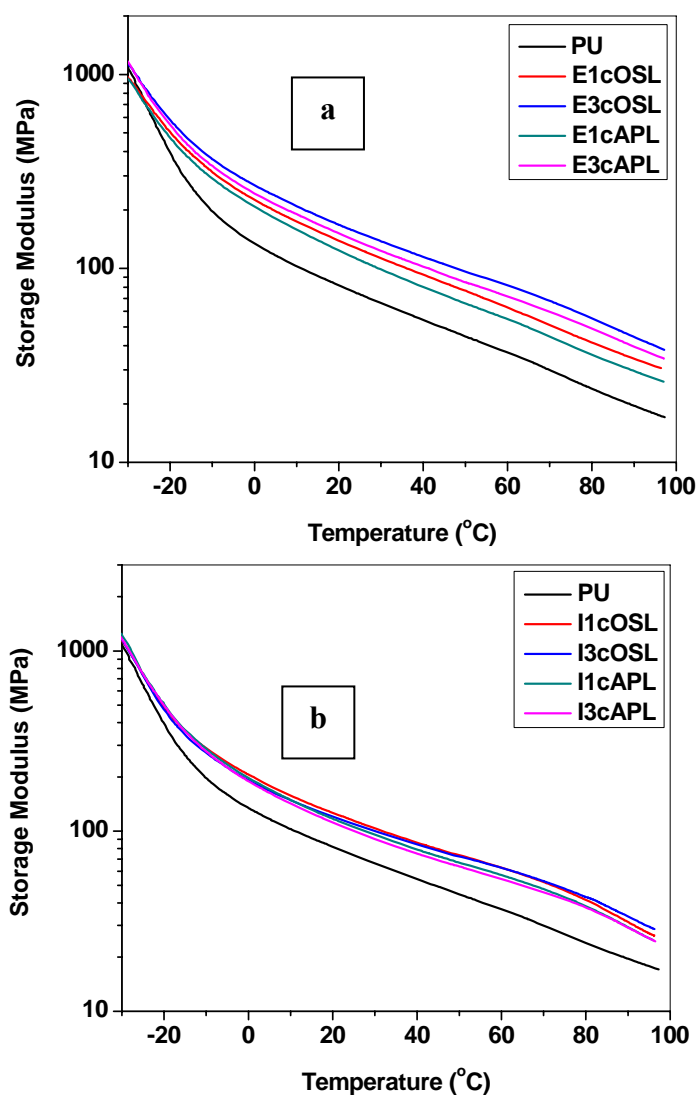


Figure 7.5: DMA thermograms of the neat TPU and TPUCN prepared by (a) *ex-situ* and (b) *in-situ* techniques

The glass transition temperature is found not to follow any particular trend. However, the T_g 's of the nanocomposites are always lower than that of the neat TPU. This is possibly due to the plasticizing effect provided by the alkyl chains present in each silane units of the modifiers. The loss factor, $\tan \delta_{\max}$ values of the nanocomposites are also lower than that of the neat TPU (Fig. 7.6). Increase in clay

content for a particular type of clay further reduces the $\tan \delta_{\max}$ value. This is possibly due to the decrease in the fraction of TPU in the nanocomposite with the increase in clay content.

Table 7.3: Dynamic mechanical properties of TPU-clay nanocomposite

Sample ID	Storage Modulus (MPa)			T _g (°C)	tan δ_{\max}
	-20 °C	+20 °C	+80 °C		
PU	402.1	81.7	23.9	-22.9	0.36
E1cOSL	509.7 (26.8)	139.0 (70.1)	41.3 (72.8)	-27.5	0.26
E3cOSL	584.0 (45.3)	167.1 (104.5)	55.0 (130.1)	-27.0	0.24
E1cAPL	473.0 (17.7)	123.0 (50.5)	35.7 (49.4)	-33.5	0.32
E3cAPL	553.6 (37.7)	151.7 (85.7)	49.1 (105.4)	-27.6	0.27
I1cOSL	488.9 (21.6)	126.2 (54.5)	42.5 (77.8)	-24.9	0.29
I3cOSL	474.8 (18.1)	119.7 (46.5)	42.8 (79.1)	-24.8	0.26
I1cAPL	500.3 (24.4)	117.0 (43.2)	38.3 (60.2)	-25.4	0.29
I3cAPL	504.1 (25.3)	111.1 (35.9)	37.7 (57.7)	-25.4	0.28

(*Values given in the parenthesis represent the percentage increase in E' value with respect to the neat TPU)

7.6 Dynamic Rheological Analysis

7.6.1 Strain Sweep

Percentage drops in modulus values at different strain levels (1, 7, 20, 70 and 100%) are compared with the initial modulus for the neat TPU and TPUCNs (Table 7.4). The initial drop in modulus with strain is very sharp with respect to the initial storage modulus even in the neat TPU. This is due to the two-phase morphology and presence of hard domain (which act as a filler) in the TPU. The increase in drop in modulus values in case of TPUCN as compared to the neat TPU indicates the increased 'Payne effect'. However, the change is marginal within the nanocomposites independent of their techniques of preparation and they follow a similar trend with

respect to strain % (except at 1% strain). This is possibly due to the reason that at the initial strain level molecular chain gets aligned and hence, the effect of strain at higher strain % remains indifferent.

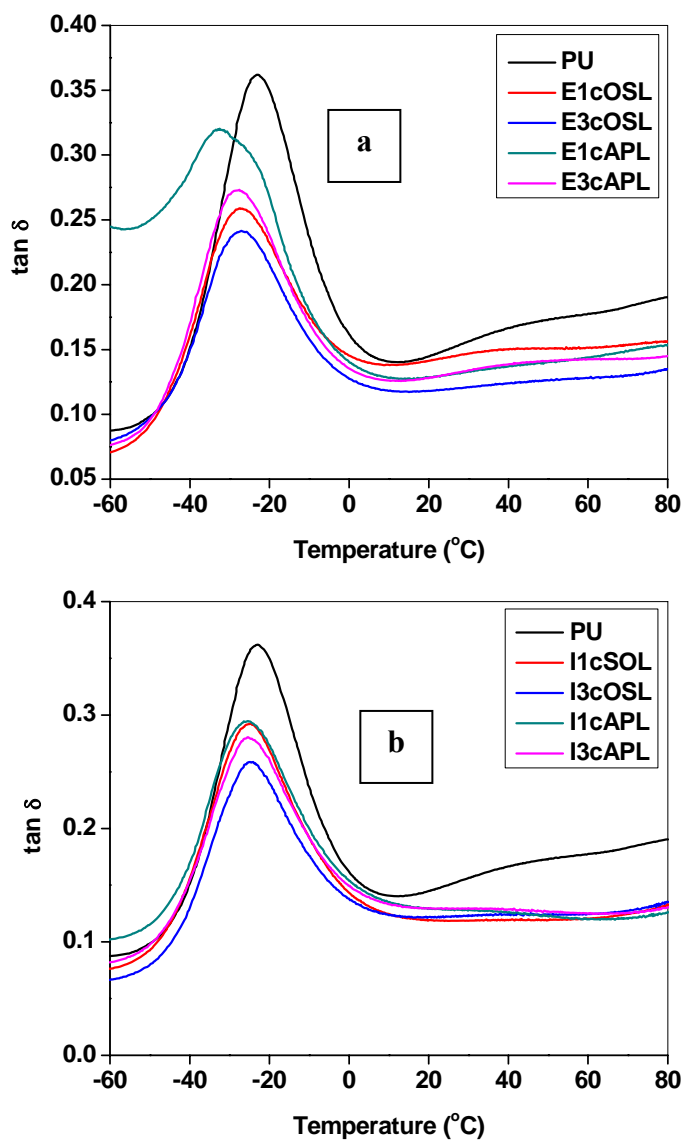


Figure 7.6: $\tan \delta_{\max}$ vs. temperature for (a) *ex-situ* & (b) *in-situ* prepared TPUCNs

Table 7.4: Percentage decrease in modulus value as compared to the initial modulus at different strain levels for the neat TPU and TPUCNs

Sample ID	% drop in modulus value at different strain levels				
	1%	7%	20%	70%	100%
PU	8.7	45.9	76.1	94.5	97.2
E3cOSL	10.1	52.7	83.2	96.2	97.8
E3cAPL	10.0	51.0	82.8	96.6	98.1
I3cOSL	9.1	53.9	85.9	97.6	98.7
I3cAPL	9.3	50.5	80.9	95.5	97.3

7.6.2 Temperature Sweep

Temperature sweep experiment was carried out from a temperature very close to the softening of the ordered hard domains of the TPU upto the ambient temperature e.g., from 180 °C to 40 °C, at a cooling rate of 3 °C/min by using RPA. This experiment was performed to observe the effect of crystallization or self organization of macromolecules during controlled cooling under a sinusoidal frequency of 1Hz. The storage modulus values of the neat TPU and the nanocomposites at different temperatures are presented in Table 7.5.

In case of the *ex-situ* prepared nanocomposites, it is observed that at a constant clay content, cOSL based nanocomposites exhibit higher storage modulus values (G') than their cAPL counterpart. This phenomenon is independent of the temperature range studied. This can be ascribed to the tubular morphology (of clay with the hard segments of TPU) of the nanocomposites with higher aspect ratio for cOSL as compared to that of the elliptical morphology present with cAPL. Increase in clay content increases the storage modulus values (irrespective of the type of clay, cOSL or cAPL). This is possible due to the increased reinforcement provided due to the increased clay content.

In-situ prepared cOSL based nanocomposites exhibits higher G' value as compared to that of cAPL based nanocomposite at a constant clay content. However, contrary to the *ex-situ* based nanocomposites, increase in clay content (of similar type) decreases the G' value in both the varieties of clays (cOSL and cAPL). This is assumed to be due to increased active functional groups present on the modified clays providing increased number of reaction sites (for the $-NCO$ group of the prepolymer). This causes hindrance to the growth of the main chain of the TPU leading to change in the molecular arrangements and the segmental mobility.

The storage modulus values (G') of the nanocomposites are always higher than that of the neat TPU irrespective of the technique of preparation of the nanocomposites and the types of clay used. The maximum improvement in G' value is observed to be with E3cOSL irrespective of the temperature studied. The percent increase in G' values are found to be 148 and 676% higher as compared to that of the neat TPU at 60 °C and 170 °C, respectively.

7.6.3 Effect on Complex Viscosity at 140 °C

Figure 7.7a and b display the complex viscosity (η^*) vs. frequency plot of the nanocomposites at 140 °C prepared by *ex-situ* and *in-situ* techniques, respectively.

Ex-situ prepared cOSL based nanocomposites show higher η^* values than their respective cAPL based counterparts, at a constant clay content. These observations are in line with our earlier observations presented in earlier section and the explanations are quite similar. Increase in the clay content leads to an obvious increase in the η^* value in both the cases due to the increased reinforcement and hydrodynamic effects (following Guth-Gold equation as explained in earlier chapters).

Similarly, *in-situ* prepared nanocomposites with cOSL possess higher η^* values as compared to cAPL based nanocomposites, at a constant clay content. However, an increase in the clay content leads to a decrease in η^* value in both varieties of clay (i.e., cOSL and cAPL). The extent of decrement is however, greater with cAPL based nanocomposites. This is assumed to be due to increased active functional groups present on the modified clays providing increased reaction sites (for the $-NCO$ group of the prepolymer). This causes hindrance to the growth of the main chain of TPU during polymerization leading to change in the molecular arrangement and the segmental mobility.

Table 7.5: Dynamic storage modulus values of TPU and TPUCN at different temperatures as obtained from RPA

Sample ID	Dynamic Storage Modulus* (kPa) at			
	60 °C	90 °C	130 °C	170 °C
PU	4821	2534	948	172
E1cOSL	11802 (144.8)	7107 (180.5)	3179 (235.5)	969 (463.2)
E3cOSL	11970 (148.3)	7226 (185.1)	3575 (277.2)	1335 (675.9)
E1cAPL	9689 (100.9)	6016 (137.4)	2789 (194.3)	921 (435.4)
E3cAPL	11168 (131.6)	6755 (166.6)	3007 (217.3)	1054 (512.6)
I1cOSL	10562 (119.1)	6132 (142.0)	2815 (197.0)	799 (364.0)
I3cOSL	9602 (99.2)	5471 (115.9)	2495 (163.3)	685 (298.2)
I1cAPL	9198 (90.8)	5446 (114.9)	2640 (178.6)	786 (356.9)
I3cAPL	9188 (90.6)	5238 (106.7)	2480.1 (161.2)	642.8 (273.5)

(* Values within the parenthesis indicate % improvement in dynamic storage modulus with respect to the neat TPU)

η^* values of the neat TPU is always less than that of the *ex-situ* prepared nanocomposites but the reverse is true for *in-situ* prepared nanocomposites. However, *ex-situ* prepared nanocomposite always possess higher η^* value as compared to their *in-situ* based counterpart. This is due to the difference in segmental mobility. This is also in accordance with our earlier deduction presented in Section 7.4, where DSC results reflect a clear difference in segmental relaxation process between the *ex-situ* and *in-situ* prepared nanocomposites.

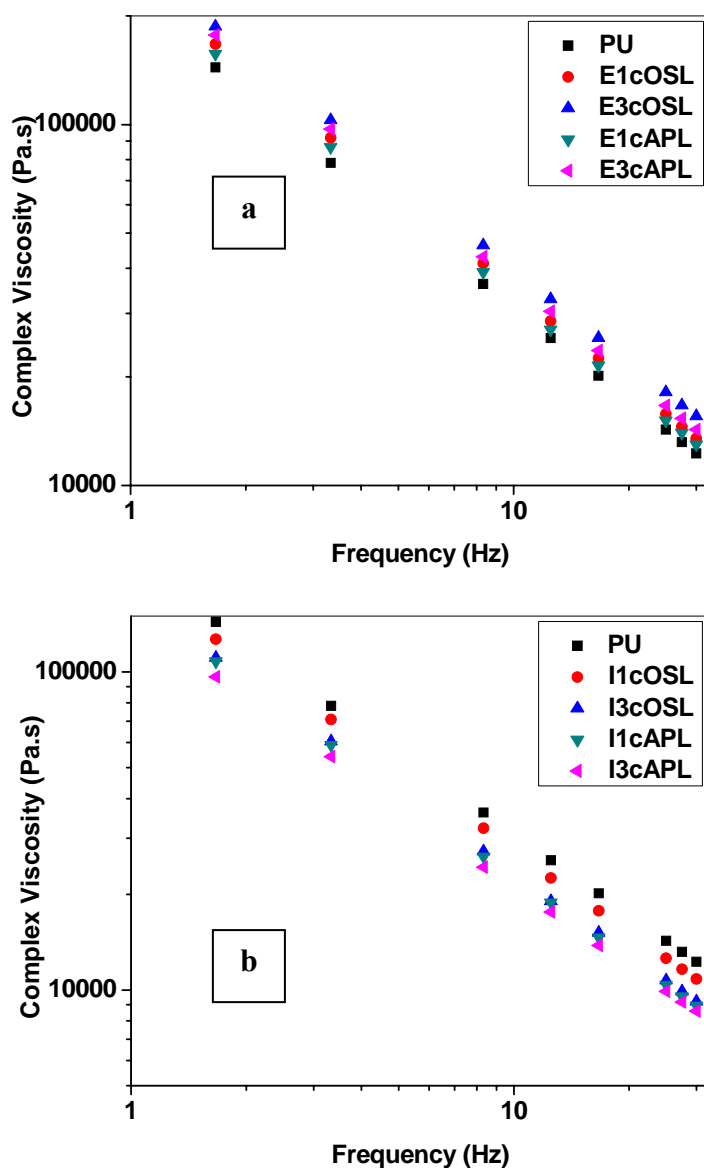


Figure 7.7: Frequency sweep at 140 °C of (a) *ex-situ* & (b) *in-situ* prepared TPUCNs

7.7 Tensile Properties

The tensile properties of the nanocomposites are given in Table 7.6.

Ex-situ prepared cOSL based nanocomposites possess higher tensile strength (TS) and elongation at break (EB) as compared to that of the cAPL based nanocomposites. Nearly 67% increase in TS, 208% increase in EB and 44% increase in modulus value at 50% elongation are observed with E1cOSL as compared to the neat TPU. Increase in clay content reflects marginal change in TS for cOSL based nanocomposites but

nearly 1 MPa increase in TS is observed when the amount of cAPL is increased from 1% to 3%. However, for both the types of nanocomposites (containing cOSL and cAPL), EB follows an increasing trend with the increase in clay content and the effect is more prominent in case of cOSL based nanocomposites. This is possibly due to the difference in morphology of the nanocomposites.

In-situ prepared cOSL based nanocomposites possess greater TS, EB and modulus at 50% strain as compared to their cAPL based counterpart. However, in these cases increase in clay content reduces all characteristic mechanical properties (TS, EB and modulus at 50% strain) of the nanocomposites independent of the types of clay used (cOSL or cAPL). This is possibly due to the increase in the amount of active functional groups contributed from the modified clay leading to shorter length of the main chain of the TPU so formed. A comparison between the *ex-situ* and *in-situ* prepared nanocomposites shows that the former registers better tensile properties than the latter. This is mainly because *in-situ* prepared nanocomposites possess different morphology due to different molecular arrangements. These structures are evolved by the reaction of the active functional groups on the modified clays with the prepolymer. However, in *ex-situ* prepared nanocomposites the clay particles do not affect the original order of the neat TPU significantly (Scheme 7.2). This feature has been elaborately discussed in Section 7.2.2.

Table 7.6: Tensile properties of the nanocomposites

Sample ID	TS (MPa)	EB (%)	Modulus at 50% strain (MPa)
PU	4.8	136	4.3
E1cOSL	8.0	275	6.2
E3cOSL	7.9	418	5.6
E1cAPL	5.9	165	5.8
E3cAPL	7.0	295	6.1
I1cOSL	6.8	246	5.3
I3cOSL	4.9	131	4.4
I1cAPL	5.5	111	5.2
I3cAPL	5.4	110	5.1

7.8 Thermogravimetric Analysis

Figure 7.8 shows the TGA thermograms of the ex-situ and in-situ prepared nanocomposites. Table 7.7 represents the temperature corresponding to 5 and 10% degradation of the neat TPU and TPUCN, respectively. Thermal stability of all the nanocomposites is higher than that of the neat TPU.

In case of nanocomposites prepared by *ex-situ* technique, cOSL based nanocomposites exhibit higher thermal stability as compared to the cAPL based nanocomposites. The thermal stability (for 5% weight loss) of E3cOSL is found to be 34.6 °C higher than that of the neat TPU. Increase in clay content increases the overall thermal stability.

In case of nanocomposites prepared by *in-situ* technique, cOSL based nanocomposites possess greater thermal stability as compared to their cAPL based counterpart. The increase in clay content also increases the overall thermal stability. I3cOSL exhibits an improvement of 34.9 °C in thermal stability as compared to the neat TPU which is comparable with that of E3cOSL. However, the temperature corresponding to 10% degradation of E3cOSL is found to be the highest amongst all the nanocomposites studied here (40.7 °C higher than the neat TPU).

Surprisingly, the presence of additional H-bonding in case of cAPL does not reflect any observable influence on the initial degradation temperature of the nanocomposites. The enhancement in thermal stability at lower temperature is mostly due to the barrier effect of the nanoclay. But at the same time, at higher temperatures the active functional groups present on the surface of the clay possibly act as nucleophiles, thereby reducing the thermal stability.

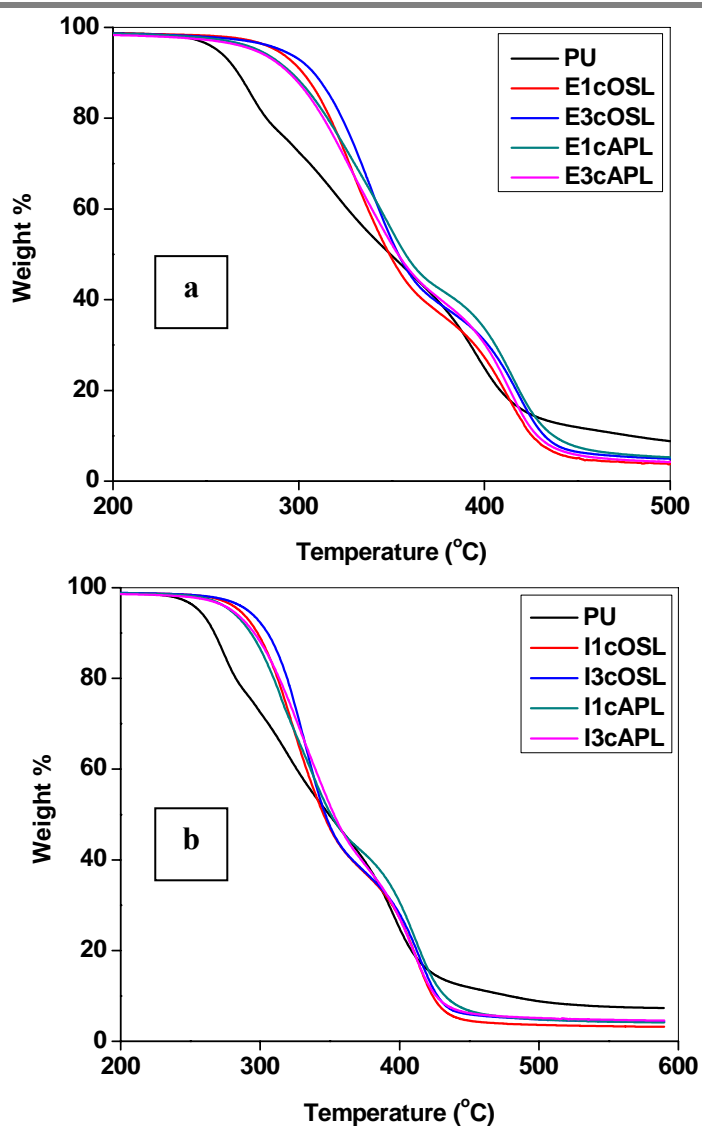


Figure 7.8: TGA thermograms of (a) *ex-situ* and (b) *in-situ* prepared TPUCNs

Table 7.6: Temperature corresponding to 5 and 10% degradation

Sample ID	T ₅	T ₁₀
PU	256.1	267.3
E1cOSL	288.0	302.1
E3cOSL	290.7 (34.6)	308.0 (40.7)
E1cAPL	278.3	296.1
E3cAPL	276.1	294.8
I1cOSL	285.1	298.0
I3cOSL	291.0 (34.9)	305.3 (38.0)
I1cAPL	278.6	293.3
I3cAPL	279.7	295.7

([†] Values presented in the parenthesis indicate the increase in thermal stability as compared to the neat TPU)

7.9. Conclusions

Ex-situ prepared nanocomposites offer greater improvements in modulus, thermal stability and tensile properties as compared to their *in-situ* based counterparts. Increase in the number of active functional groups on the modified clay is found to be detrimental to the improvements in technical properties.

7.10 References

Chen T. K., Shieh T. S., Chui J. Y. (1998) Studies on the First DSC Endotherm of Polyurethane Hard Segment Based on 4,4'-Diphenylmethane Diisocyanate and 1,4-Butanediol, *Macromolecules* 31, 1312-1320.

Dai X., Xu J., Guo X., Lu Y., Shen D., Zhao N., Luo X., Zhang X. (2004) Study on Structure and Orientation Action of Polyurethane Nanocomposites, *Macromolecules* 37, 5615-5623

Pattanayak A., Jana S. C. (2005) Synthesis of thermoplastic polyurethane nanocomposites of reactive nanoclay by bulk polymerization methods, *Polymer* 46, 3275-3288

Seymour R. W., Cooper S. L. (1973) Thermal analysis of Polyurethane block copolymers, *Macromolecules* 6, 48-53.

Shu Y. C., Lin M. F., Tsen W. C., Chuang F. S. (2001) Differential scanning calorimetry analysis of silicon-containing and phosphorus-containing segmented polyurethane. I - Thermal behaviors and morphology, *Journal of Applied Polymer Science* 81, 3489-3501

Tsen W. C., Chuang F. S. (2006) Phase Transition and Domain Morphology of Siloxane-Containing Hard-Segmented Polyurethane Copolymers, *Journal of Applied Polymer Science* 101, 4242-4252.

CHAPTER 8

SUMMARY AND CONCLUSIONS

8.1 Summary and Conclusions

Detailed investigation on the effect of modified Laponite nanoclays on the structure-property of the TPU-clay nanocomposites have been studied extensively in this thesis. Laponite nanoclays have been modified with organic entities with non-active and/or with active functional groups by ionic, covalent and dual modification techniques. The modified nanoclays have been characterized by FTIR, solid state NMR, WAXRD, and TGA. The TPU-clay nanocomposites based on various modified Laponites have been prepared by solution mixing, *ex-situ* and *in-situ* techniques. The resulting nanocomposites have been characterized by WAXRD, HRTEM, AFM, FESEM, DSC, TGA, DMA and RPA. Structure-property correlations for such novel TPU-clay nanocomposites have been established throughout the course of the thesis. An elaborate discussion on the experimental findings ultimately leads to the following conclusions:

Laponite is successfully modified by using ionic, covalent and dual modification techniques. Laponite RDS possesses additional sites for ionic modification due to the presence of $\text{Na}_4\text{P}_2\text{O}_7$ in its structure. Covalent modification of Laponite with trialkoxy silanes leads to oligomerization of the modifiers. Extent of modification in case of clay modified by covalent followed by ionic modification technique is lower than that of the ionic followed by covalent modification technique. Dual modification technique leads to greater extent of modification of Laponite RD.

TPU-clay nanocomposites have been prepared by solution mixing technique by using Cloisite[®] 20A (modified montmorillonite) and in-house modified Laponite RD (ionically modified by dodecylammonium chloride, dL and cetyltrimethyl ammonium bromide, cL). Morphological analysis by WAXRD, TEM and AFM reveals the preferential confinement of Cloisite[®] with the soft domains, dL with the

hard domains, but cL is found to be distributed in both the domains randomly. The storage modulus and thermal stability of the nanocomposites follow an order, SC>ScL>SdL. This behavior can be explained well on the basis of the combination of intercalated and aggregated structures of the nanoclay inside the TPU matrix, depending on their nature and preferential association with different segments. The onset of degradation of the nanocomposites are enhanced by 17.5, 8.3 and 11.4 °C for SC, SdL and ScL, respectively with 1% clay content as compared to the neat TPU.

The dynamic rheological behavior of TPU-clay nanocomposites have been explained on the basis of equilibrium morphology obtained from TEM observations. Cloisite[®] 20A based nanocomposites register greater decrement in dynamic modulus as compared to their modified Laponite counterparts (over a wide range of % strain) owing to the greater size of platelets and soft segment preference of Cloisite[®]. Amongst the Laponite RD based nanocomposites, cL based TPU nanocomposites display stronger 'Payne effect' as compared to that of the dL based counterparts due to the hard segment preference of the dL. In frequency sweep experiment, it is found that $G' > G''$ at 140 °C, whereas, $G'' > G'$ at 170 °C, for all the nanocomposites (irrespective of the frequency). Cloisite[®] based nanocomposites register greater η^* values as compared to Laponite RD based counterparts irrespective of the temperatures studied (140 and 170 °C). This is again ascribed to the greater size of clay platelets and greater polymer-filler interactions. Hard/Soft segment preference of nanoclays is highly reflected at 140 °C but aggregation tendency of clay platelets prevails at 170 °C. Addition of clay is found to increase the elastic component of stress relaxation for the TPU at 120 °C. This behavior is more prominent in case of Cloisite[®] based nanocomposites as compared to their Laponite based counterparts.

Overall, the size of clay platelets and morphology of the nanocomposites play vital roles in determining the dynamic rheology of TPU-clay nanocomposites.

Laponite RDS modified with two different surfactants (cetyltrimethyl ammonium bromide, cLS and dodecylamine hydrochloride, dLS) are dispersed in the TPU matrix by solution mixing technique. Morphologies of these two modified clay-nanocomposites are markedly different from each other. cLS based TPU nanocomposites exhibit partly exfoliated, intercalated and aggregated structures at lower clay content, but a network type of structure is observed at higher clay contents. However, dLS based TPU nanocomposites exhibit spherical cluster type of structure at all clay contents studied. Nearly two fold increase in storage modulus is observed in both glassy and rubbery state with merely 1% cLS addition, but gradually it decreases with an increase in clay content. However, in case of dLS filled nanocomposites, gradual increase in storage modulus is observed with the increase in clay content. The plasticizing action of surface alkyl ammonium groups resulted due to the modification of the $\text{Na}_4\text{P}_2\text{O}_7$ is highly reflected in case of ScLS, especially in strain sweep and frequency sweep test modes. Thermal stability of the nanocomposite (for 5% weight loss) is improved by 19.1 and 12.5 °C as compared to the neat TPU, with only 1% addition of cLS and dLS, respectively.

Simple covalent (alkyl silane) modification of Laponite RD provides an aggregated morphology in the TPU matrix. Similarly, initial covalent modification followed by ionic modification (OScL) reveal a combined aggregated and exfoliated morphology whereas, highly exfoliated morphology persist with initial ionic followed by covalent modification (cOSL). A combined presence of aggregated and exfoliated morphology show greater storage modulus values with moderate improvement in thermal stability. However, highly exfoliated structures provide the highest thermal

stability with moderate improvement in the storage modulus. The dual modified Laponite possess the tendency to alter the equilibrium morphology of the nanocomposite. The storage modulus value in the glassy region (at $-60\text{ }^{\circ}\text{C}$) and in the rubbery region ($+100\text{ }^{\circ}\text{C}$) are improved by 173% (with S3OScL) and 85% (with S3cOSL), respectively as compared to that of the neat TPU. Order of complex viscosities of the nanocomposites are directly proportional to the degree of dispersion of the modified nanoclays, independent of the temperatures studied. The onset of degradation is found to increase by $28.7\text{ }^{\circ}\text{C}$ in case nanocomposite containing merely 1% cOSL, as compared to that of the neat TPU. Thus, the dual modification of Laponite offers an avenue to improve the state of dispersion of Laponite RD in the TPU matrix. Higher degree of dispersion of Laponite can significantly improve the technical properties and thermal stability of the TPU matrix.

Significant changes in the morphology are observed between the two types of nanoclays used in the TPU matrix for the preparation of nanocomposites by *ex-situ* and *in-situ* techniques. This is basically due to the change in number of active functional groups (tethering) on the dual modified Laponite surface. Among the two techniques of preparation of nanocomposites, *ex-situ* prepared nanocomposites offer better property spectrum as compared to the *in-situ* prepared nanocomposites. In case of *ex-situ* prepared nanocomposites, increase in clay content increases the complex viscosity, dynamic storage modulus and tensile properties but the reverse trend is observed in case of *in-situ* prepared nanocomposites. cOSL (with lower degree of tethering) based nanocomposites exhibit better mechanical and rheological properties along with thermal stability as compared to its cAPL counterpart (with greater extent of tethering). The dynamic storage modulus value of the nanocomposite containing 3% cOSL is found to be enhanced by nearly 148 and 676% as compared to the neat

TPU at 60 °C and 170 °C, respectively. Almost 67% increase in tensile strength, 208% increase in elongation at break and 44% increase in modulus value are observed for the *ex-situ* prepared nanocomposites containing cOSL. The onset of degradation of the cOSL based nanocomposite is found to be ~35 °C higher than that of the neat TPU. Overall, it may be summarized that increase in polar functionalities in the modifier and the supramolecular structure of the modifier within the clay platelet and the polymer chains play vital roles in the development of morphology & change in molecular relaxation, mechanical properties and rheological characteristics of the TPU based dual modified Laponite clay nanocomposites.

8.2 Contributions of the Present Work

The thesis delineates the preparation and the state of the art of structure-property relationships of the TPU-modified Laponite clay based nanocomposites. Laponite RDS and dual modified Laponite RD have been used for the first time in the TPU matrix. Modified Laponite clays have been found to show a distinct affinity towards the hard domains of the TPU. Novel tubular and elliptical morphologies have been noticed in the TPU-dual modified Laponite clay nanocomposite system. Higher degree of tethering has been found to be detrimental to the improvement in technical properties of TPU-dual modified Laponite clay nanocomposite. *Ex-situ* prepared nanocomposites have resulted in the greater improvement in technical properties than its *in-situ* based counterpart. The maximum improvement in thermal stability of the dual modified Laponite based nanocomposites has been observed to be 35 °C higher than the neat TPU.

8.3 Limitations and Scope for Future Work

A series of silanes with monoalkoxy functionality would have yielded more interesting results to the TPU-dual modified Laponite clay nanocomposites (minimizing the oligomerization of the alkoxy silanes during modification of clay). Detailed investigation on the exact changes those are occurring in the crystalline structures of the nanocomposites could have been studied utilizing small angle and variable temperature X-ray analyses. Also modulated DSC analysis would have been performed to separate various relaxation processes those are occurring in the novel nanoscale structures in the TPU-modified Laponite clay nanocomposites, especially those involving dual modified Laponites. These could not be completed either due to the time limitations or due to the unavailability of experimental facilities. However, those can be extended as scopes for future research.

The results obtained in this thesis may be extended for other systems based on semicrystalline block copolymers, in general. There is a tremendous scope for the TPU-Laponite nanocomposites in a number of applications, where improvements in properties especially the thermal properties do play a major role.

CURRICULUM VITAE

Name: ANANTA KUMAR MISHRA
Date of Birth: 06-08-1980
Sex: Male
Nationality: Indian
Marital Status: Unmarried
Address: Apamara
P.O. Bhutiar Bahal
Dist. Balangir, ORISSA
PIN: 767029

Educational Qualification: M.Phil. (Organic Chemistry):
2003: 1st Class
Sambalpur University, Burla
M.Sc. (Organic Chemistry):
2002: 1st Class,
Sambalpur University, Burla
B. Sc. (Hons. in Chemistry):
2000: 1st Class & Distn.,
Sambalpur University, Burla

Experience in Research Senior Research Fellow (SRF)
Rubber Technology Centre
Indian Institute of Technology,
Kharagpur. (May 2006– July 2010).

List of Publications in International Journals

- **A. K. Mishra**, S. Chattopadhyay, G. B. Nando, E. Devadoss, “Synthesis and Characterization of Elastomeric Polyurethane-Laponite Nanocomposite” *Designed Monomers and Polymers* 11 (2008) 395-407
- **A. K. Mishra**, G. B. Nando, S. Chattopadhyay, “Exploring preferential association of Laponite and Cloisite with soft and hard segments in TPU-clay nanocomposite prepared by solution mixing technique” *Journal of Polymer Science Part B: Polymer Physics* 46 (2008) 2341-2354
- **A. K. Mishra**, S. Chattopadhyay, G. B. Nando, “Effect of modifiers on morphology and thermal properties of novel thermoplastic polyurethane-peptized Laponite nanocomposite” *Journal of Applied Polymer Science* 115 (2010) 558-569
- **A. K. Mishra**, S. Mushtaq, G. B. Nando, S. Chattopadhyay, “Effect of Cloisite and modified Laponite clays on the rheological behavior of TPU-clay nanocomposites” *Rheologica Acta* 49 (2010) 865-878

-
- **A. K. Mishra**, Rajamohanam P. R., G. B. Nando, S. Chattopadhyay, “Structure-property of TPU-clay nanocomposite based on covalent and dual-modified Laponite” *Advanced Science Letters* (In Press) 4 (2011) 1-9
 - **A. K. Mishra**, Rajamohanam P. R., S. Chattopadhyay, G. B. Nando, “Effect of tethering on the structure-property relationship of TPU-dual modified Laponite clay nanocomposites prepared by *Ex-situ* and *In-situ* techniques” *Polymer* (2010) **accepted**

Conference Presentations

- **A. K. Mishra**, S. Chattopadhyay, G. B. Nando, “*Synthesis and characterization of polyurethane Laponite nanocomposite*” in *Polychar-16*, Lucknow, 2008.
- **A. K. Mishra**, S. Chattopadhyay, G. B. Nando, “*Polyurethane-Laponite clay nanocomposite*” *Rubber Expo 09*, Kolkatta 2009.
- **A. K. Mishra**, S. Chattopadhyay, G. B. Nando, “*Preparation and Characterization of Segmented Polyurethane-Laponite clay Nanocomposites*” ICHTM-09, IIT Kharagpur, 2009.
- **A. K. Mishra**, G. B. Nando, S. Chattopadhyay, “*Effect of aspect ratio and state of dispersion on the rheological behavior of TPU-clay nanocomposite*” PPS-25, Goa, 2009.